Adhesively Bonded Composite Repairs in Marine Applications and Utility Model for Selection of Their Nondestructive Evaluation

by

Dimitrios Panagiotidis
B.S., Marine Engineering
Hellenic Naval Academy, 1999

SUBMITTED TO THE DEPARTMENT OF MECHANICAL ENGINEERING IN PARTIAL FULFILLMENT OF THE REQUIREMENTS FOR THE DEGREES OF

NAVAL ENGINEER
AND
MASTER OF SCIENCE IN OCEAN SYSTEMS MANAGEMENT
AT THE
MASSACHUSETTS INSTITUTE OF TECHNOLOGY

June 2007

Signature of Author _____
Department of Mechanical Engineering
May 10, 2007

Certified by _____
James H. Williams, Jr.
School of Engineering Professor of Teaching Excellence
Thesis Supervisor

Certified by _____
Henry S. Marcus
Professor, Mechanical Engineering - Marine Systems
Thesis Supervisor

Accepted by _____
Lallit Anand
Professor of Mechanical Engineering
Chair, Department Committee on Graduate Students

Adhesively Bonded Composite Repairs in Marine Applications and Utility Model for Selection of Their Nondestructive Evaluation

by

Dimitrios Panagiotidis

Submitted to the Department Of Mechanical Engineering, on May 11, 2007 in Partial Fulfillment of the Requirements for the Degrees of Naval Engineer and Master of Science in Ocean Systems Management

Abstract

During the last half century, the use of composite materials and structures has been increasing within many industries: aerospace, automotive, civil, marine, and railway engineering, wind power generation, and sporting goods, to name a few. There is, however, only a small open literature base concerning adhesively bonded composite repairs, primarily originating from within the aerospace industry. Moreover, little work has been done toward the optimization of repairs on marine composite structures, despite a growing number of such applications.

Few decision-making procedures leading to the undertaking of composite repairs have been articulated. Among these, the selection of the most appropriate nondestructive evaluation (NDE) scheme is acknowledged as an important aspect in determining the extent and the type of repair, and ultimately assessing its quality. Such selections of NDE technique(s) currently appear to be largely based upon qualitative engineering judgment, which is likely to lead to long-term sub-optimal remedies.

An open literature review of various repair schemes and the parameters that affect their mechanical properties is undertaken, and conclusions on adhesively bonded composite repairs for marine applications are summarized. Particular attention is given to the effects on the repaired composite of the mechanical and geometric properties of the adhesive and patch materials, fabrication procedures, as well as the environmental and loading conditions in which the repair is expected to function. It is thusly concluded that among the essential parameters for cost and reliability optimization of composite marine repairs are the following: NDE of the region under consideration for repair; adhesive thickness and spew fillet size; membrane and flexural stiffness, overlap length, scarf angle, shape, fiber orientation percentage, and tapering of the repair patch; in-plane bondline length; out-of-plane curvature of the substrate; repair curing and subsequent operating temperature; and moisture absorption. Accordingly, recommendations for further studies are based on these summaries and conclusions.

It is also determined that the selection of the optimal NDE technique(s) for field inspection is a complex function of the structure's geometry, construction of the composite material (such as single-skin, sandwich, or laminate), type and orientation of defect sought (such as interlaminar or intralaminar), accessibility of the site to be inspected (such as single-sided versus double-sided), and cost. To facilitate this multi-attribute decision-making, decision theory is used to generate a value model for the determination of the optimum NDE scheme in marine applications. The decision criteria for this multidimensional assessment of NDE methods are derived from the marine-related open literature. The reliability of such a value model will ultimately depend on the quality of the available data for its formulation.

Thesis Supervisor: James H. Williams, Jr.
Title: School of Engineering Professor of Teaching Excellence

Thesis Supervisor: Henry S. Marcus
Title: Professor, Mechanical Engineering - Marine Systems

Acknowledgements

To my thesis advisor, Professor James H. Williams, Jr., for his valuable suppervision and guidance throughout the completion of this work, thank you. With your suggestions, questioning of my approaches and unlimited availability for discussion, you provided me with meaningful support.

To my thesis supervisor, Professors Henry S. Marcus, for his academic aid, thank you.

To my parents Georgios and Areti, for their love, thank you.

To the Hellenic Navy for financially supporting my academic pursuit, thank you.

To Mr. Richard L. Duffy for his valuable editorial assistance, thank you.

I am also grateful for the financial contribution of the DDG-1000 Program Manager (NAVSEA PMS 500) and the technical guidance of the DDG-1000 Ship Design Manager (NAVSEA 05D).

This work is dedicated to the love of my life, and wife, Melina Chatziefstratiou.
Κορίτσι μου,
Your love is my compass.
Your smile is the wind in my sails.
You have been the anchor and anchorage during the heaviest seas of our journey.
Without you, everything would be futile.
Thank you.

To Melina

Table of Contents

List of Figures

List of Tables

1. Introduction

1.1. General Context

During the last half century, the use of composite materials and structures has been increasing within many industries: aerospace, automotive, civil, marine, and railway engineering, wind power generation, and sporting goods, to name a few. This was inevitable since composites posses unique mechanical properties, such as the high values of specific strength (strength of the material divided by its density) and specific stiffness (stiffness of the material divided by its density), that are crucial for the accomplishment of modern structures in a cost effective manner.

Especially for the transportation-related industries those advanced properties were acknowledged and appreciated early after the introduction of **glass** fibers in 1938 (by Russell Games Slayter). Later on, as fibers with improved properties appeared—boron (1966), **carbon** (1968), aramid (1972), and high-performance polyethylene (1987)—the use of composites was pursued and established as a means of achieving increased fuel savings.

1.2. Definition of Problem

Although the related work and literature is rich and the exceptional mechanical properties of composites are substantially comprehended and utilized to solve engineering challenges, their use for the **adhesively bonded repair** of damaged composite and metallic structures is under development. Particularly, the aerospace industry is currently pioneering work on the improvement of composite repairs for metallic and composite structures, while only a small number of bonded composite repairs are documented in the marine industry, most of which were applied on metallic structures. Thus, there seems to be a technological gap emerging from the constantly increasing use of composites for marine constructions and the low technology readiness level (TRL) of adhesively bonded composite repairs for composite structures. The pursuit to bridge this gap and establish reliable cost effective repairs is constrained by a number of singularities presented by composite materials.

In specific, composites are produced by bonding at two levels: first in each lamina, between the matrix and reinforcements (fibers, chips, particles etc.), and second in the bonding of the laminae that constitute the composite laminate. Consequently, the strength of

composites depends significantly on the quality of these two bonding levels. Furthermore, the through-thickness strength of the laminate is usually very low compared to its strength in other orientations, due to lack of reinforcements in the plane perpendicular to the laminae lay-up. Thus, when an additional bonding is introduced in order to adhesively join the damaged laminates with the repair patch, there is uncertainty about the loci of a potential structural weakness; whereas in the case of metallic adherends, weakness evolves in the region directly adjacent to the joint bondline. Moreover, composite adherends need special care during the surface preparation, prior to any repair, since their surfaces consist of a thin resin layer covering load carrying fibers. Additionally, the anisotropy of composites produces complex coupling mechanisms in the deformations and stresses. The above singularities limit the capability to predict accurately the performance of adhesively bonded repairs and have been targeted by researchers in the effort to establish cost effective repair methods for composite structures.

Unfortunately, proprietary restrictions deprive the open literature of know-how gained by research or in-the-field operations, by a number of companies and the armed forces. Additionally, few decision-making procedures leading to the undertaking of composite repairs have been articulated. In specific, although the use of Nondestructive Evaluation (NDE) methods is admissibly essential for the achievement of safe and cost effective repairs, the selection of an NDE scheme is often totally based upon engineering judgment. This practice, when deprived of a methodology, although effective, could lead to sub-optimal remedies in the long run. Hence, the lack of a method for the determination of the optimum NDE method seems to conflict with the constant need for cost effectiveness.

1.3. Overview of Thesis

The bulk of the existing literature available to the public is related to the aerospace industry, where the thickness of laminates and face-sheets, in the case of sandwich composites, is very **small** (usually less than 3 mm)[1]. From this niche pool of knowledge, repair principles can be extracted, providing a valuable base of comprehension for the use of composites in repairs in other industries. Following the above approach, general trends can be deduced, from the aerospace-gained know-how, about the application of composite repairs on

[1] For simplicity, structural thickness less than 3 mm will be referred to as **thin**, while thickness exceeding 3 mm will be referred to as **thick**.

contemporary marine structures, an industry that is aggressively introducing composites in structural design during the last two decades.

A review of the major parameters affecting and most basic principles concerning composite repairs is pursued in this thesis. The utilized literature basis originates from technologies pertinent to NDE methods, composites, adhesives, bonded **joints** and repairs related to the aerospace, automotive and marine industries. Primarily the family of composites with fibers (including fabrics) as reinforcements and various thermosetting matrices is examined. Conclusions derived from one field may not be readily applicable to any other. However, potential influencing parameters can be determined and accordingly fields of further research can be recommended in an attempt to facilitate the establishment of reliable cost effective bonded composite repairs for marine structures.

Moreover, decision theory is used to generate a value model for the determination of the optimum NDE scheme in marine applications. The decision criteria used for this multidimensional assessment of NDE methods are derived from the marine-related open literature. The reliability of the value model partially depends on the operator's ability to obtain the required inputs, and on his engineering expertise.

2. Composites, NDE, and Repairs

The specifics of the procedure assumed to remedy a damaged composite structure depend on a number of parameters. Among them, one could distinguish Mode of damage, criticality of the damaged part for safe operation of the structure, availability of time for repair, materials-tools availability, and cost effectiveness. Ideally the sequence of steps in a composite repair would be to:

- detect and assess/categorize the damage,
- repair the damage,
- assess the repaired structure properties (e.g. strength, stiffness, stability, fatigue life expectancy).

In order to detect and assess damage without affecting the functionality of a structure, NDE methods need to be applied. Following the damage assessment a repair design has to be sought. The design should incorporate all the relevant parameters of composite repairs and take into account the cost effectiveness of each of the available repair schemes.

Before proceeding with the parameters that influence a bonded composite repair design (Section 3), we quote a description of the major classes into which composite structures can be categorized. The mechanical properties' diversity of composite structures can be appreciated taking into consideration these classes and the wealth of different composite configurations, depending on the fabrication procedure, lay-up sequence of the plies, core or matrix material, type, orientation and material of the reinforcements. Bearing in mind this diversity, the lack of a universally optimal NDE method and repair scheme for the numerous combinations of composite materials and damage Modes can be better comprehended.

Accordingly, an open literature-based review of NDE methods and repair schemes that are used for the assessment and remedy of damaged composite structures is given. Reliant on this review, the determination of the most appropriate NDE method and repair scheme, related to adhesively bonded repairs of **thick** marine structures, is attempted. Finally, a value model for the determination of the optimum NDE scheme is generated using decision theory (Section 7).

2.1. Types of Composite Structures

Simplifying their classification, composite structures can be divided into the following three categories:

- solid laminates, composed of a combination of laminae lay-ups,
- sandwiches, consisting of a core (honeycomb, foam, etc.), whose both sides are covered by plies of non-composite material (face-sheets),
- sandwiches with composite laminates as face-sheet plies.

The first and third categories are mainly examined in the open literature related to the marine industry. Hence, the following study mainly addresses these two types of composite structures.

2.2. NDE of Damaged Composite Structures

The value of detecting and assessing the damage in the effort to minimize the required repair size, while at the same time ensuring the soundness of the structure, is underlined by Armstrong et al. [4]. When one refers to composite damage it should be kept in mind that this includes not only voids, delaminations, and truncations of the constituent parts of the structure. In addition, moisture absorption is also considered a major damage mechanism, for reasons elaborated in paragraph 3.2. The performance of several detection/assessment techniques in aerospace applications is summarized in Table 1. Among them, the most broadly established in the aerospace industry are the following.

2.2.1. Visual Inspection

Visual inspection is one of the most popular techniques of preliminary inspection [4], [12], [13]. Airbus, for example, claims that **carbon** fiber reinforced plastic (CFRP) structures (parts, assemblies, etc.) are designed in such a fashion that if there is no visible evidence of damage then the structure "will not have sustained damage to an extent where aircraft safety is affected" [4]. Moreover, under the same assumption of no visible evidence, this manufacturer states that fatigue life and ultimate loads are sustained, and minor visually undetectable damages will not propagate to a significant extent through the lifecycle of the structure.

However, the above statements sound rather overoptimistic if certain Modes of damage are considered. For instance, moisture ingress, whose deteriorating effects on the mechanical properties of a laminate are developed in paragraph 3.2, might not be visually detectable unless extremely high levels of uptake induce laminate swelling. Moreover, for the case of oversized, **thick** marine structures that present high geometric complexity, the visual detection of moisture uptake seems impossible. Furthermore, the application of a repair in a structure often comprises a path to moisture uptake if not properly sealed. In many cases the repair scheme spoils the uniformity and smoothness of the structure, making the visual detection of defects, especially that of moisture uptake, burdensome.

Additionally, exposure of laminates to impact loading can induce significant structural defects with minor visible evidence. Specifically, large delaminations have been detected on the back surface of S2-**glass/vinyl ester** laminates impacted at velocities below the ballistic limit; that is with no or partial perforation of the structure [31]. In all the examined cases the delaminated area of the back surface was significantly larger than that of the impacted side. The minimum and maximum percentage differences of the front and back surface's area delaminations were 259% and 1473%, respectively, among 12 specimens.

Hence, it seems that the evaluation of a marine composite structures using visual inspection might be unreliable if not combined with other NDE methods.

2.2.2. Tap Testing

Tapping the suspect area manually or automatically may provide useful information on the condition of the examined structure [4], [12], [13], [41], [59]. Higher frequency sounds, electronically detected, indicate good bonding quality as opposed to dull sounds (lower frequencies) that are usually produced when tapping disbonded areas.

One of the disadvantages of tapping inspection is that it can only detect delaminations in the first few layers within a solid laminate. Moreover, it is generally not by itself sufficient for impact damage evaluation. This latter deficiency is attributed to the fact that impacts often produce damage that is deeper within and even on the back face of a laminate. However, coin tapping outperforms other NDE methods when certain parameters of field inspection on marine structures are considered, as indicated in Table 2. The unique performance in these

parameters could place coin tapping among the candidates for a combinatorial NDE scheme for field inspection in the marine industry.

2.2.3. Ultrasonic Inspection

This method is based on measurements of the attenuation and velocity of ultrasonic stress waves that propagate through the examined structure [4], [7], [12], [13], [41], [59]. The trade-off between high frequencies, that present higher sensitivity for detecting defects, and lower frequencies, that have better penetrability, is one of the main considerations when using this method.

There are a number of different ultrasonic inspection schemes. With regard to the inspection geometry, through-transmission refers to a system of a separate receiver and a transmitter, each at one of the opposite sides of a structure. The need for accessibility on both sides and alignment of the transmitter and receiver restrict the practicality of the through-transmission configuration for field inspection. Another method is the pulse-echo, which uses an integrated transmitter-receiver for one-sided inspection. These two techniques use transmission angles perpendicular to the examined structure but oblique angles could also be used in certain configurations. One of these, the polar backscatter, presents unique advantages in the characterization of matrix cracking, the detection of voids and porosity, and the determination of various levels of impact damage.

In spite of the unique advantages of ultrasonic inspection, there are fields of composite repair that are hardly benefited by its use. Specifically, honeycomb structures are difficult to inspect because the propagation of the ultrasound is limited by the inconsistencies in the impedance between the air and the solid walls of the cells [4]. Additionally, liquid ingression reduces the reflection coefficient of the ultrasound, thus deteriorating the detection of defects [7]. Moreover, the presence of compressive loading, pressing the disbanded faces closer, and large bondline thickness lead to increased uncertainty in the results of the inspection [7].

Nevertheless, this NDE method provides some exceptional characteristics, as indicated in Table 2, which can afford reliable field inspections when used separately or in combination with other methods.

2.2.4. X-ray Inspection

X-rays may be used to provide in-depth and in-detail inspection, usually in cases where other methods are inapplicable [4], [12], [13]. For instance, this technique can detect defects in planes perpendicular to those examined with the ultrasonic method. However, in many instances this NDE technique is limited by the X-ray absorption characteristics of the materials. For instance, the similarity of the absorption in **carbon** fibers and certain resin matrices could significantly limit the applicability of X-ray inspection [4].

Unfortunately, the use of this technique is constrained by the high safety precautions that need to be taken in order to protect the operating personnel from the harmful effects of X-radiation exposure. This limitation is more restrictive for field inspections, where personnel evacuation and discontinuity of operations is often unacceptable. Consequently X-rays could not be considered as a practical NDE alternative for regular field maintenance inspections of marine constructions.

2.2.5. Thermography

This technique comprises one of the most broadly used NDE methods in the aerospace industry [4], [7], [13], [41], [59]. The presence of defects on a uniformly preheated structure is determined at areas where rapid changes in the distribution of temperature are observed. This method is alleged to be more reliable than ultrasound for the detection of defects closer to the structure surface [4]. However, its applicability is found to be significantly reduced when used in complex marine composite structures [41].

Nevertheless, the capabilities of thermography are proven in field inspection of composite marine structures. Certain inherent disadvantages of this method could be completely compensated for by other NDE techniques as indicated in Table 2. Altogether, thermography seems to be positioned among the major candidates for a multi-method scheme in marine field inspections.

2.2.6. Interferometry/Shearography

Another NDE technique with significant acceptance in the aerospace industry is interferometry [4], [7], [13]. The structure under examination is subjected to loading or heating and thus displacements are induced on its surface. The magnitude of these

displacements is affected by the presence of defects. Before and after the displacement generation the surface is exposed to a monochromatic light and alterations of the light phase, caused by relative changes of the surface position, indicate the presence of a defect. Some devices measure the first derivative of displacement; this is known as shearography [4].

A comparative assessment of this technique for marine field inspection is not available in the open literature. Nevertheless, it is clear that loading large marine structures is difficult to achieve, while uniformly heating them is conditionally impractical, as in the case of thermography.

2.2.7. Bond Testers

These devices can measure local changes in mechanical impedance around defects (delaminations or disbonds) in a structure that is excited at certain frequencies [4], [7], [13]. Another type of bond tester uses the fact that the presence of a defect can cause resonance of disbonded surfaces when the structure under examination is subjected to certain vibration frequencies. Ultrasonic resonance is utilized in order to detect gross defects and is particularly useful in complex bonded structures [13]. In such cases the use of ultrasonic through-transmission is limited by reduced accessibility and pulse-echo testing is unreliable due to the complex internal signal reflections. However, for the determination of small defects loci, other methods are preferable than bond testers.

2.2.8. Eddy Currents

Eddy currents can be utilized to detect certain defects in composite structures [4], [13]. This method is based on dynamic magnetic fields that are produced by an alternating current flowing into a conducting coil, the probe. When the probe approaches a conductive structure under examination, electromagnetic induction will occur and eddy currents will be induced in that structure. Disruptions of the eddy currents indicate defects on the structure.

This method is mostly used to detect fiber breakage at moderate depths from the laminate surface, as it is relatively insensitive to porosity and delamination [4]. The physical principle on which this method is based limits its application to the inspection of materials with conductivity.

2.2.9. Moisture Meters

Basically, in composites, the ingress of moisture induces an increase in conductivity. This conductivity change can be measured in non conductive composites and then the percentage of humidity absorption is estimated [4]. It is obvious that this method is not applicable to **carbon** or any other conductive fiber composite.

Unfortunately, the existence of such a device with proven reliability and accuracy in the determination of moisture absorption for **thick** composite structures is not documented in the open literature, although there are a number of commercial moisture meters on the market. Besides, the utility of a device that simply detects the presence of moisture in composites is questionable, since there are indications correlating the degradation of composite properties with specific moisture absorption levels, as developed in paragraph 3.2.

2.2.10. Other NDE Methods

There are a number of methods that were developed but are little used in field inspections or remain as laboratory tools [13]. Among them the X-ray backscatter imaging, computed tomography, neutron radiography, acoustic emission, acousto-ultrasonics, and finally microwave testing. A summary of the most commonly used NDE methods and their applicability in aerospace structures can be found in Table 1. The comparison of the individual attributes of the most commonly used NDE methods, based on the available open literature, is tabulated in Appendix A.

2.2.11. NDE of Composites Used in Marine Industry

It should be noted that all the aforementioned NDE features of paragraph 2.2 are derived from the aerospace-related open literature. Assuming that the same properties are applicable to other industries would not be justified. Especially for the case of **thick** composite structures, often met in marine industry, of both single-skins and sandwiches, it has been determined that certain NDE methods are inapplicable or unreliable. Specifically, the impedance method and an automated tap method, both developed for aerospace applications, have been tried for the evaluation of **thick** marine composite structures (with artificial delaminations) without any success [41], [59].

A comparison of certain NDE methods, used to assess marine **glass** fiber reinforced structural components, has revealed their relevant importance for field inspection, along with a number of limitations that are introduced by the particularities of marine composite structures [41], [59]. These NDE methods were ultrasonic pulse-echo, infrared thermography, and automated coin-tap. A microwave method was also utilized but, given its low technology readiness level, its practicality for field inspections was regarded as questionable [59]. Panels, T-**joints**, and top-hat stiffeners were fabricated with engineered defects. The tested panels were **thin** and **thick** single-skin glass-reinforced polyesters, and sandwich composites with balsa and PVC cores. Additionally, a 2/3 scale section of a single-skin GRP minesweeper and another sandwich composite construction, with PVC core, of a small ship that was exposed in explosion trials, were examined (core and skin thicknesses used were 60-100 mm and 4-15 mm respectively). The findings of the above benchmark studies are summarized in Table 2.

Table 1: Relative comparison of NDE methods derived from aerospace applications [13].

Flaw Type	*Visual*	*Tap test*	*UT through-transmission*	*UT pulse–echo*	*UT polar backscatter*	*UT resonance*	*UT correlator*	*X-radiography*	*X-ray backscatter*	*Computed tomography*	*Neutron radiography*	*Acoustic emission*	*Acousto-ultrasonics*	*Eddy currents*	*Thermal IR*	*Shearography*	*Microwave*
Porosity			1	1	2		2	1		1	1		2				2
Foreign material	3		2	1	2	2	2	2	2	2	2				2	3	
Shallow delamination		2	1	1	2	1	1		1	1		3	2		1	1	
Deep delamination			1	1	3	3	1		1	1		3			2	2	
Matrix cracks	3				1			1		2		2	1		3		2
Fiber breaks								2		2		2	2	1			1
Impact damage	3	2	1	1	2	2	1	2	2	1		3	2	1	1	1	1
Skin/skin disbond	3	2	1	2		1	1	2	1	2	2	2	3		1	1	
Skin/core disbond		3	1	2		2	1	3		3	2	2			1	1	
Crushed core			1	3			1	1		2					2	2	
Condensed core								1		1							
Blown core			1				1	1		1							
Core node disbonds								1		1							
Water intrusion			3	2			3	2		2	1	2			2		
Corroded core			2				2	2		3	1	3					
Fatigued core			2				2	1		2							
Foam adhesive voids							3	2		1	2						
Bondline adhesive voids			1	2		1	1	2	2	2	1				2	1	

Key:
1. Good sensitivity and reliability. Good candidate for primary method.
2. Less reliability or limited applicability. May be good supplementary method.
3. Limited applicability. May provide some useful information.

Table 2: Comparison of NDE methods for field inspection of **glass** fiber marine composites (constructed based on [41], [59]).

Defects Inspected and Other Attributes	Ultrasound Pulse-Echo	Infrared Thermography	Automated Coin Tapping
Single-skin Delamination	Yes	Yes	Yes
Sandwich Delamination	No	Yes	Yes
Core Damage	Yes*	Yes	Not evaluated
Impact of Thin/Thick Single-skin	A	B	C
Impact of Sandwich with PVC Core (Balsa Core)	A (B)	B (C)	Not evaluated (Not evaluated)
T-Joint Delamination at Base (Fillet)	A (A)	C (C)	Not evaluated
Top Hat Stiffeners Delamination at Base (Fillet)	A (C)	C (C)	A (Not evaluated)
Sandwich Beam Stiffener-Panel Delamination	C**	C	Not evaluated
Equipment Flexibility	A	C	A
Inspection Time	C	B	A
Effective Near Complex Geometries ***	Yes	No	Yes
Time Demanding Preparation	No	Yes	No
Use in Access Restricted Areas ****	Yes	Scaffolding structures needed	Yes

"A", "B" and "C" are qualitative ranks of relative performance. "A" indicates the best performance, "C" the worst while "B" is in between.

* Only for core thickness less than 30 mm.

** Some delaminations between the sandwich panel and stiffeners were observed.

*** Closer than 300 mm to stiffeners or bulkheads.

**** Provided there is accessibility by the operator.

From Table 2 it becomes clear that the optimal choice of an NDE method is a complex function of the structure's geometry, construction of the composite material (such as single-skin, sandwich, or laminate), type and orientation of defect sought (such as interlaminar or intralaminar), accessibility of the site to be inspected (such as single-sided versus double-sided), and cost. It is also worth mentioning that, for the two examined sandwich composites, NDE methods performed differently for two different cores. Specifically, although there was

variable capability of detecting core damage and skin-core delamination in PVC cores, the results of all NDE methods were characterized as "very bad" [59]. This poses some skepticism regarding the generality of Table 2, since similar differentiation of NDE performance could be found in sandwiches or single-skin laminates for different fibers and polymers.

Equally, it is probable that the classification of NDE methods based on the experience of the aerospace practices is inadequate for **thick** marine composite structures. A comparative assessment, relying on parameters such as those of Table 17, for reinforcements other than **glass** fiber, various matrices or core materials, different construction geometries and with more NDE methods is not documented in the open literature. Moreover, there is no reference assessing the use of different NDE techniques for post-repair evaluation of adhesively bonded composites in the marine industry. The criticality of this literature deficiency can be better appreciated when introducing the two major schemes used in contemporary adhesively bonded composite repairs. As clarified in paragraphs 2.3.1 and 2.3.2, although both can be effective as repairs they present certain peculiarities (e.g. geometry, distribution of stress and strain in the adhesive) that could significantly affect the reliability of any NDE method in their assessment, at various levels.

2.3. Repair Configurations

In terms of the geometrical design of the repair patches, any of the adhesively bonded repairs falls into one of two categories: lap and scarf patch repair. The physical specifics and mechanical properties of each are elaborated below.

2.3.1. Lap Patches

This design requires the application of repair material on top of one or both sides of the damaged area. Single side lap repairs are less efficient than the double ones, since the increased eccentricity that they introduce in the structure induces bending moments even when the primary load is just tensile or compressive. However, the application of double-side lap repairs is not practical in the context of marine structures. This is because double-side laps need alignment, a procedure that is easier for assembling parts in the aerospace industry, but generally inapplicable in naval constructions. Although double lap repairs are considered

more effective than single lap, a potential misalignment of the double lap patches could deteriorate the properties of the repair due to the development of local bending [56]. In addition both single and double-side lap patches are prone to failing in the high peel and shear stresses that develop at the end-zones of the patch-parent overlap [23], [32]. A representation of these stresses is given in Figure 1.

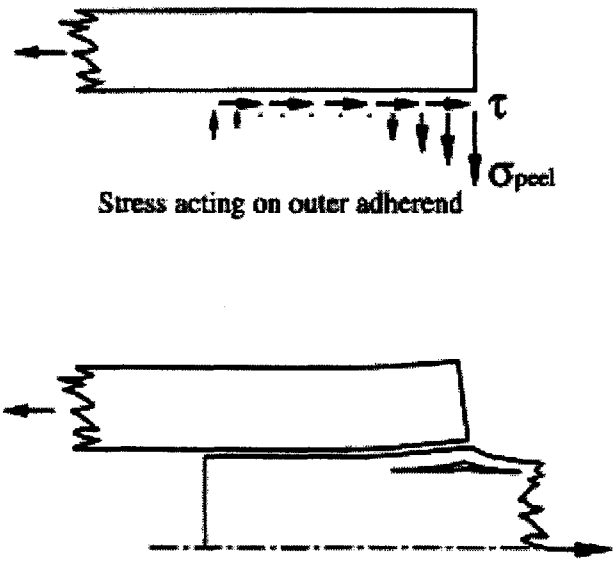

Figure 1: Peel and shear stresses on the end-zone of a lap patch repair joint [23].

Lap patches are usually applied in a stepped configuration, where the lengths of the repair layers increase as they are applied farther from the damaged area, or in a uniform configuration, where the lengths of the repair layers are the same. Both stepped and uniform lap repair configurations are shown in Figure 2.

2.3.2. Scarf Patches

This design usually requires the removal of material around the damaged area and the insertion of the repair material in its place. The fabrication of this design requires a thorough and work-intensive preparation in order to achieve the required scarf angle. Scarf repairs provide increased strength compared to any other repair configuration [23]. Hence, this repair scheme is broadly used for critical structural components. Another advantage of the scarf repair is that, unlike the external lap patch, it does not direct the load over and around the

damaged area, but it restores in the most efficient manner the properties of the damaged material by physically replacing it. In order to maintain the continuity in the region of the repair, scarf angles of approximately 1:30 (scarf thickness to length, ratio) are used for aerospace composite repairs. A representation of this repair scheme is illustrated in Figure 2.

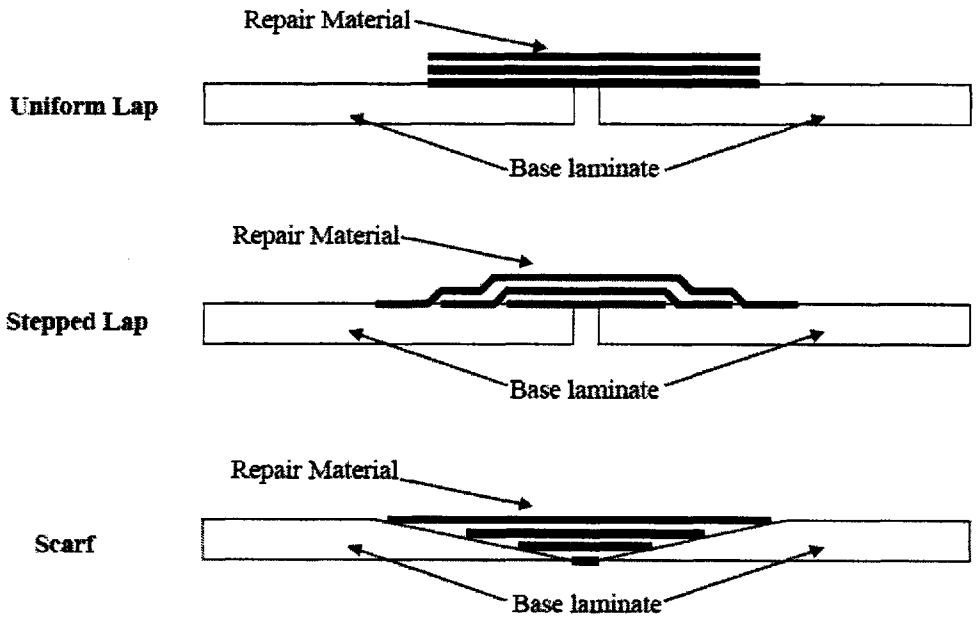

Figure 2: Characteristic schemes of scarf and lap repair.

2.3.3. Repair Efficiency of Lap and Scarf Configurations

The repair efficiency of various properties for lap and scarf repair configurations, found in the open literature, is illustrated in Table 3. It is clear that Table 3 cannot provide safe conclusions regarding the relative effectiveness of lap and scarf **joints** in repairs. Neither can it be used to extract useful conclusions about the repair efficiencies of combinations of materials, properties, thicknesses, and geometries other than the ones included in it. However, it indicates a number of potential research areas. For instance, there are only a small number of studies regarding the efficiency of bonded composite repairs for structures with thickness more than 3 mm. Moreover, among the researches that deal with thick substrates, none addresses reinforcements other than glass or compressive strength efficiency of the repair. The single study related to repaired glass vinyl ester substrates does not expand its examination of repair efficiency for properties beyond fatigue performance. Unfortunately, unawareness of

the maximum efficiency that each repair scheme yields for different combinations of materials, loadings, thicknesses, and geometries can lead to unreliable repair designs. Hence, it is recommended that Table 3 is utilized as an indicative basis of the open literature deficiencies for further research.

Table 3: Efficiencies % of lap and scarf repair schemes.

	Material: Parent (patch)	Tensile	Compressive	Flexural	Fatigue (flexural load)	Thickness mm	Geometry	Ref.
Lap	3 **Carbon** Epoxies (3 **Carbon** Epoxies, ***)	30-78 *				< 3	Double stepped (entire panel width)	[15]
	Carbon Epoxy (Same)		68-83			3	Double (round)	[23]
	Carbon Epoxy (Same)		63-85			3	Double (round)	[44]
	S2-Glass/Vinyl Ester (3 Repair Schemes Using S2-Glass/Vinyl Ester)				51-115 **	6.3	Double	[36]
Scarf	**Carbon** Epoxy (Same)	80-96				< 3	(round)	[18]
	Carbon Epoxy (Same)	81-93				< 3	(round)	[19]
	3 **Carbon** Epoxies (3 **Carbon** Epoxies, ***)	60-96 *				< 3	Full thickness (entire panel width)	[15]
	2 **Carbon** Epoxies (Same)	45-99				< 3	Full thickness joint	[17]
	3 **Carbon** Epoxies (Same)			34-95		< 3	Full thickness joint	[17]
	Glass Isophthalic Polyester (2 Glass Epoxies) (Glass Vinyl/Ester) (Same)	33-52 35-37 20		29-36 40-50 40-45		15	Full thickness **stepped** (entire panel width)	[9]
	Glass Isophthalic Polyester (Glass Epoxy) (Glass Vinyl/Ester)	71-72 55-59		57-69 61-64		30	Half thickness **stepped** (entire panel width)	[9]

* Values were geometrically extracted from graphical representations of experimental data (Figure 11, [15]).
** In addition to the double lap, an epoxy plug was used to fill the open-hole damaged panels.
*** Different from parent.

2.4. NDE for Marine Composite Repairs

From Figure 2 it becomes clear that there are significant geometric differences between the two repair schemes of lap and scarf repairs. These differences are strongly

correlated to different stress and strain distribution in the repaired region of the two configurations. It is not clear how the various physical and mechanical properties of repair schemes can influence the ability of NDE methods to detect defects on adhesively bonded repaired composites. Without such knowledge it seems that any post-repair evaluation of a structure is unreliable.

3. Parameters That Affect Bonded Repair Durability

Depending on the application (aerospace, marine, automobile, etc.) a composite structure may be subjected to a great diversity of loadings, and may operate under various combinations of environmental conditions. This variety of operational parameters creates an enormous field of patterns under which the composite structure could be damaged. Thus, the intrinsic complicated mechanical properties of composites can be affected in Modes that are significantly more complex than those usually developed in metallic structures. This complexity can be better confronted, and a composite repair better designed, when all the affecting parameters are considered and assessed. These parameters that can seriously affect, negatively or positively, the mechanical properties of a repaired structure and their influence on a composite repair are elaborated in Section 3. This section focuses on the qualitative fashion with which each parameter influences the adhesively bonded composite repair. In addition, a number of parameters with coupled effects are presented; however, there might be additional parameter interactions that are not outlined in this thesis.

3.1. Geometrical Configuration

There are certain geometrical characteristics of a repair that can severely influence its performance. Among them, adhesive thickness and spew fillet size; membrane and flexural stiffness, overlap length, scarf angle, shape, fiber orientation percentage, and tapering of the repair patch; in-plane bondline length; and out-of-plane curvature of the substrate; have been proven to significantly affect the quality of a repair and are presented below.

3.1.1. Adhesive Bondline Thickness

The effect of the adhesive thickness on the tensile strength of **thin** composite plates with a hole, repaired with a circular CFRP patch, has been approached with the use of finite element analysis (FEA) [46]. The study showed that there is a certain adhesive thickness value above or below which the ultimate failure stresse decreases, as illustrated in Figure 3.

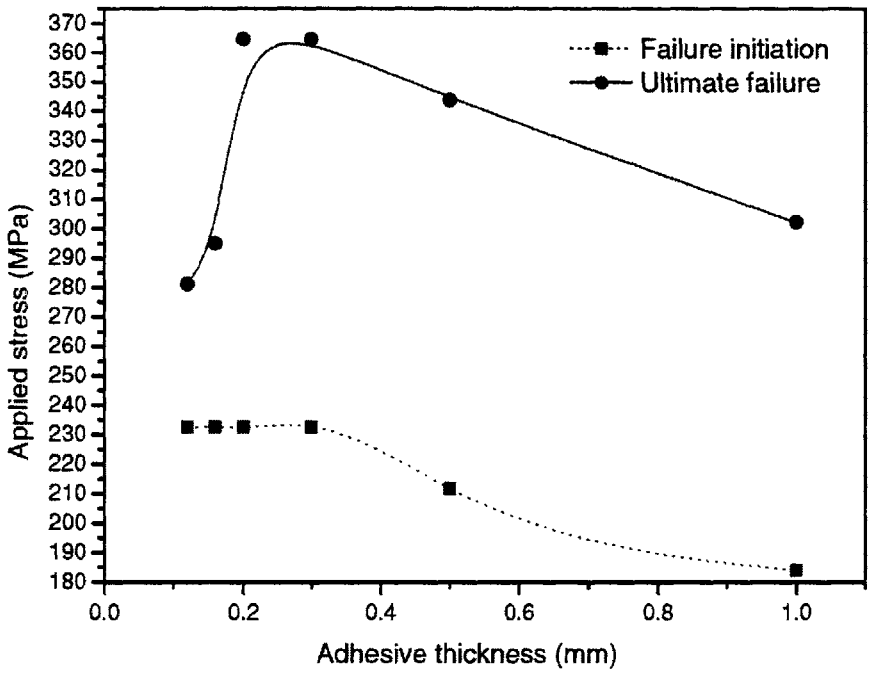

Figure 3: Variations of failure initiation and ultimate stress with adhesive thickness [46].

The existence of an optimum adhesive thickness has been further verified by experiments on Mode I fracture resistance of lap **joints** with metal substrates, as elaborated in paragraphs 3.1.1.2, 3.1.1.3, 3.1.1.4. Of course in the absence of experimental evidence it is not safe to deduce that such an optimal adhesive thickness value exists when considering the performance of a bonded composite repair in tensile, compressive, flexural, or fatigue loading. Nevertheless, it should be expected that the quality of bonded repairs, that essentially are bonded **joints**, is correlated to adhesive thickness. Moreover, attempting a parallelism with studies on bonded **joints**, this correlation could be anticipated to be dependent on adhesive ductility, bondline width, loading rate, and temperature, as detailed below.

3.1.1.1. Ductility

The durability of a repair can be affected by the adhesive bondline thickness and its uniformity throughout the patch and parent material interface. It should be noted that the magnitude of this influence is dependent on the adhesive ductility [7], [20]. Tests on Mode I fracture resistance of **glass/vinyl ester** bonded **joints**, using more than 500 data points for each of two adhesives with different ductility, confirmed this dependency [7]. Specifically, the

Mode I fracture toughness of a **joint** with rigid **epoxy** (Young's Modulus 1.8 GPa, strain to failure <5%) presented little or no dependency on the adhesive thickness. On the contrary, despite the higher variability in the data values (indicated by the higher standard deviation), **joints** bonded with a significantly more ductile polyurethane (Young's Modulus 50 MPa, strain to failure >50%) presented substantially higher fracture toughness for increased adhesive thickness.

Similar conclusions can be deduced from Figure 4, where clearly the polyurethane presents a significant difference (increased value) in fracture resistance when a thick bondline is applied, while such a difference does not seem to occur for the resistance of the brittle **epoxy**, [20].

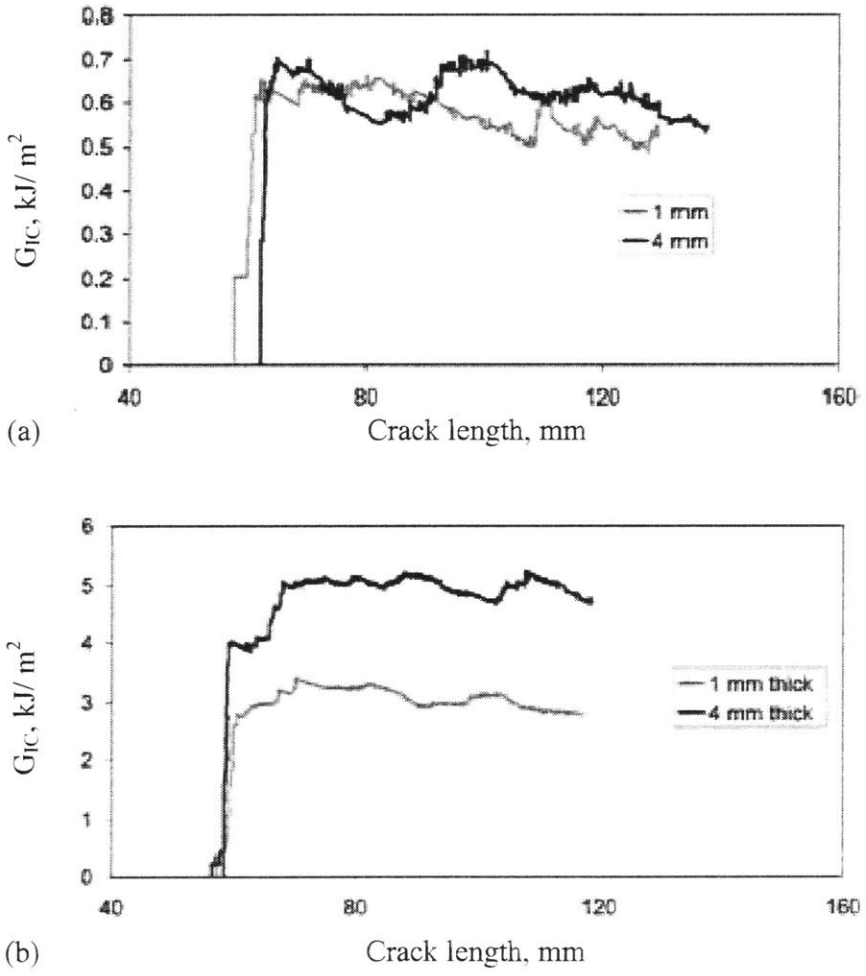

Figure 4: Mode I fracture toughness for adhesive between infused glass-reinforced vinyl ester substrates, influence of bondline thickness on G_{IC}. (a) Epoxy adhesive. (b) Polyurethane adhesive [20].

Although the data of Figure 4 correspond only to Mode I fracture toughness tests of bonded **glass/vinyl ester joints**, they indicate an unchallengeable correlation between bondline thickness and the strength of composite structures. As previously underlined, the magnitude of this correlation depends on the ductility of the adhesive[1].

Consequently, a repair, being essentially a **joint**, should be expected to be directly affected by the thickness and ductility of the adhesive that is used to bond the parent material and the patch. The usual practice in aerospace industry is to bond composites with adhesive layers of specific thickness, that are most commonly maintained on carrier fabrics—woven nylons or **carbon** fiber polyesters. Moreover the usually small dimensions of the required repairs allow the achievement of uniform bondline thicknesses, usually less than a millimeter, using an autoclave to cure the repaired part.

In marine applications the size and geometrical variability of the structures dictates the manual application of adhesives, often in the form of pastes. This latter technique in conjunction with the unfeasibility of autoclave curing, due to size limitations, increases the variability of the bondline thickness [7], [20]. Thus, it seems that special care should be taken for the achievement of uniform bondline thickness in marine composite repairs, in order to maximize Mode I fracture toughness, bearing in mind the dependency of toughness upon the ductility of the adhesive used. However, it should not be readily assumed that the ductility of the adhesive affects the influence of adhesive thickness on the fracture resistance of other Modes (fracture Mode II and Mode III) or the failure stress and strain in the same pattern as it affects Mode I. Moreover, the adhesive thickness and ductility-correlated effects could be somewhat or completely different in substrate composites, other than **glass/vinyl ester**.

It seems that the use of adhesives in composite repairs should follow experimental tests that would reveal the effect of adhesive thickness-ductility correlation on the mechanical properties of the repaired structure. An experimental study examining different adhesives and substrates is lacking in the marine-related open literature. The conclusions of Section 3.1.1.1 are illustrated qualitatively in Table 4.

[1] Especially, for the category of ductile adhesives it has been shown that the bondline thickness has a major influence on the formation of the adhesive plastic zone, whose characteristics are essential for the fracture toughness of any bonded **joint** [7], [25].

Table 4: Effect of adhesive thickness on the strength of glass/vinyl ester bonded repairs.

	Dependency On Adhesive Bondline Thickness	
Adhesive Ductility	Mode I Fracture Resistance	• Mode II-III-Mixed Fracture Resistance, • Ultimate Stress-Strain (Tensile-Compressive), • Fatigue.
Brittle	Insignificant	**
Ductile	Significant Increase *	**

* With increasing adhesive bondline thickness.

** Lacking in marine-related open literature; needs to be determined.

It should be noted that the Mode I fracture resistance dependency as indicated in Figure 4 might be an unrepresentative part of the actual correlation with adhesive thickness, since only two thicknesses, 1 mm and 4 mm, were used to study the variation in Mode I fracture resistance of two different adhesive ductilities. A higher number of thickness data points could reveal the complete trend with which ductility-thickness correlation affects Mode I fracture resistance, and maybe indicate the ideal ductility-thickness combination for fracture resistance maximization.

3.1.1.2. Width of Adhesive Bondline

Experimental tests with **metal** substrates revealed that the influence of thickness on the Mode I fracture toughness of lap **joints** is moreover dependent on the width of the adhesive bondline [25]. This dependency is illustrated in Figure 5, where values of the Mode I fracture energy are given for various adhesive thicknesses in five different **joint** bondline widths, maintaining a constant loading rate and temperature (loading rate and temperature are additional parameters that influence the Mode I fracture resistance of a bonded joint, as elaborated in paragraphs 3.1.1.3 and 3.1.1.4, respectively).

The presence of any of these geometrical constraints (bondline width increasing or adhesive thickness decreasing) increases the length of the plastically deformed region directly ahead of the crack tip, affecting the toughness of the adhesive. There is a specific value of bondline thickness, t_m, which corresponds to the maximum Mode I fracture resistance. For values below or above t_m the adhesive fracture energy is reduced (maintaining the loading rate, bondline width, and temperature).

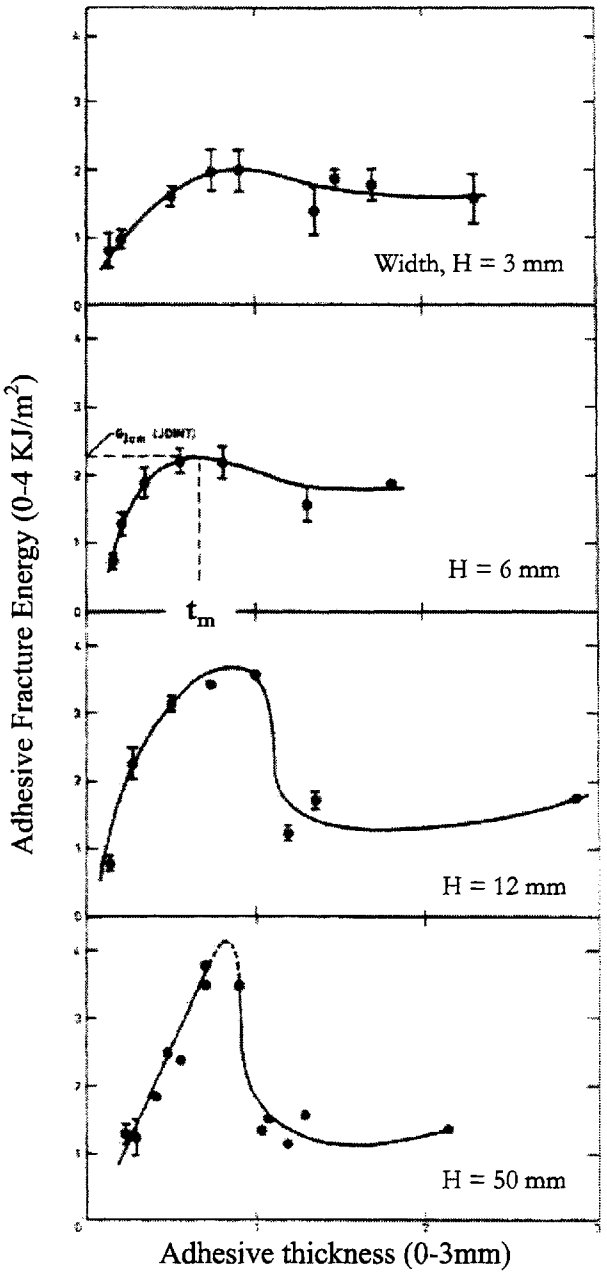

Figure 5: Adhesive fracture energy, G_{Ic}, as a function of bond thickness, t, for various joint widths, H. (Temperature: 20°C; loading rate: 1.67×10^{-5} m/s) [25].

In order to explain this behavior it should be considered that Mode I fracture toughness is provided by the ability of the material to dissipate the energy of the applied load by forming the plastic zone around the crack tip. When the adhesive thickness is equal to a certain value, t_m, it has been shown that the plastically deformed region ahead of the crack tip assumes its maximum volume. Hence, the maximum fracture energy is required to achieve

fracture. This value, t_m, is twice the radius of the plastic deformation zone that can be developed in the bulk adhesive. For adhesive thickness below t_m the plastic zone is restricted from being fully developed by the high-modulus substrates, and the fracture energy is reduced. On the other hand, for adhesive thickness above this critical value t_m the developed plastically deformed volume is again reduced, and this is attributed to the reduced presence of constraints (width increasing or thickness decreasing).

It would not be prudent to assume that the specifics of the above thickness-width dependency, derived from metal **joints**, are directly applicable to composite **joints** and repair patches or to other combinations of temperature and loading rates. Nor would it be safe, without experimental justification, to postulate that this dependency identically affects the resistance in other fracture Modes, the failure stress and strain, and fatigue life. However, there seems to be no reason inhibiting the assumption that the same thickness-width dependency exists, at least qualitatively, in adhesively bonded composite repairs. The open literature lacks an experimental or theoretical justification of such an assumption.

3.1.1.3. Rate of Loading

It is experimentally shown that the value of bondline thickness t_m depends on the rate of loading for metal **joints** [25]. The dependency of Mode I fracture resistance on the rate of loading, for a fixed temperature and bondline width, is illustrated in Figure 6. From this it becomes evident that the value of t_m, which is the peak of each curve, changes for different loading rates. Additionally, it is clear that the type of change (increasing or decreasing) in the Mode I fracture energy with increasing loading rate can be tremendously different for different bondline thicknesses. The effect of the loading rate on the fracture resistance of a metal **joint** for two different adhesive thicknesses is qualitatively illustrated in Figure 7. The magnitude of these rates, roughly 10^{-6} to 10^{-3} m/s, is small and consequently gives practically no information about the t_m behavior in impact loading.

Although the applicability of the above results cannot be effortlessly expanded for the case of adhesively bonded composite **joints** and repairs, a unique correlation of the adhesive thickness and the loading rate is indicated. It seems that the determination of the adhesive thickness, besides other considerations, should also be based on the expected loading rates that the post-repair structure is expected to suffer.

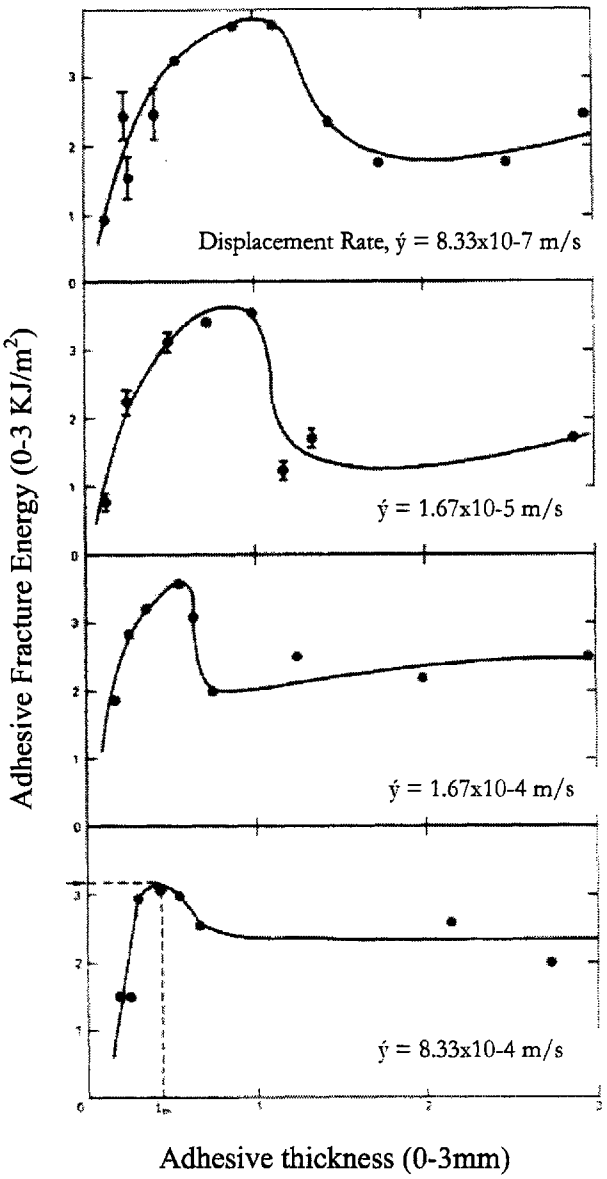

Figure 6: Adhesive fracture energy, G_{Ic}, as a function of bond thickness, t, for various constant rates of displacement, ẏ. (Temperature: 20°C; joint width: 12 mm) [25].

The consideration of the expected loading rates should also be followed in the case of marine structures. Unlike the small loading rates, illustrated at Figure 6, a vessel will more probably be exposed to higher rates. For instance the rates of cyclical loadings, that are induced from hogging and sagging conditions; heave, pitch, roll and maneuvering accelerations; slamming, whipping and springing of the hull; and gunshot pounding, affect different parts of a ship's structure at various magnitudes and periodicities. The expected

loads and their corresponding rates could be modeled based on known characteristics of the ship (such as seakeeping performance, wave spectra of the regions where the ship operates, among other parameters related to the operational profile of the vessel).

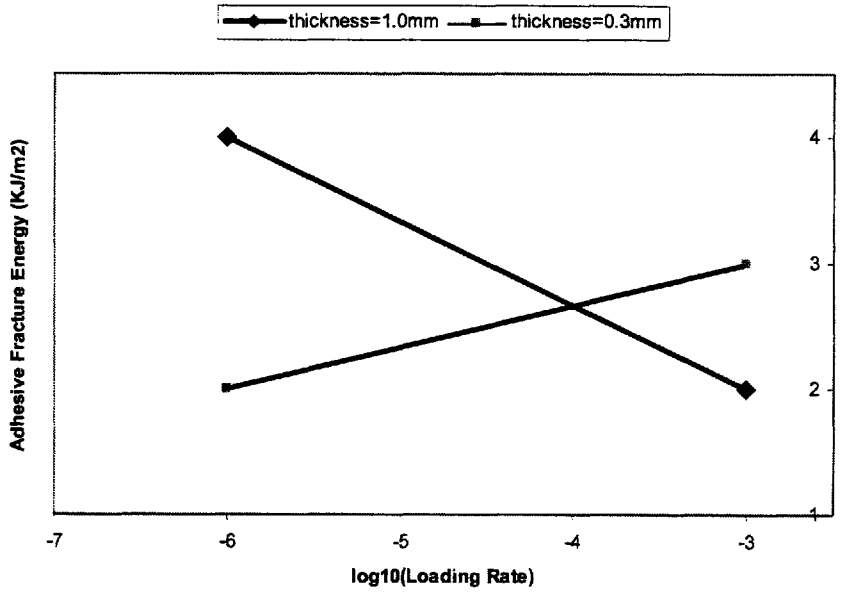

Figure 7: Dependency of Mode I fracture resistance on loading rate and adhesive thickness (constructed based on [25]).

Unfortunately, the open literature lacks an experimental base that addresses the dependencies of fracture resistance (of any Mode), failure stress and strain, and fatigue life on loading rates for adhesively bonded composite repairs (for various temperatures and bondline areas). Taking into consideration the numerous dynamic loads and varied conditions that marine structures are expected to withstand, it seems that the lack of such knowledge is a potential path to sub-optimal composite repairs.

3.1.1.4. Operating Temperature

Another parameter that influences the effect of adhesive bondline thickness is the temperature. As far as Mode I fracture resistance is concerned, increasing temperatures yield increased values of t_m, for fixed values of bondline width and rate of loading, as can be seen in Figure 8 [25].

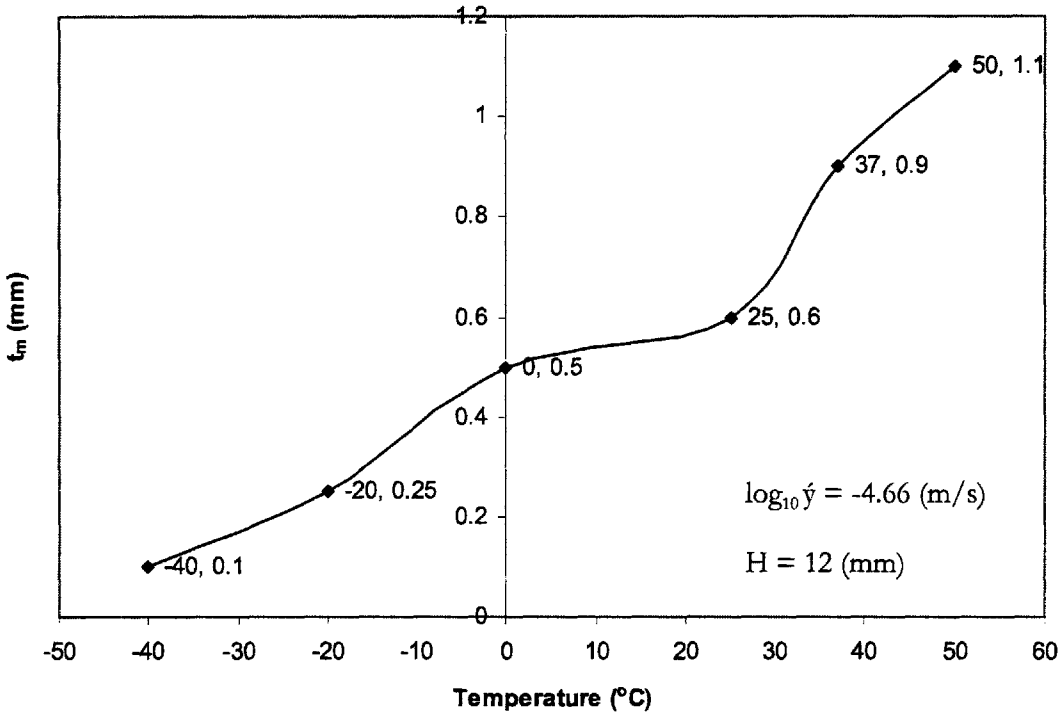

Figure 8: Effect of temperature on t_m (adhesive thickness yielding maximum Mode I fracture resistance). Constructed based on [25].

Again, it would not be wise to postulate that similar correlations between temperature and the effect of the adhesive thickness on toughness exist in other fracture Modes, failure stress and strain (tensile or compressive), and fatigue life. Nor would it be logical to assume that the trend of Figure 8 would hold, qualitatively or quantitatively, for other combinations of loading rate and bonding width. However, it appears that temperature is another parameter that could prove to be significantly influential on the selection of the optimum adhesive bondline thickness, especially in diverse environments such as those in which marine repairs are exposed. A venture to explore the effect of adhesive thickness on the mechanical properties of bonded repairs for different combinations of temperature, loading rate, and bondline area is missing from the marine-related open literature.

3.1.1.5. Considerations Concerning Adhesive Bondline Thickness

Summarizing the discussion of paragraph 3.1.1, it can be stated that the influence of bondline thickness on the performance of a composite repair is expected to be a complex function of the following parameters:

1. **ductility of the adhesive**[1],
2. **adhesive bondline width**,
3. **loading rate**,
4. **temperature**.

As far as composite repairs to marine structures are concerned, there are a lot of patch schemes and geometries (e.g. scarf, stepped lap, uniform lap, oval, circular etc.), and sizes that can be applied, depending on the magnitude and type of the damage, the accessibility of the damaged structure, etc.. It is expected that the effect of the adhesive thickness on the properties of the repaired structure will be influenced by the size of the adhesive layer in the other two dimensions, i.e. width and length (or radius for circular patches) of the overlap. Moreover, it is expected that this influence will vary with respect to the loading rate and temperature—two parameters that cover long ranges of possible values in the marine environment. The qualitative and quantitative specifics of the fashion in which the above parameters are correlated and interact should not be expected to resemble the trends presented in Section 3.1.1; valuable results could only be extracted from carefully designed experiments that would reveal the underlying relations of the pertinent parameters. Hence, the data of paragraph 3.1.1 should be thought of as a proposed base for research and experimentation and not as a pool of readily applicable knowledge for adhesively bonded composite repairs in marine applications.

3.1.2. Tapering of Adhesive at End of Overlap

The high-shear strains that develop in the plastic zones, at the ends of bonded composite lap **joint** overlaps, can be significantly reduced with a local increase of bondline thickness at the ends of the overlap [23], [43]. The distribution of adhesive shear strains at the end of the **joint** overlap, under tensile loading, for various adhesive thicknesses is illustrated in Figure 9.

[1] It should be taken into consideration that ductility is dependent on the temperature. Moreover, the ductility rate of change, with temperature, differs between materials as indicated in paragraph 3.3.2.

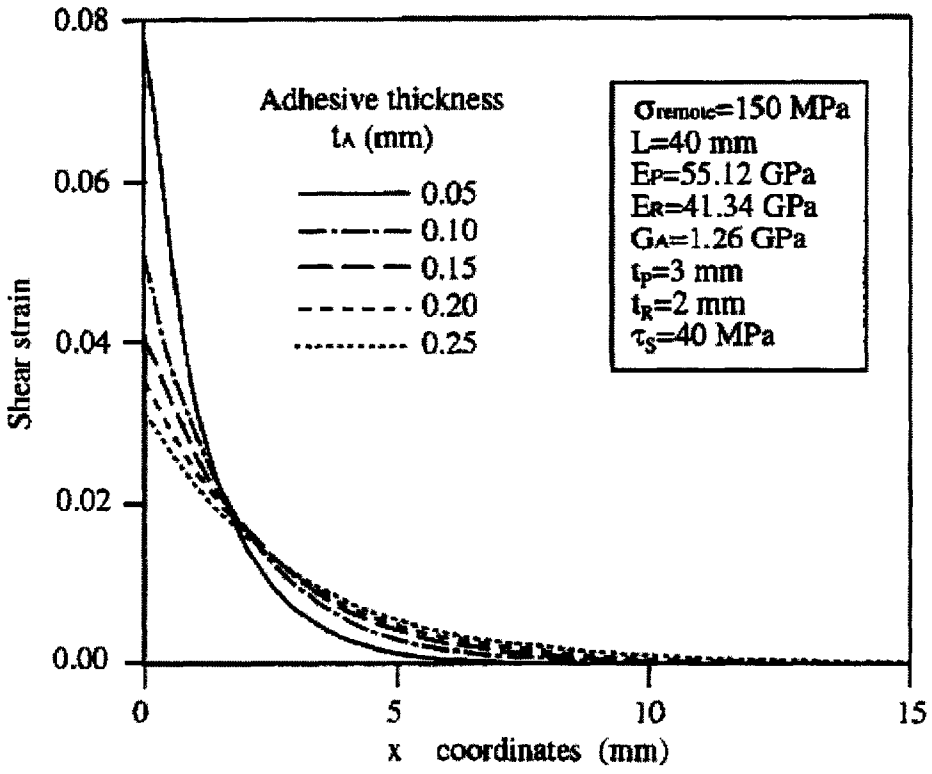

Figure 9: Distribution of adhesive shear strains at the end of the overlap for various adhesive thicknesses [23].

The "x" coordinate measures the distance of a point in the overlap from the overlap-end (x=0 mm). The subscripts "P", "R" and "A" indicate that the property refers to the parent, repair and adhesive material respectively.

Moreover, it has been determined that the maximum peel stress suffered by the adhesive and neighboring adherend of a double lap bonded **joint** depends on the thickness of the patch and the adhesive, besides depending on shear stress [23]. Specifically, the peel stress decreases for decreasing values of the patch thickness and increasing values of the adhesive thickness. In the regions adjacent to the end of the overlaps, where the shear stress gets its maximum values, the peel stress assumes peak values as well. Thus, exploiting the dependency of peel stress on patch and adhesive thickness, it is recommended that gradually thinner patches and thicker adhesive bondlines should be used as approaching the ends of the double lap joint overlaps. This technique, referred to as tapering, is illustrated on Figure 10. It should be noted that in Figure 10 the different taper designs are sorted with shear and peel stress—that is (d) has lower shear and peel stresses than (a).

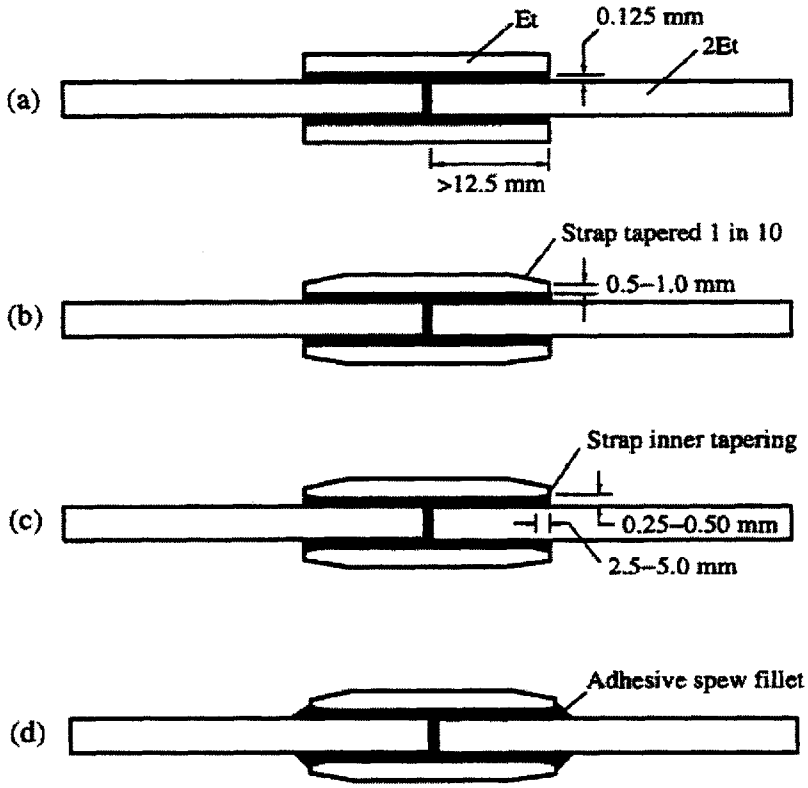

Figure 10: Various tapering designs for a double lap joint [23].

Furthermore, tapering of the patch end on double lap **joints** has been found to significantly decrease the high adhesive shear strains developed at the bondline ends [28], [29].

However, it is not clear whether and to what extent tapering can be applicable in marine repairs. In such applications the thickness of the repair adhesive layer is significantly larger than repair designs of the aerospace industry. The thicker the adhesive layer is, the more porous it tends to be and especially in the marine realm the adhesive thickness of a repair is expected to be fabricated with great uniformity tolerances, due to limitations imposed by size. Hence, before praising tapering, studies should be conducted in order to determine its utility. It seems that among the related parameters at least angle and length of the taper should be examined to determine their optimum combination in each of the tapering configurations (inner, outer, inner-outer tapering), based on a number of considerations. Table 5 qualitatively presents the impact of each configuration on a number of proposed considerations.

Table 5: Proposed considerations in the assessment of tapering configurations for marine repairs.

	Considerations				
	Advantage		Disadvantage		
Configuration	Reduction of peel and shear stresses	Prolongation of fatigue life	Cost added on repair	Increased porosity of adhesive	Degradation of patch membrane stiffness***
Inner** patch taper	2	*	1	1	1
Outer** patch taper	1	*	1	N/A	1
Inner-outer patch taper	3	*	2	1	2

Key: Greater values indicate stronger impact of a configuration on a consideration.
* Lacking in marine-related open literature; needs to be determined.
** A taper is called "inner" when the shortest side of the patch is closer to the parent material. Otherwise it is called "outer".
*** Membrane stiffness is defined in paragraph 3.1.4.

A fine patch tip at the end of the bondline overlap can theoretically alleviate the concern about high shear and peel stresses near the end of the overlap. However, the finer the patch tip is, the costlier is its fabrication and with patch ends correspondingly more prone to fatigue failure. Additionally, the membrane stiffness imbalance between the patch and the parent material could lead to deterioration of the ultimate stress of the repair, as is elaborated in paragraph 3.1.4.

As stated above, the findings from **thin** bonded **joints** should not be applicable, without justification, in **thick** bonded composite repairs of marine applications. Nevertheless, the beneficial properties of tapering are confirmed in repairs of **thick** aluminum ship decks with CFRP patches [43]. In this specific composite repair application, it is experimentally proven that tapering the adhesive is more effective than tapering the patch. Thus, in the CFRP patch lay-up the shorter lamina of the taper should contact the parent metallic plate (inner tapering).

3.1.3. Adhesive Spew Fillet

The use of a spew fillet at the end of the overlap is considered as a design feature that reduces the increased peel and shear stresses in the region of the overlap end in bonded **joints** [4], [7], [1, ch.1], [23]. However, it appears that the beneficial properties of a spew fillet are related to adhesive formations at the end of the overlap with specific geometric characteristics and not to arbitrarily formed fillets that result from the squeezed-out excessive adhesive (uncontrolled spew fillet).

Experiments on **thin glass vinyl ester** joggle lap **joints**, as illustrated in Figure 11, showed that the tensile failure loads for **joints** with and without a spew fillet were improved by 54% and 46%, respectively, relative to specimens having an uncontrolled spew fillet [56].

Figure 11: Joggle lap joint.

The results of those experiments show that squeezed-out adhesive can be harmful for the bonded **joint** properties if not removed. On the other hand if the excessive adhesive is formed in a spew fillet (or adhesive is added at the end of the overlap after the **joint** fabrication to form the spew fillet) with specific geometric characteristics, it can improve the **joint** tensile strength. It was also determined that the influence of the spew fillet on the tensile strength of the **joint** depended on both the ductility of the adhesive and the stiffness of the adherends; the increase of the **joint** tensile strength was the highest with the most ductile adhesive and least stiff adherend, as illustrated in Table 6.

Table 6: Percentage increase of joggle lap joint tensile failure load with spew fillet, compared to that without spew fillet [56].

	More stiff adherend*	Less stiff adherend**
Tough adhesive	5.22	9.21
Ductile adhesive	2.16	15.43

* [0/90] lay-up was used with respect to the load orientation.
** [±45] lay-up was used with respect to the load orientation.

In addition, tensile loading tests of **thin** aluminum/**epoxy** single lap **joints** determined that a 25% increase of the tensile strength is introduced with the use of an adhesive spew fillet [57]. When the spew fillet is combined with rounding of the edge of the adherends the increase of the **joint** tensile strength surpasses 50%. The geometric specifics of the specimens used are illustrated in Figure 12 (it is not specified why the fillet angle is 45° or why the adherend edge is tapered with a specific radius).

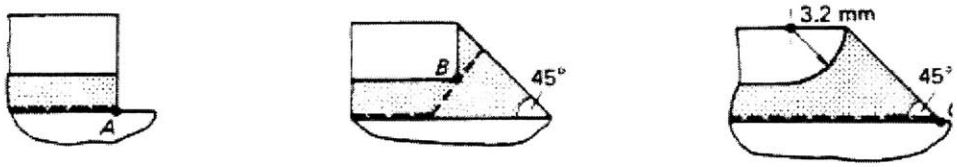

A B C

Figure 12: Aluminum/epoxy single lap **joints**: a) no spew fillet; b) with spew fillet; c) with spew fillet and radiused adherend [57].

However, experiments using CFRP (and steel) patches to reinforce **thick** aluminum plates of a type 21 frigate superstructure led to disappointing conclusions regarding the beneficial properties of using a spew fillet [43]. Specifically, for the CFRP patches the introduction of an **epoxy** spew fillet over the region of the end of the patches did not yield a significant improvement in fatigue tensile loading. Further, in the case of the steel patch the specimens with the spew fillet yielded significantly lower static strength and fatigue life[1]. The discrepant findings of the adhesive spew fillet effect on different applications are illustrated in Table 7.

The aforementioned failure to improve the repair mechanical properties should not be perceived as a generalized inability of spew fillets to benefit adhesively bonded repairs. Rather it seems that unless the geometric specifics of the adhesive spew fillet are determined for the various repair designs, it is not safe to apply it on bonded repairs. Furthermore, it is not clear whether a spew fillet design that is beneficial for a certain mechanical property will improve or deteriorate other properties and to what extent.

[1] In both CFRP and steel cases the patch adhesive cracked at the point of the maximum adhesive thickness of the fillet.

Table 7: Repair efficiency difference, for configurations with and without spew fillet.

Repair configuration, Material	Tensile Loading	Compressive Loading	Fatigue (Tensile Loading)	Thickness mm	Ref.
Joggle Lap **Joints**, Glass Vinyl Ester	17% increase	*	*	< 3	[56]
Single Lap **Joints**, Aluminum Epoxy	25% increase	*	*	< 3	[57]
Single Lap Patches on Aluminum Substrate, CFRP (Steel)	* (decrease)	*	Insignificant (decrease)	> 3	[43]

* Not evaluated

An organized study that determines the geometric specifics of an optimal spew fillet for various adhesive and substrate materials, and illuminates the spew fillet effect on the different mechanical properties of adhesively bonded composite repairs, is absent from the marine-related open literature.

3.1.4. Membrane Stiffness of Repair Patch

Compressive tests on double lap **joints**, conducted in order to identify critical parameters for the improvement of external patch repair efficiency, revealed the importance of the patch geometric characteristics for the repair quality [1]. Experiments proved that there is an ideal value of the membrane stiffness[1] ratio (the ratio of patch to parent material membrane stiffness) corresponding to the maximum failure stress. Both soft and tough[2] patches (with membrane stiffnesses less than and greater than the ideal value, respectively) failed at lower stress values than that corresponding to the ideal membrane stiffness. The determination of the optimum patch membrane stiffness, for a double lap composite **joint,** is illustrated in Figure 13. It should be noted that the factor of 2, in the ratio $2E_Rt_R$ / (E_Pt_P), is introduced to account for the thickness of both patches of the double lap **joint**.

The effect of the membrane stiffness ratio on the tensile strength of **thin** open-hole CFRP plates, repaired with double-side CFRP circular lap patches, was further verified with a FEA method [46]. Specifically, it was indicated that the thickness ratio (patch to parent material thickness) presented a specific value above or below which both the initiation and

[1] Membrane stiffness of a plate is the product of its thickness and stiffness.

[2] It was determined that tough patches (high thickness) can cause premature failure of a repaired structure, by increasing the stress concentrations in the region of the repair.

ultimate failure tensile stress decreased. Using the properties[1] of the prepreg[2] which was used for the fabrication of both parent plate and the repair patch, the tensile stiffnesses of both laminates can be calculated (the corresponding calculations are included in Appendix C— $4.214*10^{10}$ Pa and $6.232*10^{10}$ Pa for the patch and parent plate, respectively). The value of patch to parent plate thickness ratio yielding the maximum tensile failure load lies between 0.6 and 0.7, as indicated in Figure 14.

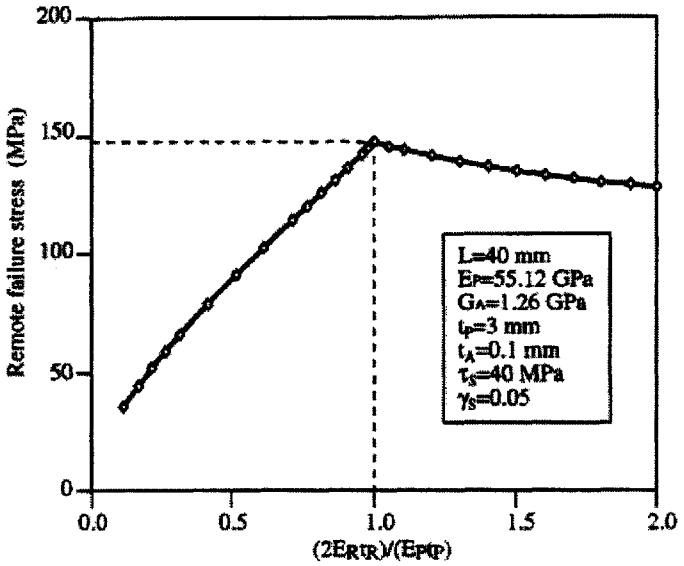

Figure 13: Determination of the optimum patch membrane stiffness of a double lap joint [23].

The subscripts "P", "R" and "A" indicate that the property refers to the parent, repair and adhesive material respectively.

Thus, the ratio of patch to parent material membrane stiffness ($2E_Rt_R$ / E_Pt_P) yielding the maximum ultimate tensile strength is between 0.811 and 0.947, closely approaching the value of 1.0 that has been experimentally determined as the ideal for double lap **joints**.

In addition, the membrane stiffness imbalance (high differences between parent and patch membrane stiffness) of repair and parent material could be correlated to the deterioration of the quality of adhesively bonded composite scarf repairs. Although a scarf **joint** is an oversimplification of the scarf repair, some parallelism of their properties could be

[1] The parent lay-up is [(0/90/±45/90/0)2]s and the repair patch is made from ±45 plies.

[2] Intermediate sheet material of reinforcing fibers impregnated with a polymer matrix resin system. Matrices are typically thermosetting resins in a partially cured (B-staged) form, though thermoplastic resins are also employed.

exploited. It has been determined that in scarf **joints**[1] membrane stiffness imbalance among different adherends can provoke high unevenness in the shear stresses throughout the bondline, with higher values being developed at the end of the repair overlaps [1, ch.6]. Marine field repairs are often applied under vacuum in the absence of an autoclave and often use different repair layers and resins than the original structure. These unavoidable practices can introduce high stiffness and thickness variability in the adhesive and repair patch, hence varying the membrane stiffness ratio of the parent and repair material. Consequently, it is possible that field scarf repairs are prone to high shear stress unevenness, which is directly linked to failure susceptibility.

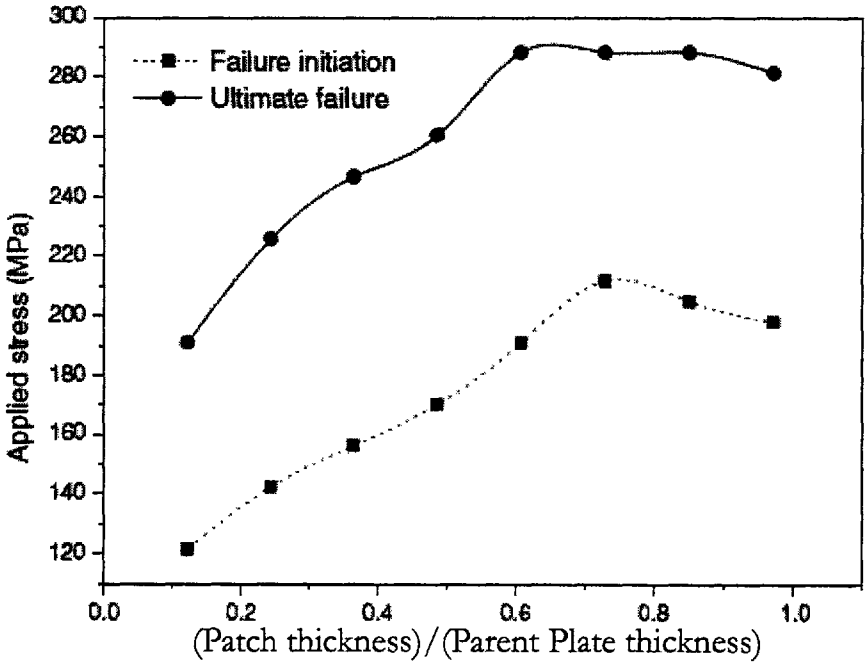

Figure 14: Failure initiation and ultimate tensile stress for various CFRP patch-parent thickness ratios [46].

As indicated by the nomenclature of Figure 13, the dimensions of the examined **joint** (overlap length, thickness) are not representative of the usual marine industry repair magnitudes. Thus, it would not be safe to assume that the strength of a repair **joint**, with significantly larger scantlings, would maintain the same dependency on membrane stiffness.

[1] In scarf **joints** the thickness of the un-scarfed (constant thickness) part of the adherends is considered in the determination of the membrane stiffness ratio.

Neither would it be justified to postulate that the strength of any repaired structure depends on the membrane stiffness of the patch in an identical qualitative or quantitative fashion as the one presented, in paragraph 3.1.4.. There are indications, however that membrane stiffness ratio affects the properties of composite repairs in almost the same fashion as in bonded composite **joints**. Using a FEA package to calculate the stresses developed (in 3 dimensions) in the patch, parent laminate and adhesive of a repaired plate, under compressive loading, it was determined that the optimum membrane stiffness ratio was in accordance with that corresponding to a double **joint** [23]. Specifically for a double-side lap patch repair of an open-hole plate, with identical stiffness for parent and repair material, it was determined that the optimum patch thickness was half the thickness of the parent material, corresponding to membrane stiffness ratio of 1. Furthermore, it is interesting that the same value of membrane stiffness ratio (1.0) has been found to be ideal in the case of bonded composite repairs of **thick** metallic substrates [48]. It was determined that when the membrane stiffness of a single-side unidirectional [1] boron/**epoxy** patch has the same membrane stiffness as the aluminum panel (substrate), then the repair is the most effective under tensile loading.

It is obvious that the patch and the parent structure properties (thickness and stiffness) are correlated, at least for the cases of tensile and compressive loading. Yet, the effect of membrane stiffness ratio is not examined for bending loading and fatigue in the open literature. Hence, the influence of this ratio on the quality of bonded composite repairs should further be explored if an optimization of the repair design is sought (e.g. reduced additional weight, increased durability). Unfortunately, the marine-related open literature completely lacks an endeavor that would clarify the influence of the membrane stiffness ratio on the mechanical properties of adhesively bonded composite repairs on **thick** composite substrates for various materials, repair schemes and loading conditions.

3.1.5. Overlap Length of Repair Patch

Examining, with an analytical non-linear model, the double-side lap **joint**, as an idealized case of the double-side lap patch repair, yielded a valuable insight regarding the optimum overlap length [23]. When considering such a **joint** under compressive loading, it is logical to assume that the adhesive layer is mainly subjected to shear stress in the plane

[1] The lay up was $[0]_n$, where n is the number of layers.

parallel to the bondline. Hence, meaningful conclusions can be extracted from the shear stress distribution in the adhesive. The variation of the stress distribution for different overlap lengths is illustrated in Figure 15. In this figure, the plateau values of the shear stress correspond to the plastically deformed end-zones of the adhesive, while the troughs indicate the elastic regions of the adhesive. Clearly in the case of short overlaps the elastic region is more heavily loaded than in the case of longer overlaps. The plastically deformed end-zones are completely formed when the overlap length reaches a certain value, above which these zones essentially undertake the entire load. Hence, there is theoretically no reason to design an overlap length beyond this value, as is indicated in Figure 16.

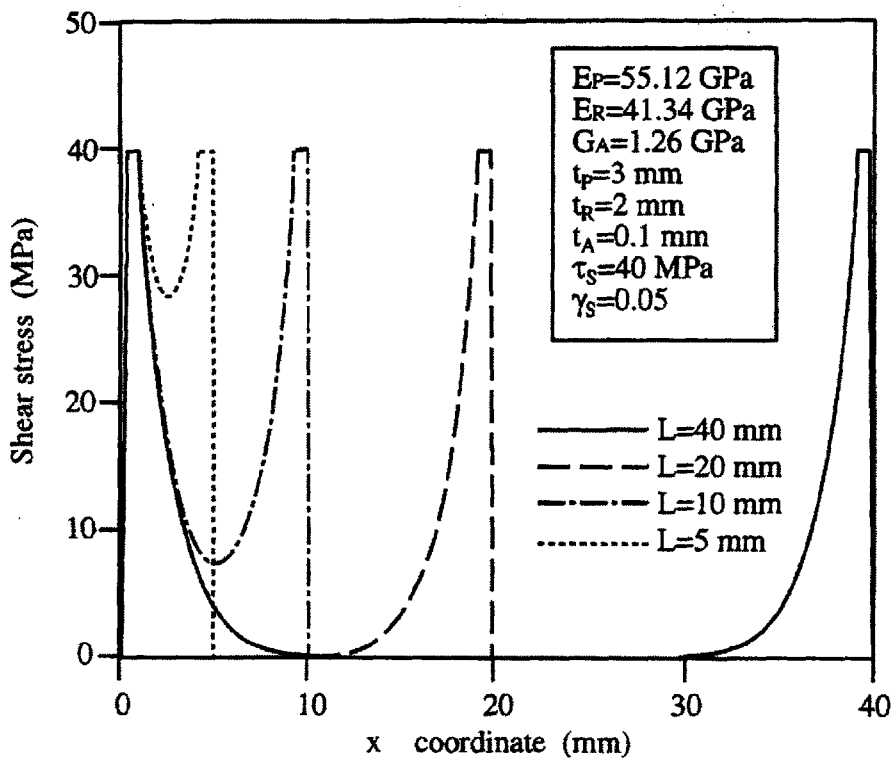

Figure 15: Adhesive shear stress distributions for various double lap joint overlap lengths [23].

It should be noted that for constant adhesive and adherend thickness the length of the plastic shear zone in single lap **joints** was found to increase with increasing stiffness of the

adherend[1] [4]. Thus, it should be taken into account that the ideal overlap length is a function of the adherend stiffness.

Experimental tests using **glass** fiber **vinyl/ester** joggle lap and L-section **joints** verified that the applied tensile load is supported essentially by the ends of the bonded overlap [56]. Specifically, a Teflon layer was introduced in the middle of the overlap length of both **joint** configurations to simulate a disbond defect. It was determined that above a certain value the increase of the **joint** bonded surface had insignificant influence on the **joint** tensile strength. Thus, it seems that special attention should be given to any parameter that can affect the load-carrying capability of the overlap ends, such as the adhesive spew fillet (elaborated in paragraph 3.1.3). The value of protecting the overlap ends from exposure to environmental effects (solar radiation, heat, moisture, chlorine ions), using sealants or covering the repair with insulating patches, is apparent.

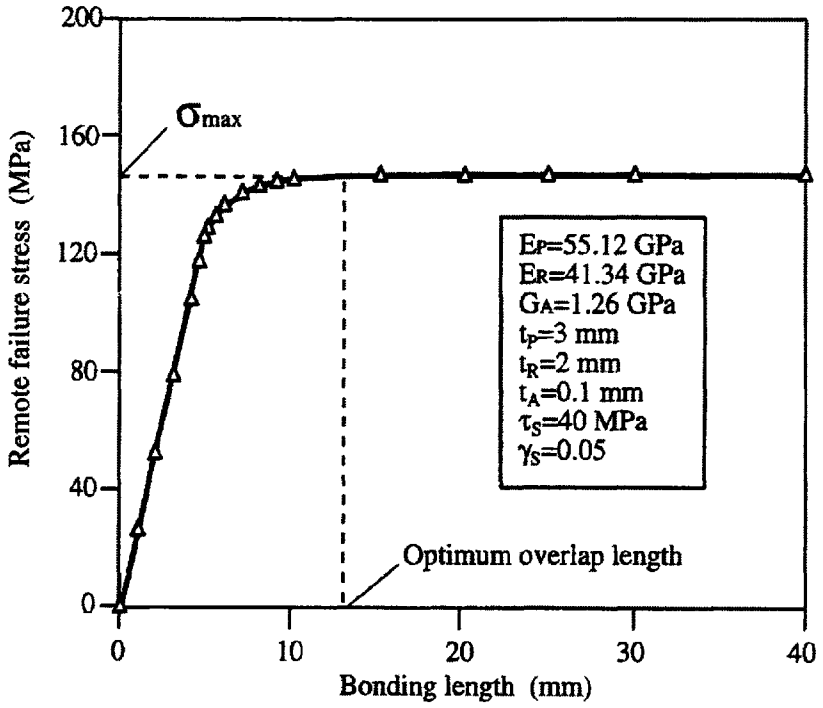

Figure 16: Determination of the optimum overlap length for a double lap joint, under ultimate load. [23].

[1] Steel, aluminum, titanium, **carbon,** and **glass** adherends were examined.

The existence of an optimal overlap length was further verified with tests on stepped and uniform lap repaired composite specimens [15]. Although, the optimal length is not the same in each of the above schemes, and varies depending on the number of the repair layers, it is present in all cases and defined as the length of the overlap above which there is no gain in the strength of the repair. Additionally, the existence of an optimum patch size for the repair of **thin** open-hole composite CFRP plates[1] is verified with a FEA method [46]. The effect of the patch diameter in the failure initiation and ultimate tensile stress is illustrated in Figure 17. According to this figure it would clearly not be cost effective to use a patch diameter larger than the value corresponding to the plateau of the ultimate failure curve, namely 70 mm. This value, of course, reflects the optimal size only for the tensile strength of a specific **thin** composite lay-up.

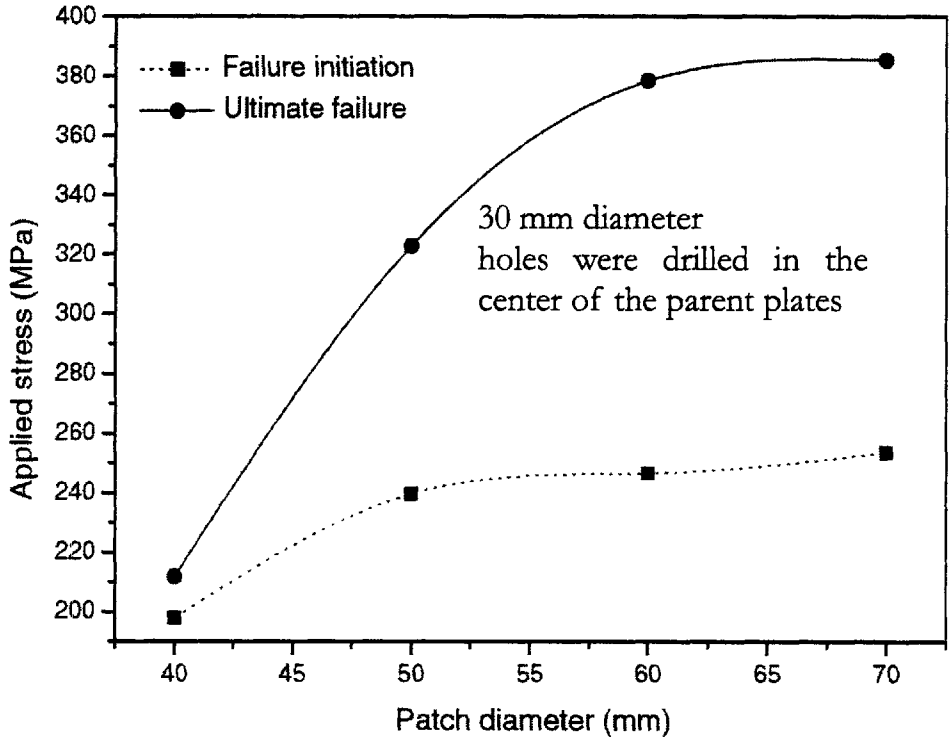

Figure 17: Effect of repair patch size on failure initiation and ultimate tensile stress [46].

[1] The parent plate and patch lay-ups were ([(0/90/±45/90/0)$_2$]s) and [0$_2$/±45/90] respectively, both fabricated with the same prepreg.

The issue of cost effectiveness gains more gravity in the field of marine repairs where the sizes of a patch could reach several square meters (5 m^2 patches were used for repairs on board a RAN FFG-7 frigate [40]). Unfortunately, all the studies related to optimum overlap size originate from **joints** and repairs of **thin** aerospace composite structures and are limited to cases of tensile and compressive loadings. For marine structures with higher thickness, different composite materials, and variety of loading conditions, it is clear that the knowledge gained from aerospace industry is inadequate to guaranty reliable repairs. Unfortunately, the marine open literature lacks a study that would determine optimum repair patches for various materials and loading conditions.

3.1.6. Scarf Angle

The effect of the scarf angle is a trivial consideration in the assessments of scarf patch repairs. There is general concurrence in aerospace composite repair-related literature that smaller scarf angles produce stronger repairs [1], [11], [15]. However, smaller scarf angles have a number of disadvantages. The most severe among them are the removal of more undamaged material volume, which deteriorates the strength of the repaired laminate, and the increased fabrication cost.

Especially for naval structures the scarf repair configuration seems ideal for a number of reasons. Specifically, a significant part of composites used for navy vessels consists of panels with thicknesses on the order of several centimeters. Such **thick** structural composites would require an analogously **thick** external patch repair, if the scarf technique was not utilized. A **thick** external patch would probably cause unacceptably high peel and shear stresses, besides increasing the electromagnetic signature (radar cross section), exposing more surface of the repair patch to severe corrosion conditions and reducing the aesthetics of the repair. Thus, determining the optimum scarf angle for marine repairs is crucial for the development of effective repair procedures in this field.

The optimization of repair scarf angle should not be based solely on results obtained from tensile experiments on **thin** scarf **joints**. Specifically, using FEA to model a scarf patch-repaired laminate under tensile loading (a 3-dimensional problem) yielded an optimum scarf angle (7°) that was significantly larger than the one obtained with the simplified study (4°) of a repaired scarf **joint** (a two-dimensional problem) [1]. Hence, unjustified correlations with

scarf **joints** and lack of experimental verifications could lead to sub-optimal scarf repair designs. The open literature needs enrichment with studies that investigate the ideal repair scarf angle for **thick** structures under various loadings for the variety of composite materials that are used for naval composite constructions. Since dynamic loads are characteristic of the marine environment, fatigue should be addressed as well.

3.1.7. Patch Fiber Orientation

Frequently, the repair material is different than that of the parent composite. Such a difference could arise from the use of dissimilar resins, fibers, or even fiber orientation among the repair and parent material. Fiber orientation, in particular, can significantly affect the properties of a repair, as it directly influences in-plane Poisson's ratios.

Mismatches of in-plane Poisson's ratios can be induced depending on ply orientation [4]. These mismatches can lead to the development of high interlaminar stresses, one of the main failure mechanisms of composite materials. In order to avoid increased interlaminar stresses it was suggested that the fiber orientation differences between adjacent plies should be maintained to a minimum [4]. For instance the transition from a ply of 0° fiber orientation to a ply of 90° should be made with one or more 45° intermediate plies. Nevertheless, the suggestion does not answer the question of what combination of fiber orientation percentage and lay-up sequence should ideally be chosen for the repair of each specific parent material lay-up, repair scheme, and loading condition.

As far as lap patch repairs of **thin** composite structures are concerned, there are a number of studies addressing the effect of fiber orientation on repair quality. Using FEA, Gunnion (2006) determined that patch fiber orientation has little influence on the tensile strength of **thin** CFRP open-hole plates repaired with a circular CFRP lap patch [46]. The small variation in failure initiation and ultimate failure stresses for various patch lay-up cases examined are illustrated in Figure 18.

Liu (2006) utilized a FEA method to investigate the effect of fiber orientation mismatching, with constant fiber orientation percentage, on the properties of **thin** CFRP bonded scarf **joints** [45]. The study indicated low sensitivity of shear and peel stresses to mismatched adherend lay-ups. The findings of both Gunnion (2006) and Liu (2006) appear to

be in agreement with classic laminate theory [50], [51][1]. According to this theory the percentage of fibers in each orientation determines the mechanical properties of a laminate, and hence of the repair. Thus, as long as the orientation percentages are the same, variations in the lay-up sequence should not induce changes in the properties of laminates.

Case	Patch lay-up
1	[0/45/-45/45/90]
2	[45/0/±45/90]
3	[±45/0/45/90]
4	[90/45/-45/45/0]
5	[45/90/±45/0]
6	[±45/90/45/0]

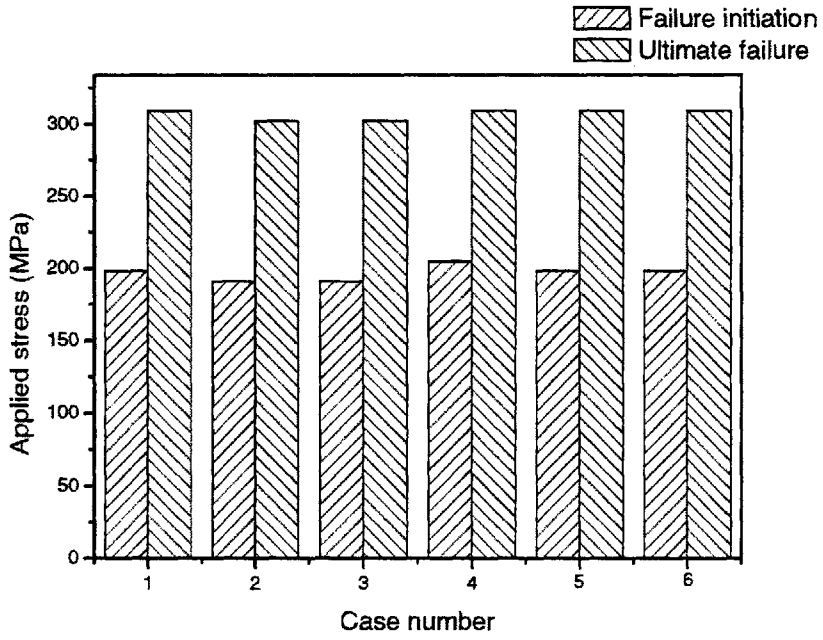

Figure 18: Influence of various lay-up orientations on tensile strength of lap patch repairs [46].

The numerical conclusions of the above studies were not followed by experimental justification. Nevertheless, different experimental studies confirmed that variations in the fiber orientation percentage can alter the properties of a bonded composite repair. In particular, **thin** substrates of **glass/vinyl ester** (of continuous swirl mat), damaged by central impact and bending, were repaired with **glass** fabrics of plain weave (fill and warp fibers were of 0° and 90° orientation, respectively) using double lap patches with several orientation angles[2] [35]. Due to the small number of specimens (three per lay-up), the experimental

[1] Cole, (1999), provides the properties of tensile strength, tensile modulus, shear strength, shear modulus and Poisson's ratio for carbon, aramid, glass and hybrid preimpregnated lay-ups with epoxy resins for various percentages of fibers at 0°, ±45° and 90° orientations.

[2] [0,90]2, [45,-45]2, [0,90,45,-45], [30,60]2 and [15,-75]2.

results only allowed for qualitative conclusions. It was deduced that the orientation of the repair patches influences the bending strength of the repaired panel.

Additionally, a quantitative correlation of the orientation percentage with the properties of a composite repair was achieved [44]. Using two different multidirectional symmetric CFRP lay-ups, L1 and L2[1], for both parent and patch materials, the effect of the patch orientation on the compressive strength of lap patch repaired **thin** specimens was indicated. Specifically, L1 parent laminates repaired with L2 patches yielded an increase of up to 8% in the compressive strength, compared to the repair scheme where both parent and patch material was L1 lay-up.

As far as scarf repairs are concerned, the ideal patch fiber percentage orientation is thought to be one that matches that of the parent material. This might be the case assuming that both repair and parent materials consist of the same components and are of the same fabrication quality[2]. However, the assumption of identical parent and repair materials is often proven erroneous by a number of limitations imposed by field repairs (e.g. curing under vacuum or at atmospheric pressure instead of an autoclave, humidity presence, inability to apply a uniform adhesive thickness), especially in the marine industry. Consequently, the repair patch properties can differ significantly from those of the parent material, and even in scarf repairs it might be probable that the ideal patch fiber orientation will be different than that of the parent structure.

Although the materials and loading conditions of the limited existing open literature studies differ, their results tend to the same conclusion: fiber orientation percentage, and not fiber orientation by itself, is correlated to the properties of **thin** lap patch and scarf composite repairs. Unfortunately, such a correlation cannot be justified for the class of **thick** composite structures due to a lack of pertinent studies.

3.1.8. In-Plane Bondline Length and Out-of-Plane Substrate Curvature

Among the reasons that scarf designs are used in bonded repairs is that scarfing improves the repair strength by increasing the bonding area. However, adequate bonding area cannot be achieved with scarf designs if the thickness of the damaged laminate is small (e.g.

[1] L1: [(±45/02)3]s, L2: [(±45/0/90) 3]s.

[2] The deteriorating effect of patch and parent ply orientation mismatch on the tensile strength of a thin scarf repaired CFRP panel is elaborated in paragraph 3.5.

in the case where one of the **thin** face plies of a sandwich composite is damaged). In such cases a lap patch repair can be assumed. Usually, this practice entails that the damaged material is either cut out and the void filled with a resin or a plug[1], or left as it is and reinforced with resin before being covered with the lap patch. An alternative procedure providing sufficient bondline area for the substrate can be achieved with the increase of the in-plane bondline length. In **carbon**-reinforced epoxy open-hole panels it has been experimentally determined that the introduction of a resin plug can increase the compressive failure load of a double patch repaired panel by almost 20% [44].

Moreover, it has been experimentally shown that the angle between bondline and bending axis influences the bending strength of **thin glass**-reinforced composites repaired with lap patches. Maximization of this angle (90°) can yield bending strengths similar to the undamaged structure that is reinforced with the same number of lap patches. In detail, adhesively bonded repairs of **thin glass vinyl ester** and polyester panels, using various in-plane bondline angles[2], including the ones illustrated in Figure 19, were tested under bending loading [11], [35].

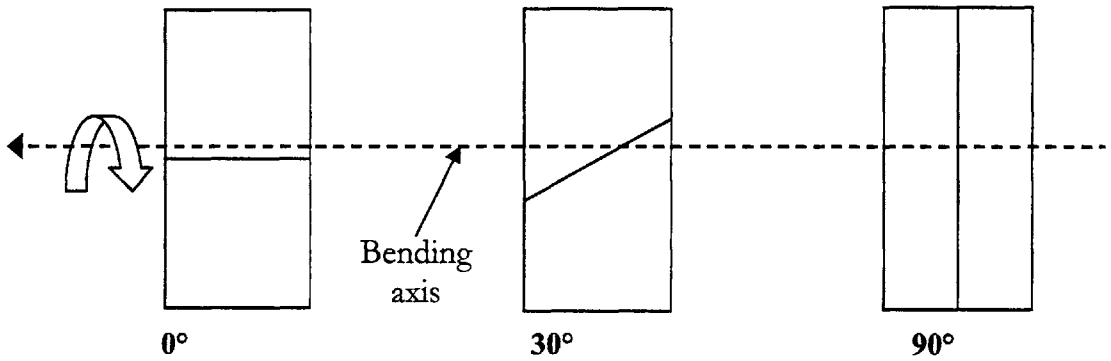

Figure 19: In-plane Bondline configurations.
Values represent angles between bondline and bending axis.

All specimens had two **glass**-reinforced patches on each side (not shown in Figure 19). It has been experimentally shown that bending strength of the repaired specimens reached similarly high values for in-plane bondline angles above 60°. These values were on average comparable to the flexural strength of undamaged specimens reinforced with the same type

[1] In carbon-reinforced epoxy open-hole panels it has been experimentally determined that the introduction of a resin plug can increase the compressive failure load of a double patch repaired panel by almost 20% [44].
[2] Additional in-plane bondline patterns are illustrated in Figure 20.

and number of lap patches. Thus, 60° was determined to be the optimal angle as far as bending loading is concerned, since any value above this would produce similar strengths with the penalty of a significantly more complex fabrication.

The studies mentioned in paragraph 3.1.8 reveal a strong correlation between repair effectiveness and in-plane bondline angle/length of **thin** structures under bending loading. This correlation might prove to be particularly useful in the reinforcement of composites when scarfing is unacceptable for a number of reasons (e.g. small substrate thickness, shallow/superficial damage). Especially for naval constructions where the large size of repairs necessitates cost effectiveness of repair schemes, exploiting the beneficial properties of in-plane bondline angle/length, if any, seems a promising alternative to scarf configuration. In the marine environment structural composites cover a broad range of fiber and matrix materials, and repairs will be exposed to a variety of intense loads, besides bending. The effect of various in-plane bondline configurations on fatigue, compressive/tensile and flexural strength for different types of marine composites should be sought, since pertinent studies are missing from the current open literature.

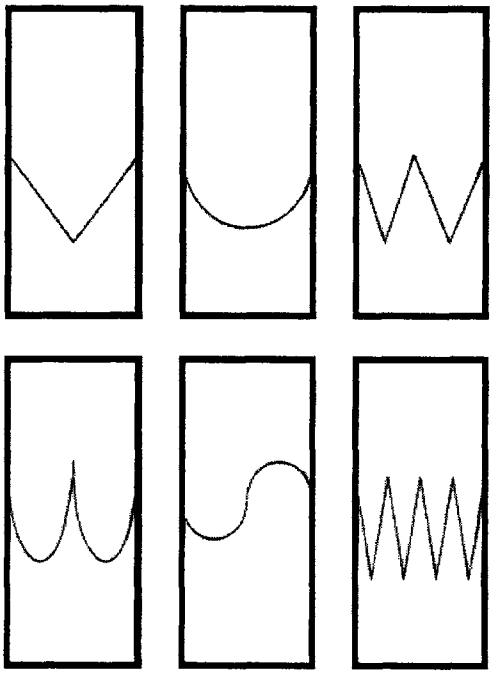

Figure 20: Various in-plane bondline configurations.

Moreover, a number of **thin glass** fiber-reinforced polyester panels with different out-of-plane curvatures, loaded in bending until fracture and repaired with two **glass**-reinforced patches on each side, were tested in bending [11]. The repair procedure followed in each of the five cases was the same. The specimens used for the discussed experiment are illustrated in Figure 21. The experimental results showed that although the undamaged strengths were completely recovered in all repaired specimens, the efficiencies of their strength recovery presented noticeable fluctuations.

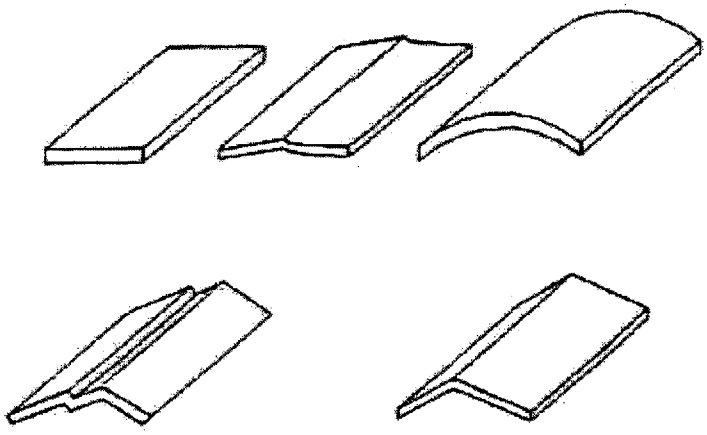

Figure 21: Specimens with various out-of-plane curvatures [11].

Attention should not be concentrated on the geometrical specifics of Figure 21, but rather on the fact that out-of-plane curvature of a substrate comprises an additional affecting parameter of a repair quality. Although the specimens were only tested in bending, it should be expected that the out-of plane curvature affects the performance of bonded repairs in other types of loading. Hence, it might be inferred that different repair procedures could be found to be optimal for each of the various out-of-plane curvatures. For marine structures, often consisting of joined cells and plates with various out-of-plane curvatures, the determination of optimal bonded repair schemes, if any, for each of the commonly used specific geometries seems a valuable area of research.

3.1.9. Repair Patch Shape

It is not clarified in the literature how the repair patch shape influences repair properties. However there are a small number of references dealing with the properties of various repair patch shapes. Circular and square patches were used to compare the strength of repaired **thin carbon**-reinforced **epoxy** specimens in compression [23]. It was determined that circular patches performed slightly better. Moreover, using a FEA method to calculate the stress intensity factor (SIF) of centrally cracked **thin** aluminum sheets, repaired with unidirectional CFRP double-side patches (skewed, rectangular, elliptical, square, and circular patches were examined), revealed a strong correlation of the results with the repair patch shape [47]. It was additionally found that increased thickness with decreased bonding area, for the same volume of the repair patch, is related to lower SIF[1]. Additionally, four different repair patch geometries were assessed in fatigue: small round, large round, rectangular, square (one specimen at each geometry) [10]. Due to the limited number of specimens, however, no conclusion was reached regarding the effect of repair size and patch geometry on the fatigue performance.

Perhaps the lack of studies pertinent to the optimum repair patch shape is justified because usually the repair extents are of very small sizes in aerospace applications, from where the bulk of the repair-related literature originates. However, when considering composite repairs in marine structures, which can extend to several square meters, the shape of the repair patch could become an important parameter for the durability and cost effectiveness of the repair. Hence, the influence of the patch shape on the compressive, tensile, and bending strength and the relevant fatigue performances seem to be valuable regions of potential experimentation.

3.2. Moisture Absorption

One of the most severe degrading affects for the quality of a repair is that of moisture ingress in the parent material, the repair patch, or the adhesive of the repair. If the parent material is moisturized, it is certain that moisture will diffuse from it to the repair adhesive in different levels during the heat-up, curing cycle, and operational life of the repair [17], [24]. Moisture can attack the repair adhesive directly or permeate the patch lay-ups and

[1] For the same volume and a decrease of 1mm in the patch thickness the SIF of three various patch shapes (skewed, rectangular and elliptical) increased by more than 20%.

subsequently the repair adhesive, if the repair area is not isolated from the environment, a practice that is usually followed with the application of protective sealants on top of the repair.

Practically any percentage of moisture uptake will certainly deteriorate most of the adhesive properties. Using unidirectional **carbon** fiber/**epoxy** composite substrates, aged for up to 12 months[1], the changes of the basic engineering properties of two cold-cure adhesives were examined [16]. As expected the moduli (E and G) as well as the tensile and shear strengths were impaired (only fracture strains showed a tendency to increase with aging). Moreover, moisture can induce blistering or delamination during the curing procedure of a bonded patch, or under severe environmental operating conditions. Under the same conditions sandwich panels can burst due to the boiling of the water that is contained in the honeycomb core [24].

The anisotropic fashion of water diffusion in composite materials limits the ability to predict the performance of a repair, since the mechanical properties of the repaired composite can be deteriorated in the substrate, the adhesive, or even both at different levels of severity. Moreover, the moisture uptake depends on a number of fluctuating parameters. To name the most important ones, there is a relation between the water diffusion coefficient and the stress field[2] of composite materials. In particular, this relation depends on the angle between the loading direction and the fiber orientation in **glass** and graphite epoxies (e.g. at zero angle between loading direction and fiber orientation the effect of stress is the minimum) [26]. Further, the rate of diffusion depends on the angle between the moisture penetration direction and the fiber orientation (at a penetration direction parallel to the fiber orientation the rate is much higher than at the direction normal to it). Lastly, there is a strong dependency of the moisture uptake on the temperature, for a given environmental humidity [27], [30]. This dependency is illustrated in Figure 22, which describes E-**glass** fiber **epoxy** cross-ply laminate moisture ingress when immersed in distilled water at 20°C and 90°C. It is noticeable that at 20°C water uptake reaches a saturation limit, while no such behavior is presented at 90°C, where the rate of uptake increases. Additionally, it is interesting that the moisture uptake is

[1] At 90% relative humidity and 40°C temperature, below the glass transition temperature of the adhesives.
[2] It has been shown that when increasing the stress level both penetration rate and equilibrium moisture weight gain increase, in graphite cross ply **epoxy** [26].

very similar to that described above, for other laminate geometries, like angle-ply and multidirectional.

Clearly, the correlation of the effects of moisture and temperature on the assessment of the repair durability should be examined in order to better comprehend their effect on the quality of a composite bonded repair. In one of the related studies the effect of moisture absorption on plain weave **carbon** fiber fabric[1] laminates was sought in the following two cases [15]:

- Pre-bond moisture level of parent laminate, up to 1.5% (per weight)
- Repaired parent laminate, initially dry, moisturized up to 1.1% (per weight)

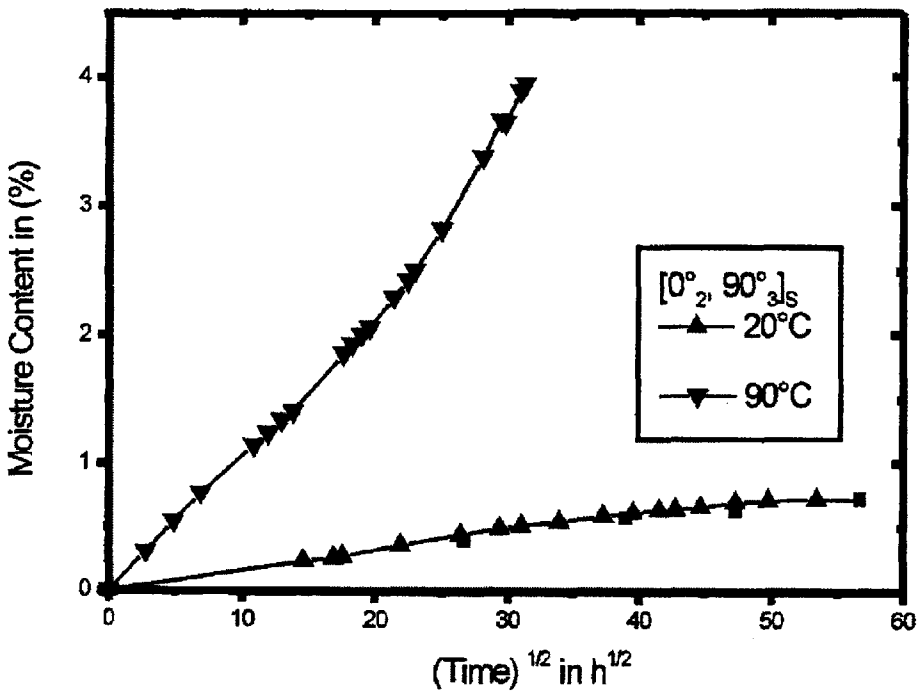

Figure 22: Variations of moisture uptake (% weight gain) with temperature [27].

Although pertinent to **carbon-reinforced** composites, the results of the above two case studies seem valuable for the development of an insight in the expected behavior of composites with different reinforcements.

[1] This fabric had fibers in orthogonal directions. Base laminate lay-ups were [(0/45)2]s for scarf repairs and [0]8 for lap repairs.

3.2.1. Pre-Bond Moisture Level of Parent Laminate, Up to 1.5% (Per Weight)

It was observed that base laminate moisture ingress had an insignificant effect on the tensile strength of the repair (at least above 80% of the pristine strength was regained) as long as the percentage of ingress was below 1.1% (per weight); above that level the effect of moisture proved to be significant. To achieve the predetermined percentages of moisture content of the specimens, two methods of moisturization were used. In the first one the base laminates were kept in an environmental chamber until the desired ingress was achieved. In the second one the base laminate was premoisturized to certain levels (1.1% and 1.5% per weight) and then dried to achieve the desired moisture content. The comparison of the two methods' test results revealed that the failure loads of the second were significantly lower than those of the first method, for the same percentage of moisture ingress. It was understood that the base laminates that were moisturized with the second method had to be almost completely dried before they could yield failure loads as high as the ones obtained with the first moisturization method.

The first important outcome of this examined case is that drying the base laminate before the repair is unnecessary if the moisture ingress is below a certain percentage (1.0% in the study of [15]). The second important conclusion is that the base laminates should be completely dried (not partially) when their moisture content, prior to the repair, is above a certain percentage (1.0% according to [15]).

The moisture percentage limits above which a complete drying is required seem to vary, depending on the materials of the substrates, the adhesives used, and the properties of the repair that are sought. For instance, a study that used **carbon** fiber **epoxy** specimens of up to 1.2% water content (by weight) determined that the drying[1] time did not significantly change the repair failure tensile and shear loads [16]. Hence, the lower limit of moisture percentage (by weight) can be stated as 1.2%; higher than the aforementioned 1.0%. This variation might be attributed to the fact that although in both studies similar fibers, reinforcements, and curing procedures were used (autoclaved curing), the repair adhesives were different. Contradicting these results, another source claims that the flexural strength of a repair **carbon**-reinforced **epoxy joint** appears to be insusceptible to the pre-bond moisture level [17].

[1] Under vacuum pressure at different periods (up to 14 days) at 80°C.

3.2.2. Repaired Parent Laminate, Initially Dry, Moisturized Up To 1.1% (Per Weight)

The examination of this case yielded that neither moisture ingress (up to 1.1%) nor high temperature 82°C can individually affect the tensile strength of the repaired structure, at least not notably. The presence of both hot and wet conditions (82°C and 1.1% moisture ingress) is required to reduce the failure load of the repaired structure significantly [17]. Similar conclusions were extracted by testing CFRP bonded **joints** both dry and moisturized [10]. When tested at 160°C, dry specimens lost roughly 20% of the pristine tensile strength (measured at room temperature). **Joints** conditioned for 42 months (in distilled water at 50°C and tested at 130°C, lost 50% of the pristine tensile strength (measured at room temperature).

In concurrence with the results from the above studies of paragraph 3.2.2 the degrading effect of moisture on the temperature resistance was determined using moisture-free metallic adherends (aluminum), wet composite adherends and a single adhesive (with curing temperature 121°C) [24]. The aluminum lap shear specimens presented similar tensile strength with the composite cured repairs up to a certain test temperature (roughly 50°C). Above that temperature the strengths of the composite specimens were significantly lower, indicating the deteriorating effect on the moisture content and high temperature interaction on the strength of the repair. This interaction is illustrated on Figure 23.

3.2.3. Consolidation of Moisture Effect Studies for CFRP

Although the examined materials and repair techniques, used by the cited references, vary, there seems to be a pattern related to the effect of moisture ingress on the mechanical properties of **carbon**-reinforced composite repair **joints**. Table 8 illustrates the comparison of **thin** laminates made with plain weaved **carbon** fiber fabric or **carbon** fiber-reinforced **epoxy** resins.

The variability in the values of the moisture percentage limits, in Table 8, could be attributed to two reasons. The first is that different materials (reinforcements, epoxies) and lay-ups are used in the two cited studies. The second is related to a study which asserts that the tensile strength of repaired **joints** correlates more with the substrate surface pre-bond moisture level than the overall moisture level of the parent structure [17]. Thus, different

values of overall moisture percentages (per weight), such as those indicated in Table 8, could correspond to identical values of surface moisture levels.

It seems that **carbon**-reinforced epoxy repairs retain at least 80% of the pristine structure strength when the overall moisture content of the parent laminate is around 1.1-1.3%. Above this level the strength of the repair is drastically affected; it is rapidly reduced to below 50% of the pristine value for moisture levels above 1.5% (not shown in Table 8). This pattern seems to hold for different parent lay-ups, repair techniques, and thickness of **carbon**-reinforced composites, such as the ones indicated in Table 8. However, these results may not extend to composite repairs with fiber reinforcements other than **carbon**, or matrices other than epoxy (polyester and vinyl ester). Since glass and **carbon** vinyl ester composites are increasingly being used in naval constructions, the determination of moisture absorption effect on their properties seems a valuable area of research.

Table 8: Effect of moisture on various **carbon**-reinforced epoxies' performances.

Parent lay-up scarf (double lap)	**Repair lay-up scarf (double lap)**	**Overall Moisture level (by weight)**	**Min. Tensile Strength regained scarf (double lap)**	**Min. Stiffness regained scarf (double lap)**	**Fatigue performance**	**Thick. mm**	**Ref.**
8-ply quasi-isotropic [(0/45)2]s (Cross-ply [0]8)	8-ply quasi-isotropic [(0/45)2]s plus extra [0]2 plies (Cross-ply [0]3 on each parent side)	≤1.1%	85% (85%)	-	-	< 3	15 *
		≥1.1% (up to 1.5%)	66% (50%)	-	-		
16-ply quasi-isotropic, [±45/0/90]2s	16-ply quasi-isotropic [0(±45/0/90)2]s	≤1.3%	80%	No effect	-	< 3	17 **
		≥1.3% (up to 1.6%)	40%	No effect	-		
12-ply quasi-isotropic [±45/0/90]2	12-ply quasi-isotropic [±45/0/90]2	N/A[1]	85.5%	-	Insignificant changes between dry and conditioned repairs	< 3	10

* Used plain weaved **carbon** fiber fabric

** A scarf angle of 1.9 degrees approximately was used.

[1] Specimens were submerged in 50°C distilled water for various periods of time (4, 11, 16, 28 and 42 months), in order to resemble the hot-wet conditions. However, the percentage of moisture ingress in the structure (e.g. per weight) is not stated.

3.3. Temperature

Temperature is a major affecting parameter when considering the mechanical properties of materials. The influence of this parameter on the quality of bonded composite repairs is complicated as it involves the parent, repair, and adhesive material in various levels, depending on their properties. The complexity of the fashion in which temperature affects a bonded composite repair could be alleviated by individually examining certain temperature-affected properties.

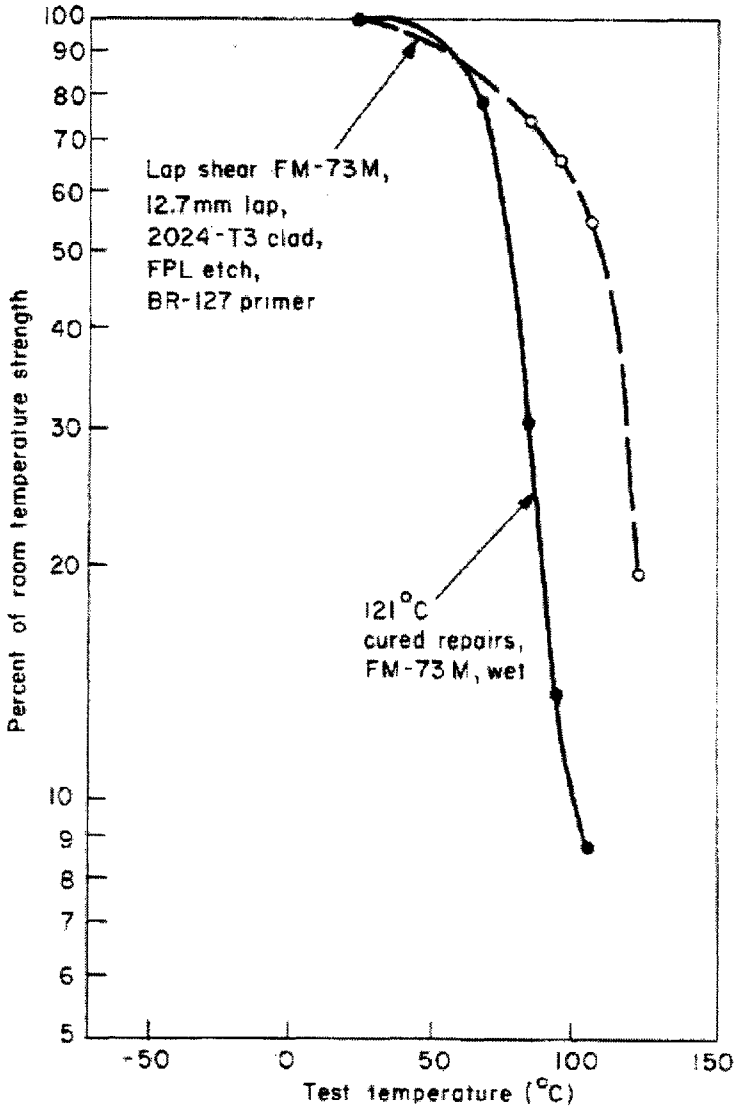

Figure 23: Reduction of joint tensile strength due to moisture uptake in high temperatures [24].

3.3.1. Glass Transition Temperature

One of the temperature-related properties that can significantly affect the properties of a bonded repair is the glass transition temperature (Tg). This property is defined as the temperature, point or narrow band, at which the material transits from being rigid and brittle to flexible and ductile. This transition is accompanied by a significant alteration of mechanical properties: strength and stiffness are reduced, while thermal expansion coefficient and specific heat may increase [4]. Thus, Tg could be considered as a metric for the evaluation of the durability of composite repairs, depending on the temperatures at which the repaired structure would be expected to operate.

However, the values of Tg change[1] depending on the moisture levels, and this dependency reduces the value of the glass transition temperature as a useful metric for the assessment of repairs [4], [16], [24], [30]. The post-curing reactions are also affected by temperature, inducing an increase of Tg, which is reduced with moisture exposure as mentioned above [16]. Furthermore, if the repair adhesive is different than the patch and parent material resins, dissimilar Tg could complicate the behavior of the repair for various elevated temperatures. This pattern in which Tg is affected by the aging parameters (temperature and moisture) renders it unavailing in the assessment of the durability of composite repairs. Nevertheless, the effect of Tg on the mechanical properties should always be considered in the design of composite repairs. Indicatively, it is suggested that in the saturated condition, for safety, the operating temperatures of **epoxy** resins should be 28°C below Tg [4].

3.3.2. Adhesive Shear Stress-Strain Curve

It has been determined that the shear properties (ultimate values of both stress and strain) of the adhesive influence the strength of a **joint** significantly [1], [23]. Specifically, higher ultimate adhesive stress and strain values produce a stronger bonded **joint**, as it is indicated in Figure 24 and Figure 25. Moreover, it has been specified that the influence of the ultimate shear strain on the strength of a **joint** is higher than that of the ultimate shear stress.

[1] As a rough rule-of-thumb it may be said that for each 1% water pick-up there is a drop in Tg of about 20°C.

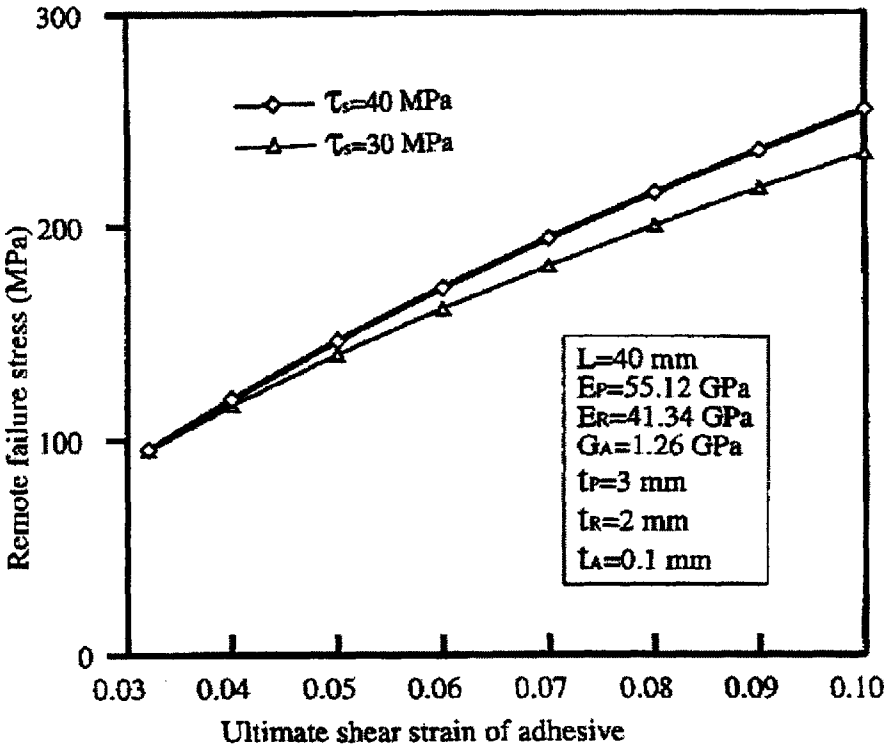

Figure 24: Influence of the ultimate adhesive shear stress on the joint strength [23].

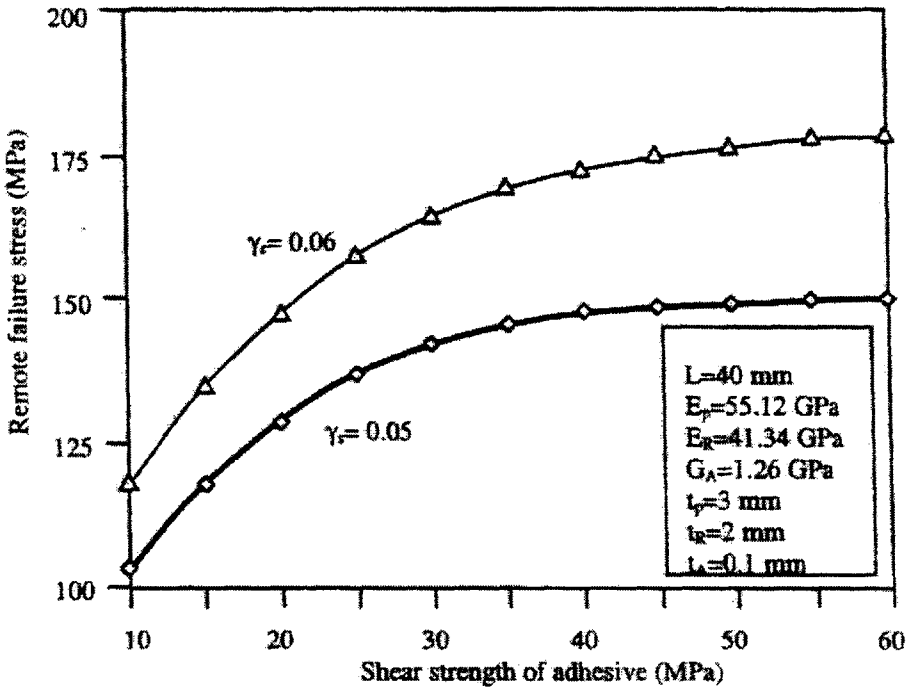

Figure 25: Influence of the ultimate adhesive shear strain on joint strength [1].

The effect of temperature on both the ultimate stress and strain of any material should not be neglected. In a bonded composite repair, all main constituents (parent, patch, and adhesive material) are influenced by temperature in various levels. The repair material is usually chosen based on compatibility with the parent composite (membrane stiffness balance of repair and parent materials are essential for the repair, as elaborated in paragraph 3.1.4). On the other hand the selection of the repair adhesive, which is essentially subjected to shear loading, is partially based on its ultimate shear stress and strain. Hence the effect of temperature on these adhesive properties needs to be determined.

As indicated by Figure 26, these adhesive properties vary significantly with varying temperatures.

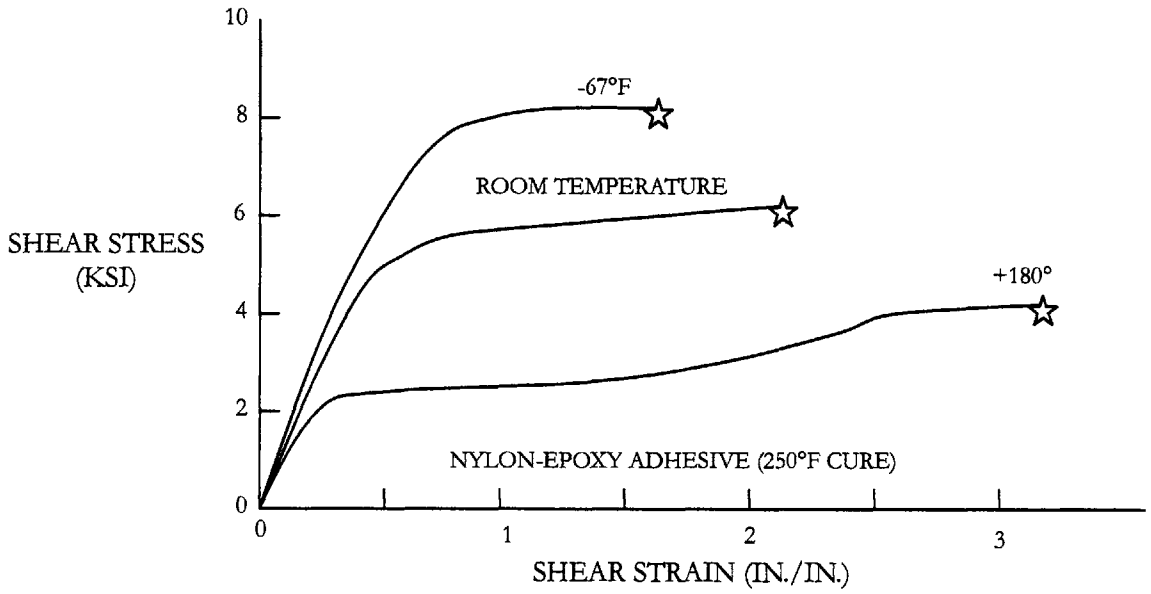

Figure 26: Variation of adhesive stress-strain curves with temperature [29].

What seems to be rather invariant is the area below each of the stress-strain curves, that is, the strain energy to failure per volume of the adhesive. Indeed, it has been shown that the shear strength of adhesively bonded structural **joints** can be determined from the strain energy per unit bond area of the adhesive [29]. It seems that such a correlation of shear strength to the strain energy, which is practically invariant with temperature, would be more valuable than a correlation with any of the other temperature-dependent properties of the adhesive (ultimate

shear stress or strain), for the selection of the repair adhesive in versatile environments. Hence, for the case of marine composite repairs, which are typically exposed to a broad spectrum of temperatures, the ultimate strain energy of adhesives seems a more appropriate metric of the repair durability.

It appears that the correlation of the ultimate adhesive strain energy with the repair strength in various temperatures should be included as a design parameter in the optimization of the overlap repair area. This can be clarified through a parallelism with bonded lap **joints**. Particularly, since the ultimate shear strain and stress are the highest and lowest respectively for the highest value of the operational temperature range, the length of plastic shear zone developed in the adhesive would be the maximum at that range, for a specific shear load. Therefore, the ultimate adhesive shear strain and stress at the highest operational temperature would yield the maximum ideal lap joint overlap length (the ideal overlap length is defined in paragraph 3.1.5). Hence, if the ideal joint overlap length is determined at the highest temperature, the resulting adhesive volume would be adequate to undertake the same strain energy in any lower value of the operational temperature range (based on the aforementioned property of constant adhesive strain energies for various temperatures).

Equally, the determination of the ideal overlap area of a bonded repair, that is in essence a joint, could similarly be correlated to adhesive shear strain energy. Such a correlation is not documented in the open literature and seems essential for the design of cost effective bonded repairs in versatile operational environments such as those to which naval constructions are exposed.

3.3.3. Cure Temperature

Tests on **carbon**-reinforced **epoxy** specimens repaired with both stepped lap and scarf patches[1] at 150°C, 175°C and 200°C curing temperatures showed that the effect of cure temperature is insignificant for the tensile failure load [15]. Hence it would seem more cost effective, since it would reduce the time to full cure and consequently the total repair time, to use the highest cure temperature (permissible for the resin system used in the repair), as is suggested by the authors of the above study. However, the term "permissible" should not only

[1] The repair materials were **carbon**-reinforced epoxies.

be correlated to the maximum temperature that the resin can withstand without losing its mechanical properties.

The thickness of the repaired composite and its moisture content should also be taken into account. Co-curing[1] the patch and adhesive of a **thick**, 50 ply, graphite/**epoxy** laminated panel that was preconditioned to 1% moisture content by weight (maximum concentration of 1.9% at the surface) under vacuum at 177°C, produced extensive blistering of the panel (roughly 60% of the area) [24]. The attempt to dry the panels only resulted in moving the blistering loci deeper in the laminate. Drying combined with a reduction of the co-curing temperature to 149°C yielded a repaired composite that was free of blistering. Moreover, it was found that using the same levels of moisture content (1% by weight) and cure conditions (177°C) for the co-curing of thinner laminates (8 to 32 plies) resulted in blistering-free repairs.

The above consideration should be given special weight for repairs of **thick** composite structures that are exposed to humidity, like those regularly encountered in naval constructions. Consequently, an optimization of the curing temperature with respect to the laminate thickness and its moisture uptake should be sought in order to achieve reliable and cost-effective repairs in the marine industry.

3.4. Extra Plies (Scarf Patch Repairs Only)

The repair patch can present diminished properties compared to the pristine structure due to a number of fabrication factors. For instance, field repair practices often dictate the curing of the repair patches under vacuum pressure only, while the whole composite structure has been originally cured in an autoclave. Thus, the repair patch could turn out to be more porous than the pristine structure [14], [17], [49]. The effect of different autoclave pressures in the fabrication of test **carbon** fiber unidirectional specimens is indicated in Figure 27.

A common practice, that is used to alleviate such demerits of the repair patches, is the introduction of extra plies in addition to the number that corresponds to the original structure. Using **thin carbon**-reinforced epoxy repair scarf **joints,** it was determined that the addition of extra plies on the repair significantly increased its tensile efficiency [15]. Specifically, several specimens were examined at both room temperature and, after hot–wet preconditioning, at

[1] Co-curing of a repair patch is the procedure where adhesive and repair patch material are simultaneously cured.

high temperatures (82°C) for one and two extra repair plies. The increase of repair efficiency, in tensile loading, is given in Table 9.

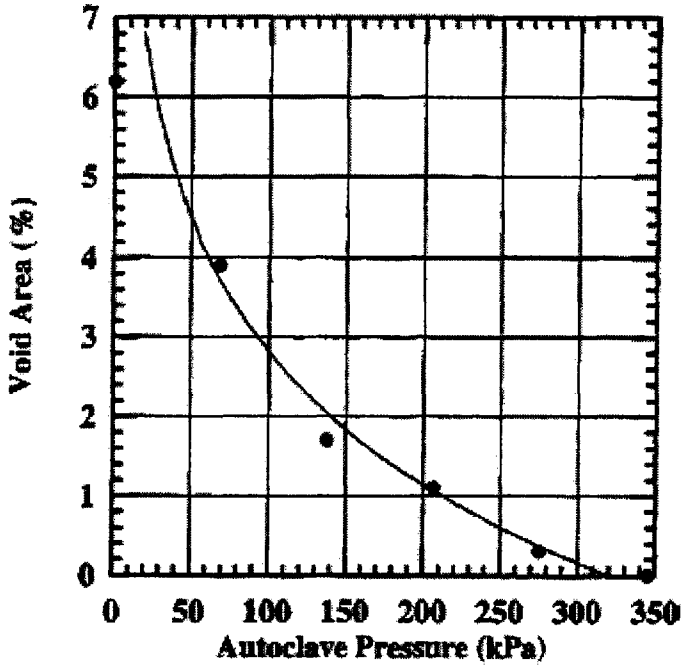

Figure 27: Void generation of unidirectional **carbon/epoxy** specimens for various fabrication pressures [49].

Table 9: Increase of scarf repair efficiency with addition of extra plies [15].

	Tensile repair efficiency (efficiency percentage increase compared to repair without extra plies)*	
Number of extra plies	Dry specimen, tested at 21°C	Hot-wet Preconditioned specimen, tested at 82°C
0	76%	56%
1	83% (9.2%)	67% (19.6%)
2	96% (26.3%)	88% (57.14%)

* Values were geometrically extracted from graphical representations of experimental data.

From Table 9 two conclusions can be deduced. First, it becomes clear that the addition of extra repair plies increases the tensile repair efficiency significantly. Second, the use of extra plies is radically more beneficial in hot-wet conditions. Particularly, the efficiency

percentage increase of hot-wet preconditioned repairs is more than double compared to that corresponding to no preconditioning and testing at room temperature.

Moreover, using a FEA method the application of extra plies was related with a dramatic reduction in peak shear and peel stresses of bonded scarf **joints** subjected to tensile loads [45]. Furthermore, Robson et al. (2002) utilized classic laminate theory to reach a set of guidelines concerning the number of extra plies and their orientation that should be used on **carbon** fiber-reinforced **epoxy** scarf repairs [14]. The properties of the repair material (including the extra plies) were derived by discounting those of the base material. This reduction was introduced in order to simulate the increased void concentration in the vacuum cured repair plies, compared to the autoclave cured parent laminates. The resulting guidelines are presented in Table 10.

Table 10: Guidelines for use of extra plies on scarf repair patches [14].

		To Restore Stiffness		To Restore Strength	
Base Lay-up	Loading	Extra Ply Orientation	Proportions*	Extra Ply Orientation	Proportions*
Quasi-Isotropic	longitudinal	0°	1 per 16 plies	0°	1 per 16 plies
Cross-Ply	longitudinal	0°	1 per 16 plies	0°	1 per 6 to 8 plies
Angle-Ply	longitudinal	±45°	1 pair per 16 plies	±45°	1 pair per 8 plies
	shear	±45°	1 pair per 16 plies	±45°	1 pair per 16 plies

* extra plies are indicated for each group, or part of plies, of the number shown in the original laminate.

In essence, this study concluded that extra plies should be aligned with the loading direction unless the structure is subjected to combined loads. In this latter case, where strength and stiffness in each different orientation should be balanced, pairs of ±45° plies are more suitable than single 0° extra plies. Additionally, the study achieved a quantification of a laminate's plies in groups that determine the number of extra plies required in the scarf repair. For instance if the base lay-up is angle-ply, consisting of 20 plies, the loading is longitudinal and the restoration of stiffness is sought, then, according to Table 10, one single extra pair of ±45° plies would be required on top of the scarf patch repair.

This rule allows for adjustments depending to the number of plies in the original structure. For instance, if in the above example the number of plies was 28, only one group of 16 plies would be contained according to the "1 pair per 16 plies" rule. However, it is suggested that the remaining 12 plies could be better accounted for if two groups of 16 plies

were to be considered; thus two extra pairs of ±45° plies would be required on top of the flush patch repair [14]. Of course, the 28-ply laminate cannot be broken down to two 16-ply groups, but from another prospective the remaining 12 plies account for 75% of the 16-ply group[1].

Thickness of the repair plies was not one of the parameters of the above study since its authors claimed that the percentage of strength drop, due to the use of vacuum curing instead of autoclave, was independent of the laminate thickness. Consequently it is alleged that the above conclusions should be valid for a broad range of thicknesses [14]. However, it should not be assumed that the results summarized in Table 10 are generally applicable to repairs of different composite materials.

For instance, the results of a study[2] using plain weave **carbon** fiber prepreg plies[3], under tensile load are not in concurrence with the conclusions of Robson et al. (2002), regarding the number of extra plies required to restore the properties of damaged base laminate plies. Specifically, $[(0/45)_2]$s lay-ups were used in the construction of the base laminates. Thus, the base laminate can be thought of as a quasi-isotropic material, consisting of 8 plies. According to Table 10, one single 0° extra ply would be sufficient to restore the strength of a 16-ply base laminate. This means that it should be more than adequate to restore the strength of an 8-ply base laminate, something that is not verified by the test results[4], since even with 2 extra 0° plies the repair strength is less than that of the pristine structure. Consequently, it can be concluded that the guidelines of Table 10 are at least applicable to the materials[5] used by Robson et al. (2002), but cannot be arbitrarily assumed for other composite lay-ups.

Nevertheless, it is clear that if patterns such as the ones summarized in Table 10 exist in composite materials, they should be sought since they are directly linked to more reliable and inexpensive repairs. Especially for the applications of the marine industry that can often require oversized patches (even up to several square meters) and are commonly performed under simple vacuum pressure, the optimization of the number of extra patches could prove to be a major contributor to cost effectiveness.

---

[1] Simplifying this, it could be stated that (32-28)=4(additional plies required to use 2 pairs of extra plies) is less erroneous than (28-16)=12(remainder of plies that cannot be assigned an additional extra ply).
[2] [15].
[3] The used fabric had fibers in orthogonal directions.
[4] Figure 16 of [15].
[5] Autoclave processed laminates of a high-modulus **carbon** fiber in an **epoxy** matrix cured at 175°C.

3.5. Repairs Defects

There are a number of defects that can be introduced in a repair. A fraction of them are attributed to wrong assessment of the damage, inadequate substrate preparation (drying, cleaning), and lack of time or special tools in the context of field repairs. In any case the presence of defects in a repair could deteriorate the ability of the repaired structure to regain the properties of the pristine state.

In order to develop an insight into the impact that a defect can impose on the repair of **carbon**-reinforced **epoxy** laminates, the effect of two types of defects were examined: inclusion of a circular defect [18, 19] and patch fiber orientation mismatching [18]. Tests conducted using six-ply quasi-isotropic [-60, 60, 0]s base laminates showed that the scarfed repairs restored 90% of the base composite pristine tensile strength, on average [18,19]. The repaired specimens with the engineered circular flaw restored approximately 83% [18] and 93% [19] of the pristine tensile strength, on average. It is interesting, considering the dimensions of the engineered flaw (100% and 14% of the smaller and larger scarf repair ply diameters, respectively, in the study), that the presence of such a fabrication defect does not appear to deteriorate significantly the static performance of the repaired structure. Furthermore, it was concluded that the repair with the circular flaw presented increased degradation in fatigue life compared to the ones without defects. It was also indicated that a mismatch between one patch and one parent laminate ply (60 degrees) slightly decreased the percentage of tensile strength restoration of the pristine laminate; approximately 85% of the undamaged laminate strength, on average, was regained. The above studies reveal certain trends that are summarized in Table 11.

Table 11: Effect of defective repairs on mechanical properties of carbon-reinforced epoxy.

	Effect on static strength *	**Effect on stiffness ***	**Effect on fatigue life ***	**Ref.**
Presence of a circular defect between two repair plies	Small reduction	**	**	18
	None	**	Increased degradation rate	19
Mismatch of repair fiber orientation of one ply	Small reduction	**	**	18

* All properties are compared with those of the pristine structure.
** Not examined.

The conclusions of Table 11 are extracted using a small number of specimens[1]. This deprives the above study of statistical precision, since only one flaw diameter and one ply orientation mismatch are examined, both at a specific ply location. Moreover, the study is deprived of a conclusion on the relevant importance of the two flaws in the performance of the repaired structure, and it does not examine the defected repair under flexural loading: a type of loading commonly applied on naval constructions. Different flaw diameters, additional ply orientation mismatches, variable locations of the previous two defects in the repair patch, and other types of laminate lay-ups could reveal better conclusions on how repair defects affect the properties of a repaired composite.

A study that would address the considerations just outlined would be valuable for the realistic assessment of field repairs. Of course, the introduction of a defect merely depends on the dexterity of the repairer. On the other hand a fraction of defects will probably emerge from the field repair procedures (increased void content due to lack of autoclaved curing, delamination generated by moisture vaporization during curing, inability of vacuum infusion processes to completely wet the fibers, degradation of prepreg properties due to inappropriate storage). The number of defects independent of the repairer competency could be modeled as a stochastic processes based on laboratory experiments. Subsequently, the most probable combination of defects could be examined for a number of composite structures and loading conditions of interest. This procedure would lead to a more realistic assessment of the expected properties that a structure would have when repaired in the field.

3.6. Adhesive and Resin Properties

The strength of composites is strongly dependent on the properties of the adhesive used to achieve the bonding of the stacking laminae [7]. This dependency, related to adhesive ductility, is additionally proven by shear lap tests on adhesively bonded composite **joints** [20], [21]. The test results of 6 different adhesives on 3 various substrate resins, shown in Figure 28, illustrate the dependency of the bonding quality on the adhesive selection (and moreover the correlation of adhesive and substrate materials on the shear strength of the bond). In addition, for **thin carbon**-reinforced epoxies, it was experimentally proven that the

[1] A total of 3 specimens with circular flaw, per each study, and 2 fiber orientation mismatches were used.

combination of resin types of the substrate and the repair patch, affects the repair tensile strength [15]. Not only did the regained tensile strength vary for different substrate and repair patch resins (using the same **carbon** fiber fabric for the fabrication of all the examined laminates), but moreover this variability fluctuated with respect to post-repair environmental conditions (hot-wet preconditioning before testing). It is also worth mentioning that the above behavior occurred in prepreg and wet lay-ups, scarf and lap schemes, unidirectional and cross ply orientations of the substrates and repair patches.

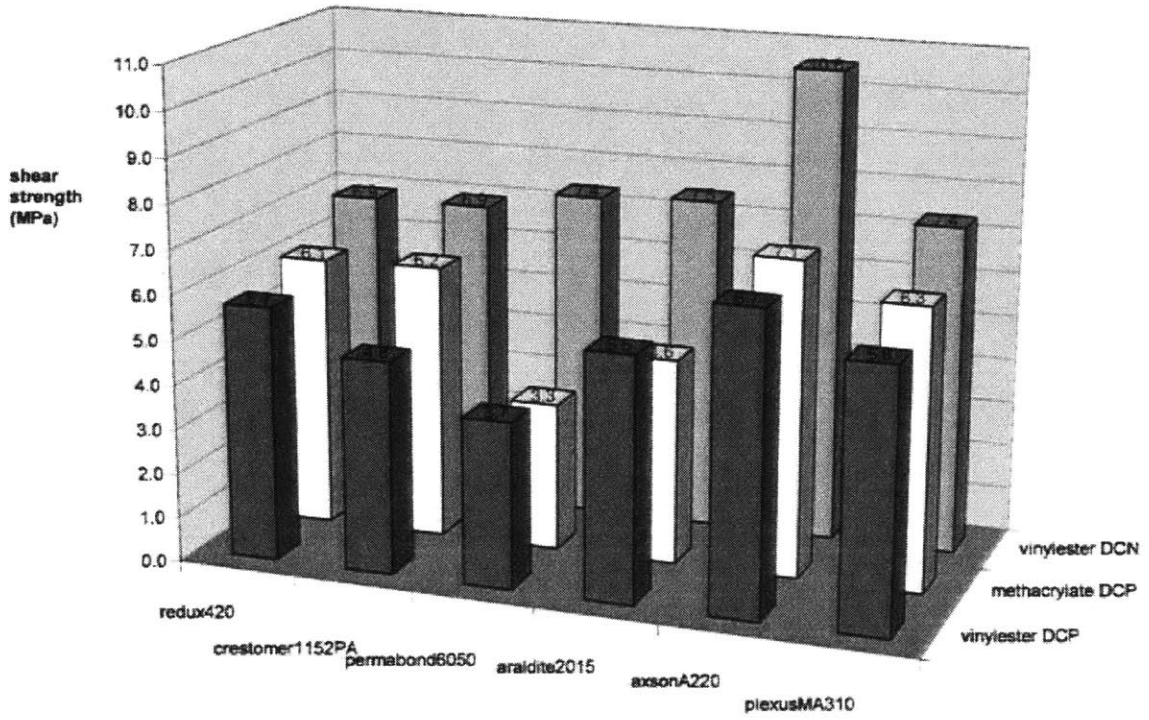

Figure 28: Shear strength of various adhesives for different substrate materials [20].

Hence, it appears that the selection of the repair patch should additionally account for the performance of its resin in the anticipated environmental exposure conditions.

4. Carbon and Glass Vinyl Ester Composite Repairs

A family of composites that is widely used in contemporary naval application is that of glass and **carbon** fiber reinforced **vinyl esters**. Vinyl ester resins have similar chemical structure with polyesters, but their specific molecular structure improves certain properties in comparison to polyesters. Vinyl ester resins are tougher and due to their lower content of ester groups, that are susceptible to water degradation by hydrolysis, they are more environmentally resilient than polyesters. These exceptional advantages are usually traded off with elevated temperature post-cure requirements, and higher costs than polyesters [38]. Nevertheless, the performance of vinyl esters in the aqueous context is proven, and their utility would increase even more through thorough design of their repairs.

The determination of an optimal repair configuration can be influenced by various damage Modes that a composite is likely to suffer in the marine environment. Most composite laminates show an increased susceptibility to impact damage, a very common Mode of damage in marine applications due to dropped heavy object (tools, cargo), impact with flotsam or other vessels, and in the case of surface combatants, impact of projectiles or shrapnel. The susceptibility to impact damage is correlated with a common characteristic of most composite laminates: the lack of through-thickness reinforcement. This property results from the absence of fiber reinforcements in planes perpendicular to that defined by the laminate lay-up. Consequently, the examination of strength in impact loading and the determination of the optimum repair schemes for the remedy of this Mode of damage should be a primary concern in the marine industry.

Damage on a composite material from impact can develop in a variety of patterns: projectile rebound, embedding, and perforation. One of the cases examined, with special interest for **thick** marine structures is that of clean perforation with minimal lateral delamination[1] [36]. Such damage is a typical result of projectile impacts. S2-glass/**vinyl ester** panels of up to 12.7 mm were used and the repair schemes included the following:

- Plugging the hole with **epoxy** (with microballoon or E-**glass** random chopped strand mat).
- Bonding a single plain weave **glass** or **carbon** /**epoxy** ply on both sides of the clean hole.

[1] Clean impact perforation was idealized by drilling holes in the examined specimens with a diamond tipped bit.

- Application of both the two previous repair schemes.

The damaged and repaired specimens were subjected to fatigue flexural loading. The fatigue life efficiencies (in flexural loading) of each repair scheme in comparison to the pristine specimens are summarized in Table 12.

Table 12: Post-repair fatigue life efficiencies (flexural loading) [36].

	Repair scheme		
Hole diameter mm (in.)	Plugging the hole	Bonded ply (both sides)	Both plug and ply (both sides) *
12.7 (0.5)	85%	84.9%	109%
25.4 (1.0)	57.5%	66%	106%
38.1 (1.5)	Not available	51.2%	115%

* Each of the repaired specimens exceeded the fatigue life of the virgin specimens (by 10% on average).

From Table 12 it is clear that the bonded ply repair scheme is more effective than the only-plug for increasing hole diameters. Moreover, it is obvious that the combination of the two schemes restores the fatigue life of the damaged composite more efficiently. However, it is not clear if the optimum repair scheme for flexural fatigue loading retains its optimality in different types of loading.

Such a discrepancy in the determination of the best repair configuration in various types of loads has been demonstrated from experiments conducted with S2-**glass/vinyl ester** panels [31]. In this latter study specimens were repaired after impact loading of metallic projectiles and the repair efficiency was evaluated in terms of flexural and impact strength. The optimal repair configuration was proven to vary for these different types of loading. Three repair schemes were examined:

- In the first, glass-reinforced patches of different shapes (to match the different area removed at various depths according to the extent of damage) were laid up, impregnated with **vinyl ester** resin, and cured at room temperature.
- In the second, patching was again used but the **vinyl ester** resin was reinforced with chopped fibers and microballoons.

- In the third, prefabricated S2-**glass/vinyl ester** single layer laminae were used on top of the patches at various depths of the repair to increase stiffness.

The performance of these repair schemes in bending and impact loading is illustrated in Table 13. Before inferring any conclusions it should be noted that the sample used for the post-repair impact loading is very small (only one panel per repair scheme) and might not lead to valid conclusions. The values of the post-repair flexural loading are the averages of three samples per repair scheme.

Table 13: Flexural and impact strength of various repair schemes [31].

Repair scheme	Flexural strength % of the pristine structure	Impact strength % of the pristine structure *
1	53	25
2	51	112
3	58.5	64

* The absorbed energy (J) was the metric for the assessment of the impact strength.

From Table 13 it appears that the 2nd and 3rd repair scheme are more efficient in restoring the pristine properties. Moreover, assuming that deceptiveness is not introduced by the small sample of post-repair impact loading tests, it can be stated that the repair scheme should be selected according to the preferred loading to be withstood. Specifically, according to Table 13, the 2nd or 3rd repair scheme should be used when the repair design criterion is the impact or flexural strength regain, respectively.

The results of the aforementioned studies, of Section 4, should not focus one's attention on the repair schemes that were presented herein, as there might be numerous others that could be implemented. Rather, the necessity to examine various repair schemes and their level of regaining each of the pristine properties should be emphasized, in order to determine which configuration is the optimal for a specific repair design criticality (stiffness, tensile-compressive strength, fatigue, and impact). The need for research in this direction is highlighted by the incomplete studies available in the open literature, as illustrated in Table 14.

Table 14: Glass/vinyl ester repair efficiency % for various repair schemes and loads.

Material Parent (Repair)	Tensile	Compr/ve	Flexural	Impact	Fatigue	Repair Scheme	Thick. mm	Ref.
Glass isophthalic polyester (Glass/vinyl ester)	35-37		45-50			Full thickness stepped (entire panel width)	15	[9]
Glass isophthalic polysester (Glass/vinyl ester)	55-59		61-64			Half thickness stepped (entire panel width)	30	[9]
S2-Glass/vinyl ester (three repair schemes using S2-Glass/vinyl ester)					51-115	Double lap	6.3	[36]
				25-112		*	N/A	[31]
			51-59			* (specimens were rectangular cuts of the repaired panels)		

* Repair layers at each depth match the contour of panel extracted damaged material.

5. Assessment of Marine Composite Repair Fabrication Techniques Originating from Composite Repairs of Metallic Substrates

An important parameter that influences the quality of an adhesively bonded composite repair is the technique utilized to fabricate the repair material. The importance of this parameter becomes clear when considering the fact that various manufacturing techniques can yield composites with different mechanical properties, even when their constituents (matrix, fiber material) are identical. Although fabrication of composite materials is fully described in the open literature (except for a number of patented procedures), a comparative assessment of the fabrication techniques related to bonded repairs of composite marine structures is missing. Fortunately, the application of bonded composite repairs on metallic structures has been established in marine industry and it is partially documented in the open literature. Hence, it would be valuable to review this available pool of knowledge, especially the portion related to marine applications, in order to develop a better appreciation of field repair fabrication techniques for composite naval structures.

In field repairs, there are certain cases[1] where the use of composite patches to repair a damaged metallic structure is preferable to the application of adhesively bonded metal patches, repair welding, and mechanical fastening. Specifically, in instances where the damaged area is large, a metallic patch would be difficult to match to the contour of the uneven substrate surface for bonding, welding, or bolting. Consequently, bonding a metallic patch would produce an uneven bondline thickness that would deteriorate the mechanical properties of the repair, as described in paragraph 3.1.1. Besides, welding would have to be done incrementally (using a number of metallic parts to match the contour) in a time-consuming procedure that would presuppose the storage of heavy metallic patches on board. Furthermore, mechanical fastening might introduce additional points of stress concentration (usually near bolt holes) and areas of compromised airtightness and watertightness.

However, fabrication is not the only constraint that limits the utilization of certain repair techniques and dictates the introduction of adhesively bonded composite repairs. Particularly, there are instances where hot work (welding) is restricted or requires a time consuming and costly preparative procedure. For instance before welding in a compartment, any hydrocarbon tank that is within one separating bulkhead from that compartment has to be

[1] A number of typical such cases are presented by Turtona (2005).

emptied, thoroughly cleaned and gas-free certified. Emptying is also required if the neighboring compartment is a magazine, a procedure that practically is infeasible for safety reasons when away from a naval base. In other cases, equipment has to be moved from neighboring apartments (like cable runs, electronic devices, etc.) to avoid exposing them to welding heat, or repairs have to be conducted at places of restricted access. In any of these cases the application of adhesively bonded composite repairs is a fast and cost-effective alternative.

A number of instances where adhesively bonded composite repairs were applied to **thick** marine metallic structures (aluminum and steel) are included in the literature [37], [40], [42], [43], [60]. Although several of these references[1] study the application of a repair patch on a cracked metallic plate after welding it, there is evidence that welding is not necessary prior to bonding the composite patch. Specifically, the fatigue performance of patched butt **joints** has been found to be equivalent to patched welded butt **joints** [43]. Hence, there are clear indications that bonded composite repairs of **thick** metallic substrates are by themselves an efficient repair scheme, independently of additional repair welding. Moreover, the increase of the residual strength and fatigue life and the reduction of crack growth rate of metallic substrates repaired with bonded composite patches are reported by many references [37], [40], [43], [47], [48], [52], [53], [54], [60].

The study of the cases presented, in Section 5, indicates that only a limited number of techniques are utilized for the fabrication of composite patches for field repairs of marine metallic structures. A comparison of the most applicable schemes among them is attempted by Turtona (2005), and their relative assessment is quantitatively summarized in Table 15. It is expected that more manufacturing techniques will be tailored to fit the field repair particularities as the use of composites in the marine industry increases. For the present, although bonded composite repair of metallic structures deviates from the scope of this thesis, Table 15 provides directions equally valuable for the selection of fabrication techniques for composite structure field repairs.

[1] [40], [43], [60].

Table 15: Comparison of most common repair fabrications for marine applications.

	Repair method			Ref.
	Hand lay-up	**Resin infusion**	**Prepreg**	
Level of Skilled operator	Low	High	High	[4], [37], [38], [39]
Vacuum Necessary	No	Yes	Yes	
Application to vertical surfaces	Easy	Hard**	Easy	
Cost	Lower	Intermediate	High	
Quality	Low	High	High	
Volatile emissions	High	Low	Low	
Fiber content achieved	Low	High	high	
High Curing temperature	No	No	Yes*	
Applicability to complex geometries	High	Low	Low	
Special storage required	No	No	Limited life out of freezer	
Resin mixing required	Yes	Yes	No	

* Low-temperature prepregs are also available (curing temperatures 60°-100°), but with reduced life (up to a few months) [38].

** On site infusion of fibers may yield dry areas that are hard to adhere to vertical surfaces [37].

6. Conclusions and Recommendations

6.1. NDE

Conclusions

The selection of the optimal NDE method for field inspection of a composite structure is a complex function of the structure's geometry, construction of the composite material (such as single-skin, sandwich, or laminate), type and orientation of defect sought (such as interlaminar or intralaminar), accessibility of the site to be inspected (such as single-sided versus double-sided), and cost. A comparative assessment of the most commonly used NDE methods related to reinforcements other than glass is not present in the open literature.

It is not clear how various physical and mechanical properties of different repair schemes can influence the ability of NDE methods to detect defects on adhesively bonded composite repairs. Without such knowledge, any post-repair evaluation of a structure is unreliable.

Recommendations

For the achievement of more reliable composite field repair designs for marine structures, a comparative assessment of NDE methods for reinforcements other than **glass** fiber, various matrix and core materials, and different construction geometries, would be valuable. A proposed value model for the determination of an optimal NDE scheme is developed in Section 7.

6.2. Efficiency of Various Repair Schemes

Conclusions

Efficiencies related to bonded composite repairs for structural components thicker than 3 mm are not covered in open literature to an extent that affords meaningful conclusions.

Recommendations

Unfortunately, unawareness of the maximum efficiency that each repair scheme yields for different combinations of materials, loadings, thicknesses, and geometries can lead to unreliable repair designs. Consequently, it appears that Table 3 (page 28) can be utilized as an indicative basis of the open literature deficiencies for further research.

6.3. Adhesive Thickness

Conclusions

There are indications, originating from Mode I fracture resistance tests of composite **joints**, for the existence of an optimum adhesive thickness for any bonded composite repair scheme. In the absence of experimental evidence it is not be safe to deduce that such an optimal adhesive thickness exists when considering the performance of a bonded composite repair in tensile, compressive, flexural, and fatigue loading. Nevertheless, it should be expected that the quality of bonded repairs, which essentially are bonded **joints**, is correlated to adhesive thickness. Moreover, from our review of bonded **joints**, this correlation could be anticipated to depend on adhesive ductility, bondline width, loading rate, and structure operating temperature.

Recommendations

Research on the determination of the ideal adhesive thickness, if any, for various repair schemes, materials, loadings, and component thickness would be valuable, especially for the family of thick marine composites that often present high adhesive thickness tolerances. In addition, the thickness dependency on ductility, bondline width, loading rate, and temperature, should be sought.

6.4. Tapering

Conclusions

There are indications that tapering of the adhesive thickness can be beneficial for bonded composite repairs. However, it is not clear whether and to what extent tapering can be applicable in marine repairs. This question is related to the fact that thicker adhesive layers are related to higher porosity.

Recommendations

Studies should be conducted to determine the utility of adhesive tapering in repairs of thick composites. It seems that among the related parameters at least angle and length of the taper should be examined to determine their optimum combination in each of the tapering

configurations (inner, outer, inner-outer tapering). A number of recommended considerations that should be accounted for in the study of tapering are specified in Table 5 (page 43).

6.5. Adhesive Spew Fillet

Conclusions

It appears that the beneficial properties of a spew fillet are related to adhesive formations at the end of the overlap with specific geometric characteristics, and not to arbitrarily formed fillets that result from the squeezed-out excessive adhesive (uncontrolled spew fillet). Moreover, the effect of spew fillet depends on the ductility of the adhesive and the stiffness of the adherends.

It is not known whether a spew fillet design that is beneficial for a certain mechanical property will improve or deteriorate other properties and to what extent, since only tensile tests were conducted in the open literature (using composite **joints** and patch repairs—both steel and CRP—on thick aluminum plates).

Recommendations

A study that would determine the geometric specifics of an optimal spew fillet, for various adhesive and substrate materials and illuminate the spew fillet effect on the different mechanical properties of adhesively bonded composite repairs, is expected to contribute to the improved repair efficiencies.

6.6. Membrane Stiffness of Repair Patch

Conclusions

A correlation exists between the patch and the parent structure properties (thickness and stiffness), at least for the cases of tensile and compressive strength. Unfortunately, the open literature does not present the influence of membrane stiffness on the mechanical properties of bonded composite repairs of **thick** composite substrates.

Recommendations

The influence of membrane stiffness on the quality of bonded composite repairs should further be explored if an optimization of the repair design is sought (e.g. reduced

additional weight, increased durability). Such a study should extend to various materials, repair schemes, and loading conditions.

6.7. Overlap Length

Conclusions

There are indications that there exists an ideal overlap size for each repair scheme. It appears that this overlap size is dependent on the stiffness of the adherends. Unfortunately, open literature studies related to optimum overlap size originate from **joints** and repairs of **thin** aerospace composite structures and are limited to tensile and compressive loadings. Taking into account the higher thickness and different composite materials used in marine structures, and the variety of loading conditions that are expected, it is clear that the knowledge gained from aerospace industry is inadequate to provide reliable and cost-effective repairs in naval applications. Unfortunately, the marine-related open literature lacks a study that would determine optimum repair patch size for various materials and loading conditions.

Recommendations

Research to determine the ideal overlap size would be significant, especially in the marine industry where repairs may extend to several square meters.

6.8. Scarf Angle

Conclusions

The optimization of repair scarf angle should not be based solely on results obtained from tensile experiments on **thin** scarf **joints,** since a lack of experimental verifications could lead to sub-optimal scarf repair designs.

Recommendations

Experimental studies that would investigate the ideal repair scarf angle for **thick** structures are missing from the open literature. Such investigations should consider various loading configurations for the variety of composite materials that are used for naval composite structures.

6.9. Fiber Orientation

Conclusions

Fiber orientation percentage, and not fiber orientation by itself, is correlated to the properties of **thin** lap patch and scarf composite repairs. Unfortunately, such a correlation cannot be readily assumed for the class of **thick** composite structures. Studies on the effect of fiber orientation for the quality of thick composite field repairs might lead to different conclusions than those of **thin** repairs. This is expected since often the properties of thick repair patches are not identical to those of the parent laminate due to limitations in the fabrication quality of field repairs.

6.10. In-Plane Bondline Length

Conclusions

There seems to be a strong correlation between repair effectiveness and in-plane bondline angle/length of **thin** structures under bending loading. If this correlation holds for the often thicker naval constructions, exploiting the beneficial properties of in-plane bondline angle/length, if any, seems a promising alternative to scarf configuration.

Recommendations

The effect of various in-plane bondline configurations on fatigue, compressive/tensile and flexural strength for different types of marine composites should be sought, since pertinent studies are not documented in the current open literature.

6.11. Out-of-plane Substrate Curvature

Conclusions

Out-of-plane substrate curvature is an additional affecting parameter of repair quality. Although only bending tests have been conducted, it should be expected that out-of-plane curvature affects the performance of bonded composite repairs in other types of loading.

Recommendations

For marine structures, often consisting of joined cells and plates with various out-of-plane curvatures, the determination of optimal bonded repair schemes, if any, for each of the

commonly used specific geometries and applied loading conditions seems a valuable area of research.

6.12. Patch Shape

Conclusions

The open literature lacks studies pertinent to the optimum repair patch shape for thick composite structures.

Recommendations

When considering composite repairs in marine structures, which can extend to several square meters, the shape of the repair patch could become an important parameter for the durability and cost effectiveness of the repair. Hence, the influence of the patch shape on the compressive, tensile and bending strength and the relevant fatigue performances seems to be worth pursuing.

6.13. Effect of Moisture Absorption

Conclusions

There seems to be a dependency of moisture absorption on:

- stress field
- angle between the loading direction and the fiber orientation
- angle between the moisture penetration direction and the fiber orientation
- temperature

Further, it appears that **carbon**-reinforced epoxy repairs retain at least 80% of the pristine structure strength when the overall moisture content of the parent laminate is around 1.1-1.3%. Above this level the strength of the repair is drastically affected; it is rapidly reduced below 50% of the pristine value for moisture levels above 1.5%. This pattern seems to hold for different parent lay-ups, repair techniques, and thicknesses of **carbon**-reinforced composites. However, it is presently unknown whether these results will extend to composite repairs with fiber reinforcements other than **carbon**, or matrices other than epoxy (polyester and vinyl ester).

Recommendations

Since glass and **carbon** vinyl ester composites are increasingly being used in naval constructions, the determination of the pattern in which moisture absorption affects their properties seems a valuable area of research.

6.14. Effect of Temperature

Conclusions

The effect of Tg on the mechanical properties should always be considered in the design of composite repairs. For the selection of the repair adhesive for marine composite structures, a correlation of shear strength to the strain energy, which is practically invariant with temperature, would be more valuable than a correlation with any of the other temperature-dependent properties of the adhesive (such as ultimate shear stress or strain). The development of delaminations during the curing process is influenced by curing temperature, moisture content, and laminate thickness

Recommendations

The determination of the ideal overlap area of a bonded repair could be correlated to adhesive shear strain energy. Such a correlation is not documented in the open literature but seems essential for the design of cost-effective bonded repairs in the operational environments to which naval constructions are exposed. An optimization of the curing temperature with respect to the laminate thickness and its moisture uptake should be sought in order to achieve reliable and cost-effective repairs in the marine industry.

6.15. Extra Plies

Conclusions

There are indications that extra plies on top of bonded composite scarf repairs can improve repair efficiency. However, the quantity of extra plies needed for the various combinations of fiber/matrix materials, parent thickness, and types of loads is not determined.

Recommendations

For applications in the marine industry, often requiring oversized patches (even up to several square meters), the optimization of extra patches could prove to be a major contributor to cost effectiveness.

6.16. Repair Defects

Conclusions

The effect of a fabrication defect on the quality of a repair is barely addressed in the open literature, examining only tensile strength of few **thin** scarf-repaired **carbon**-reinforced epoxy specimens.

Recommendations

The number of defects that is independent of the repairer's competency could be modeled as stochastic processes based on laboratory experiments. Subsequently, the most probable combination of defects could be examined for a number of composite structures and loading conditions of interest. This procedure would lead to a more realistic assessment of the expected properties that a structure would have when repaired in the field.

6.17. Resin Properties

Conclusions

The dependency of the repair quality on the adhesive properties is influenced by the properties of the substrate resin. Furthermore, the combination of substrate and patch resins affects the repair's tensile strength. The correlation of bonded repair properties with the adhesive-substrate resin and substrate-patch resin combinations, although presented in the open literature, remains in need of clarification.

Recommendations

Taking into account the variability of repair efficiencies for different combinations of adhesive-substrate-patch resins, it becomes evident that there is great value in determining the

specifics of this correlation, which moreover appears to be strongly dependent on temperature and humidity.

6.18. Vinyl Ester Composites

Conclusions

Vinyl ester composites and their repair are superficially addressed by the open literature.

6.19. Field Fabrication of Composite Repairs

Conclusions

The most commonly used manufacturing methods for adhesively bonded composite repairs of metallic marine structures were reviewed.

7. Determination of Ideal NDE Schemes for Marine Applications

From Table 1, Table 2, and Table 23 it becomes clear that the most commonly used NDE methods for marine field repairs present fluctuating performances depending on the type of the composite (sandwich or single-skin) and the type of damage. Sometimes damage can occur in the presence of witnesses, as is the common case of damages occurring during stevedoring procedures. However, possible defects are more frequently indicated after visual inspection that is part of the programmable maintenance procedure. In the latter case the operators are often incapable of determining the cause, type, and extent of the damage. Thus, NDE methods are required for a reliable assessment of the damage. The importance of the accuracy in the damage evaluation for the reliability and cost effectiveness of the repair is emphasized in Section 2.

Visual inspection, unfortunately, is not an accurate means of damage evaluation, as indicated by Table 10 and Table 23. Although these tables refer to composite structures used in aerospace industry, it is expected that visual inspection would not yield impoved results in marine composite structures that usually present greater complexity and dimensions. Hence it is essential to determine which of the available NDE methods, individually or in combination, is more appropriate for the accurate evaluation of the damaged composite structure. However, the ideal NDE method cannot be determined prior to the actual examination of the damaged structure, at least not without assuming a certain level of risk, since the operator does not possess information about the damage prior to its evaluation, other than the initial unreliable estimation given by visual inspection. Decisions under risk, such as the selection of the ideal NDE method, can be facilitated with the use of utility theory as will be elaborated in this section.

7.1. Benefits of Using Utility Theory for the Selection of NDE Method

The selection of an NDE method depends upon the evaluation of various attributes that reflect the performance of each method. Such attributes include the capability to detect various defects, depth of detection, time requirement, and cost for the application of the method (a more complete list of attributes, derived from the open literature, can be found in Table 1, Table 2, and Table 23). Thus in essence the selection of NDE methods is a multidimensional decision problem, since it is requires the assessment of various parameters,

such as distance, time, and money. In order to realize such a multidimensional assessment a common cardinal scale of measurement is required. Such a scale can be generated using utility theory.

Apart from the issue of multidimensionality, utility addresses the lack of linearity between the magnitude of decision variables and their desirability, in the context of decision-making under risk[1]. For instance, assume a gamble with an equal ½ chance to win \$10 or to lose \$2, which yields an expected profit of ½*(\$10-\$2) = \$4, and another gamble with the same probabilities to win \$10M or lose \$2M, with an expected profit of \$4M. It is certain that the number of people who would take the second gamble is significantly lower than those who would try their luck with the first one, even if the second gamble has a comparatively outstanding expected profit. That is because the outcome of losing \$2M would be rather unbearable, and thus undesirable, for most people. The same nonlinearity applies in various other decision variables, besides cost, that influence the selection of NDE methods.

7.2. Methodology

7.2.1. Determination of Candidate Alternatives

In choosing among individual or even combinations of NDE methods, each scheme (single or combined) can be thought of as a candidate alternative, $\mathbf{A_i}$ **(1≤i≤n)**. Candidate alternatives need to be mutually exclusive, meaning that if A_1 is chosen then A_2 is not. If the decision maker judges that both A_1 and A_2 can be thought of as an additional option, then these must comprise a separate candidate, say A_3. If only the most commonly used NDE for marine field repairs are considered, as illustrated in Table 2, then all their possible combinations can be accounted for as candidate alternative evaluation schemes. Namely, "U", "T", "I", "U-T", "U-I", "T-I" and "U-T-I", where the initials "U", "T" and "I" indicate Ultra sounds, Tap test and Infrared thermography, respectively.

7.2.2. Determination of States of Nature

Of course, the preference of each candidate can vary depending on certain conditions, such as the type of defects that need to be detected in a composite structure. These different conditions will constitute the **states of nature,** $\mathbf{S_k}$ **(1≤k≤n)**. Specifically, the case of a

[1] St. Petersburg paradox is a classic example that illustrates how adherence to the metric of expected values can lead to irrational decisions.

composite marine structure that is about to be visually inspected is assumed. It is further assumed that areas of visible defects will subsequently be examined by NDE methods. From a practical point of view due to the extensive sizes of marine structures, only defects that are clearly or barely visible can be considered for further evaluation, as is emphasized by D. Zenkert et al. (2005). A list of suggested states of nature is illustrated in Table 16.

Table 16: States of nature for the NDE method selection in composite marine applications.

State of Nature	Description	Probability
S_1	Delamination	P_1
S_2	Core crush	P_2
S_3	Skin-skin Disbond	P_3
S_4	Skin Core Disbond	P_4
S_5	Matrix cracking	P_5
S_6	Fiber Breakage	P_6
S_7	Moisture ingress	P_7
S_8	Impact damage	P_8
S_9	No Damage	P_9
		$\Sigma (P_k)=1.0., 1\leq k\leq 9$

The selection of the states of nature must take into consideration that they must be mutually exclusive and exhaustive, that is, their probabilities must sum to one. The logic for the formulation of Table 16 is based on the assumption that in a damaged structure only one of all possible defects has the most severe impact in the performance of the structure. Of course this is done for simplicity and does not imply that damage cannot consist of various defects. For instance, impact can cause matrix cracking, fiber breakage and severe deep delaminations, while indentation, which is caused by core crushing, can present some disbond of the core and skin. Although it consists of several defect types, impact damage is included in the considered states of nature examined here, due to its severe effect on composite structures[1]. In a more ideal representation, the sum of the combinations of all the considered

[1] In composite structures the effect of impact damage can induce a decrease of the static compressive strength of 65% and 80% for the cases of "easily visible" and "barely visible" damage, respectively [61].

defects should be used. For the case of the first seven types of defects, described in Table 16, all possible non-empty combinations would yield a total of 127 states of nature since:

$$\sum_{i=1}^{7} \frac{7!}{(7-i)!\cdot i!} = 127$$

In order to retain manageability of the represented methodology, the simplified vector of states of nature that is presented in Table 16 will be retained. The last state shown "No Damage", is included to account for the cases where visual inspection dictates further NDE examination, which subsequently reveals that no damage has occurred other than superficial abrasion. The corresponding probabilities of the states can be generated by historical data, e.g. maintenance records, or can be formulated utilizing direct probability assessment by the decision-maker; both techniques are elaborated by Lifson (1972).

7.2.3. Determination of Decision Criteria and Value Model

The assessment of the candidate alternatives is based upon a number of **decision criteria** $\mathbf{Y_j}$ **(1≤j≤n)** that comprise the decision criteria vector [Y]. The selection of a candidate alternative A_i under a state of nature S_k will yield a specific **outcome** $[Y]_{ik}$. In order to reduce the complexity of the **value model**, u_i, that describes the preference of each alternative, an additive model can be assumed, meaning that it consists of the sum of the utilities of each decision criterion, u_j.

Equation 1

$$u_i(Y_1, .., Y_j, .., Y_n) = u_1(Y_1) + .. + u_j(Y_j) + .. + u_n(Y_n)$$

The outcome of Equation 1, u_i, will be referred to as the "**value**" of each alternative. Later, in 7.2.7.1, it will be clarified that the value model is in essence the weighted sum of the decision criteria utilities, u_j, where each weight represents the relative significance of a decision criterion for the value model, u_i.

7.2.3.1. Requisites of an Additive Value Model

Assuming an additive model, such as the one described by Equation 1, requires additive independence of the decision criteria that form vector [Y]. According to Keeney and Raiffa (1976) *"Attributes Y1, Y2, ..., Yn are additively independent if preferences over lotteries on Y1, Y2, ..., Yn depend only on their marginal probability distributions and not on their joint probability distributions"*. An illustration of the above definition is that the effect of each individual criterion of vector [Y] on the value of a candidate alternative is independent of the level of any other individual criterion of [Y]. For instance, if the criteria of ticket price and departure time were used to assess the value of different flights during a day, the two criteria would be additively independent if the utilities of each attribute were unaffected by the other attribute's level. Namely, additive independence would entail that the utility of a morning flight would be higher than that of an evening flight independently of the price of the ticket. Likewise the utility for an inexpensive ticket would be higher than that of an expensive one regardless of the flight time. Hence the value of the ticket alternatives could be the sum of the utilities of departure time and ticket price.

Although additive independence of the attributes relies on the judgment of the operator, it appears that for the case of NDE method assessment the most important decision criteria retain additive independence, as defined above, and hence the utility model can be assumed to have additive form (see Equation 1). The set of decision criteria that can be utilized for the selection of NDE methods is illustrated in Table 17.

7.2.4. Determination of Range of Interest for Decision Criteria

Perhaps the only attribute of Table 17 that could violate the additive independence requirement is cost, since improved performance in any of the NDE characteristics is almost always correlated to higher cost. At this point it should be noted that the assumptions of additive independence are correlated to the range of magnitude of each attribute. For instance, considering again the example of section 7.2.3.1, the utility of a morning flight could be higher than an evening one, independent of the ticket price, if the range of the price is $200-$250 ($200 and $250 for the evening and morning flight, respectively). However, a decision-maker might feel that the assumption of additive independence does not hold for a ticket price range of $200-$2000 ($200 and $2000 for the evening and morning flight, respectively).

Equally, for the selection of an NDE scheme, if the magnitude range of cost is limited to that determined by the available market alternatives, excluding exotic equipment developed for niche applications, the property of additive independence can be assumed to retain its validity. If the operator decides that the cost is invalid for additive independence then a multilinear value model could be utilized, based on the methodology developed by Keeney and Raiffa (1976). Alternatively, cost could be excluded from the formulation of the value model and the final assessment of each NDE scheme could be based on two parameters: its value determined by an additive value model that excludes cost, and the cost of each scheme.

Table 17: Suggested decision criteria in the NDE method selection.

Decision Criterion	Description
Y_1	Single-skin delamination detection
Y_2	Sandwich delamination detection
Y_3	Impact damage detection in single-skin composites
Y_4	Impact damage detection in sandwich composites
Y_5	Core damage detection
Y_6	Fiber breakage detection
Y_7	Matrix cracking detection
Y_8	Detection of delamination at base of T-joints
Y_9	Detection of delamination at base of Top-hat stiffened panels
Y_{10}	Detection of delamination between sandwich beam stiffener and panel
Y_{11}	Detection of water intrusion
Y_{12}	Indication of damage depth (essential for the minimization of undamaged material extraction)
Y_{13}	Accuracy in size estimation(essential for the minimization of undamaged material extraction)
Y_{14}	Equipment flexibility
Y_{15}	Preparation time
Y_{16}	Inspection time
Y_{17}	Use in access restricted areas
Y_{18}	Cost of NDE

From the discussion of the preceding paragraph it becomes clear that determining the range of magnitudes for each attribute, as illustrated in Table 18, is essential. The corresponding magnitude ranges for each decision criterion should be used to generate their utilities. It is essential to avoid using a random magnitude range to obtain the utility function of any attribute and then extrapolating to represent the utility at the required range. The

necessity of determining utility at the applicable magnitude range of any attribute stems from the fact that utilities are generated by the assessment of certainty equivalent values[1] that are preferred over lotteries consisting of two outcomes.

Table 18: Determination of lower and upper values for each decision criterion.

Decision Criteria	Lower value	Upper value
Y_1	Y_{1L}	Y_{1U}
.	.	.
.	.	.
.	.	.
Y_j	Y_{jL}	Y_{jU}
.	.	.
.	.	.
.	.	.
Y_{17}	Y_{17L}	Y_{17U}

The maximum and minimum magnitudes among the lotteries, used to determine utility, correspond to the limits of the magnitude range, and varying them would vary the utility function itself. The determination of the utility function and its dependency on the magnitude range is clarified through an example in Appendix B.

7.2.4.1. Determination of Magnitude Range for Qualitative Decision Criteria

A number of decision criteria can be qualitative, as it is the case with Y_{14} and Y_{17} (see Table 17). In order to determine a quantitative scale for these criteria the below procedure might be followed[2].

Assume that the magnitude range of Y_{14} (equipment flexibility) needs to be established for a specific candidate alternative NDE scheme. The operator could determine an NDE method, NDE_1, that provides the maximum equipment flexibility and assign to it a value of 10. Then, he could determine another NDE method, NDE_2, that is the worst in terms of equipment flexibility, according to his judgment, and assign to it a value of -10. The operator could determine yet another NDE method, NDE_3, that can be regarded as neutral (neither

[1] Certainty equivalent of a lottery is defined as the value of any attribute for which a decision maker would be indifferent between having this value with certainty, that is probability of one, and having the lottery.

[2] The example is inspired from the procedure followed for the determination of "company image" by M. Lifson (1972), p. 112.

good nor bad), in terms of flexibility, and assign to it a value of zero. It should be noted that NDE_1, NDE_2, and NDE_3 could be either individual NDE methods or combinations of them. Hence Y_{14} of any candidate alternative NDE method could be subsequently assessed based on the generated scale that is illustrated in Table 19. If both NDE_1 and NDE_2 methods are included in the candidate alternatives, the magnitude range of Y_{14} would be from -10 to 10 units of the determined scale. In any other case the magnitude range would be determined by the highest and lowest value of Y_{14} among the considered candidate alternatives.

Table 19: Determination of quantitative scale for NDE equipment flexibility.

	NDE_2	NDE_3	NDE_1
Quantitative scale	-10	0	10

7.2.5. Determination of Utility Functions for Decision Criteria

The generation of Table 18 is the basis for the formulation of the utility functions of the decision criteria. Each utility can be assessed by the operator using a series of standard gambles or direct assessment as is described by Lifson (1972). An example of utility determination by means of the standard gamble method is included in the Appendix B for illustrative purposes. One of the initial steps for the generation of any utility function is the determination of a threshold value, Y_{j_T}, which lies in the magnitude range for each decision criterion.

7.2.5.1. Determination of Threshold Values for Decision Criteria

The threshold value, Y_{j_T}, divides the decision criterion's magnitude range into two regions that yield positive and negative utility values, respectively. For instance, an operator might want to use NDE methods to examine a 15 mm composite structure. Assume that he requires a capability of depth detection of at least 3 mm. Thus, the utility of the Y_{12} decision variable (Table 17) should be set to 0 for maximum depth detection capability of 3 mm. Consequently, NDE methods with maximum depth detection capabilities above and below 3 mm would be assigned positive and negative utility values, respectively. Moreover, a utility value of 1 could be assigned to depth detection capability of more than 15 mm. Hence, in the additive value model of any candidate alternative, Y_{12} would contribute positive or negative

utility values if the alternative provides a depth detection capability of more than or less than 3 mm, respectively.

Likewise, an array of threshold values has to be formed for every decision variable, Y_j, whether qualitative or quantitative. The determination of thresholds for qualitative criteria follows the determination of a quantitative scale, as developed in paragraph 7.2.4.1. Threshold values should correspond to 0 utility of any decision variable, and they usually divide the utility function of an attribute into two different functions, both increasing or both decreasing, with different marginal utilities above and below the threshold value. Figure 29 illustrates the form of a typical utility function of a decision criterion, Y_j, is illustrated. The function is monotonically increasing for increasing values of Y_j, clearly showing the increasing and diminishing marginal utilities below and above the threshold value, respectively.

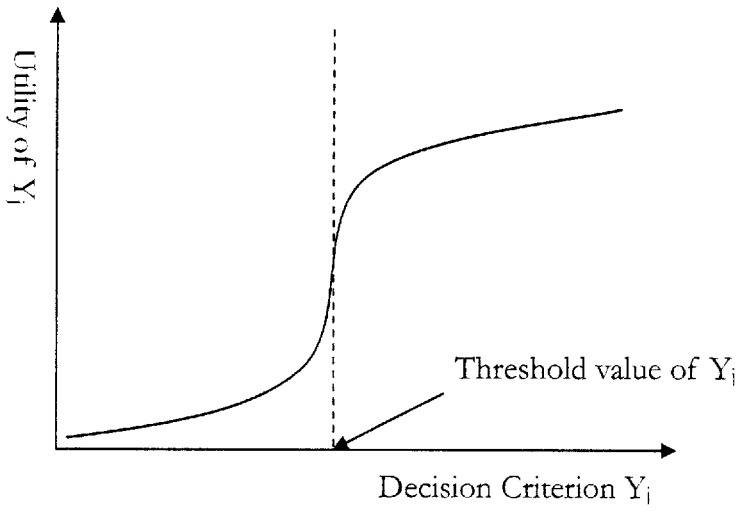

Figure 29: Typical form of utility function for decision criterion Y_j.

Following the determination of the threshold array, the procedure described in Appendix B can be used to determine the array of utility functions for each candidate alternative. Table 20 illustrates the utility function array for candidate alternative A_i.

Table 20: Array of utility functions $u_k(Y_j)$ for candidate alternative A_i.

States of Nature					
Decision Criteria	S_1 $Y_{j,k} < Y_{j,k\_T}$	S_1 $Y_{j,k} \geq Y_{j,k\_T}$	. . .	S_9 $Y_{j,k} < Y_{j,k\_T}$	S_9 $Y_{j,k} \geq Y_{j,k\_T}$
Y_1	$u_{1\_b}(Y_1)$	$u_{1\_a}(Y_1)$	. . .	$u_{9\_b}(Y_1)$	$u_{9\_a}(Y_1)$
.	.	.	. . .	.	.
.	.	.	. . .	.	.
.	.	.	. . .	.	.
Y_j	$u_{1\_b}(Y_j)$	$u_{1\_a}(Y_j)$	. . .	$u_{9\_b}(Y_j)$	$u_{9\_a}(Y_j)$
.	.	.	. . .	.	.
.	.	.	. . .	.	.
.	.	.	. . .	.	.
Y_{17}	$u_{1\_b}(Y_{17})$	$u_{1\_a}(Y_{17})$	. . .	$u_{9\_b}(Y_{17})$	$u_{9\_a}(Y_{17})$

In Table 20 it should be emphasized that utility functions consist of two segments that correspond to magnitudes below and above the threshold value of each decision criterion. Namely,

$$u_k(Y_j) = \begin{cases} u_{k\_a}(Y_j) & \text{if } Y_j \geq Y_{j\_T} \\ u_{k\_b}(Y_j) & \text{if } Y_j < Y_{j\_T} \end{cases}$$

7.2.6. Decision Criteria Estimates

The determination of the utility functions for each decision criterion was developed in paragraph 7.2.5. In addition, the value model should take into account the risk related to the selection of candidate alternative A_i. Such risk results from the uncertainty in the values of the decision criteria outcome vector, Y_{ijk}, which a candidate alternative, A_i, will yield for any of the states of the nature.

For instance, the specifications of an NDE method could claim that it can detect moisture absorption levels (decision criterion Y_{11} of Table 17) above 1.5% with 100% probability. This would in essence be the value of the cumulative density function of Y_{11}'s probability distribution for moisture content above the magnitude of 1.5%. Thus, the specific NDE method would detect a moisture content of less than 1.5% with a probability density function that could be provided by the NDE method specifications, be assessed by the

operator through a number of experiments, or if experimental resources are lacking, be generated from historical data. For decision criteria that have discrete values, a discrete probability distribution and a cumulative mass function can be determined likewise. A hypothetical example of Y_{11}'s probability distribution function and its related cumulative distribution function, for the aforementioned values, is illustrated below.

$$PDF(Y_{11}) := \begin{cases} 0 & \text{if } Y_{11} > 1.5 \\ 5 \cdot e^{5(Y_{11}-1.5)} & \text{if } Y_{11} \le 1.5 \end{cases} \qquad CDF(Y_{11}) := \begin{cases} 1 & \text{if } Y_{11} > 1.5 \\ e^{5(Y_{11}-1.5)} & \text{if } Y_{11} \le 1.5 \end{cases}$$

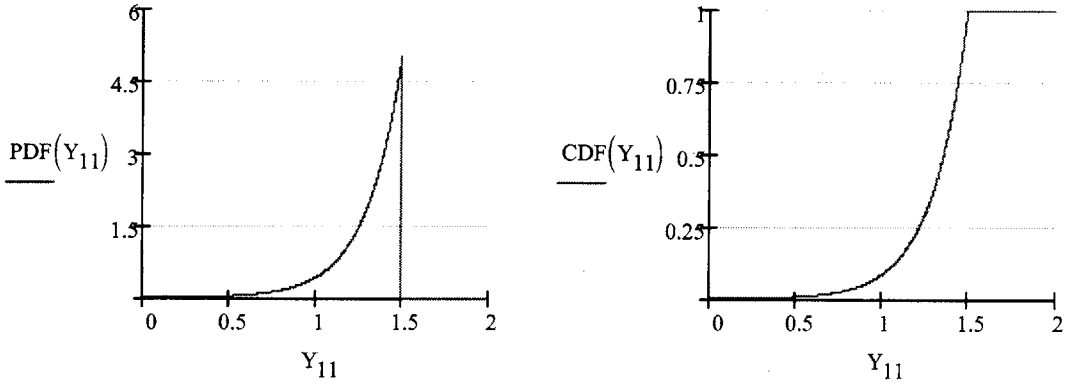

Commonly used PDFs (exponential, normal, binomial, Poisson, gamma, beta etc.) might be utilized, by manipulation of their parameters, to represent operator's uncertainty in the outcome of a decision criterion. Hence, a matrix of probability density functions, such as the one illustrated in Table 21, can be generated for each decision criterion.

Table 21: Matrix of PDFs for each decision criterion.

	$PDF_{i,k}(Y_j)$		
Decision Criteria	S1	. . .	S9
Y_1	$PDF_{i,1}(Y_1)$	. . .	$PDF_{i,9}(Y_1)$
.	.	. . .	.
.	.	. . .	.
.	.	. . .	.
Y_j	$PDF_{i,1}(Y_j)$	. . .	$PDF_{i,9}(Y_j)$
.	.	. . .	.
.	.	. . .	.
.	.	. . .	.
Y_{17}	$PDF_{i,1}(Y_{17})$	. . .	$PDF_{i,9}(Y_{17})$

7.2.7. The Value Model

In the previous paragraphs, the utility of each decision criterion for the various states of nature, and the corresponding probability density functions for each candidate alternative, have been determined. The expected utility of each decision criterion, Y_j, given a specific candidate alternative, A_i, and a particular state of nature, S_k, can now be calculated as:

Equation 2

$$u_{ijk} = \int_{-\infty}^{\infty} u_k(Y_j) \cdot PDF_{ik}(Y_j) \cdot dY_j$$

As developed in 7.2.3, an additive model (see Equation 1) can be utilized to represent the value of each candidate alternative. In order to avoid adding dissimilar quantities, such as units of length, time, and money, a normalization of the utilities, defined by Equation 2, is considered necessary. Normalization of all the decision criteria is obtained after dividing by their corresponding threshold values. In the following set of equations it is assumed that

$$Y_{j\_norm} = \frac{Y_j}{Y_{j\_threshold}}$$

It follows that, assuming equal weights of each decision criterion in the value model, the expected utility for candidate alternative A_i, and state of nature S_k can now be calculated as:

Equation 3

$$u_{ik} = \sum_j u_{ijk} = \sum_j \int_{-\infty}^{\infty} u_k(Y_{j\_norm}) \cdot PDF_{ik}(Y_{j\_norm}) \cdot dY_{j\_norm}$$

Consequently, introducing the probability of each state of nature, P_k from Table 16, the expected utility for each specific candidate alternative can now be calculated as:

Equation 4

$$u_i = \sum_k \left(P_k \cdot u_{ik} \right)$$

$$u_i = \sum_k \left[P_k \cdot \left(\sum_j \int_{-\infty}^{\infty} u_k(Y_{j\_norm}) \cdot PDF_{ik}(Y_{j\_norm}) \cdot dY_{j\_norm} \right) \right]$$

7.2.7.1. Determination of Decision Criteria Weights

The above equations include the assumption of equal relative weights for the decision criteria in the value model. This assumption, of course, does not reflect reality as the decision criteria are usually assigned various weights, which moreover are dependent on the state of nature.

For instance, assume that the operator assesses the relative importance of each decision criterion in S_2 and S_7 states of nature (see Table 16—S_2 and S_7 are the states that describe damages where the most influencing defect is "core crush" and "moisture ingress", respectively). Hence, the presence of other defects is not excluded and consequently it would be valuable to estimate their severity as well. A simple method for the designation of relative weights is to consider every decision criterion at its magnitude that yields a utility of 1. Then the operator can assign to each decision criterion a value from an arbitrary scale, e.g. 0-10, according to the relative importance of each criterion for each state of nature. It is clear that for the aforementioned states of nature, S_2 and S_7, the operator would assign the value of 10 to each of the decision criteria Y_5 and Y_{11}, respectively (see Table 17). Subsequently, the operator could assign values to the other decision criteria using the same scale to represent their relative weight in comparison to the criterion that was given the value of 10. If the operator judges that a specific criterion is insignificant, he could even assign the value of 0 to it. If, for example, the problem at hand is the NDE of a single-skin composite structure, the operator should assign relative weights of 0 to decision criteria that correspond to sandwich composites, such as Y_2, Y_4, Y_5, and Y_{10} (see Table 17). The weight of each decision criterion would then be its relative weight divided by the sum of relative weights.

With the above procedure the weights would add up to unity, yielding a consistent scale for any state of nature. This procedure for determining the decision variable weights for

state of nature S_k and a hypothetical relative weight assignment, by the operator, are illustrated in Table 22.

Table 22: Decision criteria hypothetical weights, w_{jk} (for state of nature S_k).

Decision Criterion	Relative weights using 0-10 scale	Normalized Weights[1]
Y1	6	0.08
Y2	0	0
Y3	6	0.08
Y4	0	0
Y5	0	0
Y6	4	0.053333
Y7	5	0.066667
Y8	2	0.026667
Y9	2	0.026667
Y10	0	0
Y11	**10**	0.133333
Y12	7	0.093333
Y13	7	0.093333
Y14	6	0.08
Y15	4	0.053333
Y16	4	0.053333
Y17	5	0.066667
Y18	7	0.093333
Sum	75	**1**

Taking into account the weights w_{jk}, Equation 3 and Equation 4 become Equation 5 and Equation 6, respectively:

Equation 5

$$u_{ik} = \sum_j u_{ijk}$$

$$u_{ik} = \sum_j w_{jk} \cdot \left(\int_{-\infty}^{\infty} u_k(Y_{j\_norm}) \cdot PDF_{ik}(Y_{j\_norm}) \cdot dY_{j\_norm} \right)$$

[1] As is it clarified in the text the sum of the relative weights of vector [Y] is used to normalize the vector components, and not the vector norm that is defined as:

$$|Y| = \sqrt{\sum_j Y_j^2}$$

Equation 6

$$u_i = \sum_k \left(P_k \cdot u_{ik} \right)$$

$$u_i = \sum_k \left[P_k \cdot \sum_j \left(w_{jk} \cdot \int_{-\infty}^{\infty} u_k(Y_{j\_norm}) \cdot PDF_{ik}(Y_{j\_norm}) \cdot dY_{j\_norm} \right) \right]$$

7.3. Conclusions

The importance of damage evaluation using NDE methods was emphasized in Section 2. In Section 7 a methodology was developed, using utility theory, in order to provide a means of assessing the ideal NDE scheme among all possible alternatives. The value model, described by Equation 6, yields the utility of each candidate alternative, and hence indicates the ideal one, the candidate with the highest value of utility. Of course, it should be kept in mind that the reliability of the results depends on the ability to obtain the required inputs and the validity of the assumptions.

References

1 L. Tong and K. Soutis, Recent Advances in Structural Joints and Repairs for Composite Materials, 2003.

2 M. W. Lifson, Decision and Risk Analysis for Practicing Engineers, 1972.

3 K. T. Kedward and H. Kim, Joining and Repair of Composite Structures, 2003.

4 K. B. Armstrong, L. G. Bevan, and W. F. Cole Ii, Care and Repair of Advanced Composites, 2005.

5 H. Brown, Composite Repairs-SAMPE Monograph No. 1, 1985.

6 http://www.NDT-Ed.Org, (This site was designed to be a comprehensive source of information and materials for NDT and NDE technical education), visited January 2007.

7 P. Davies, Adhesive Bonding- Science Technology and Applications, Edited By R. D. Adams, 2005.

8 K. B. Armstrong, "Eleven Years of Work to Standardize Aerospace Composite Repairs 1988-1999", International Conference on Joining and Repair of Plastics and Composites, I Mech. E, 1999.

9 D. M. Elliot and M. Mcgugan, "Performance of Stepped Repairs Utilizing 'Structural' Testpieces and As A Function of Temperature", International Conference on Joining and Repair of Plastics and Composites, I Mech. E, 1999.

10 M. N. Charalambides, A. J. Kinloch, and F. L. Matthews, "Evaluation of Durability of Bonded Repairs to CFRP", International Conference on Joining and Repair of Plastics and Composites, I Mech E, 2000.

11 K. Zimmerman and D. Liu, "Geometrical Parameters in Composite Repair", Journal of Composite Materials, 1995.

12 R. F. Wegman and T. R. Tullos, Handbook of Adhesive Bonded Structural Repair, 1992.

13 T. S. Jones, "Nondestructive Evaluation Methods for Composites", Handbook of Composites. Edited By S.T. Peters, 1998.

14 J. E. Robson, F. L. Matthews, and A. J. Kinloch, "The Strength of Composite Repair Patches: A Laminate Analysis Approach", Journal of Reinforced Plastics and Composites, Vol. 11-July, 2002.

15 S. Ahn and G. S. Springer, "Repair of Composite Laminates-I: Test Results", Journal of Composite Materials, Vol. 32, No 11, 1998.

16 S. J. John, A. J. Kinloch, and F. L. Matthews, "Measuring and Predicting the Durability of Bonded Carbon Fiber/Epoxy Composite Joints", Composites, Vol. 22, March, 1991.

17 J. E. Robson, F. L. Matthews, and A. J. Kinloch, "The Bonded Repair of Fiber Composites: Effect of Composite Moisture Content", Journal of Composites Science and Technology, Vol. 52, pp. 235-246, 1994.

18 S. Hamoush, K. Shivakumar, F. Darwish, M. Sharpe, and P. Swindell, "Defective Repairs of Laminated Solid Composites", Journal of Composite Materials, Vol. 39, No 24, 2005.

19 F. H. Darwish, K. N. Shivakumar, S. Hamoush, and D. Hsu, "Performance of Patch Repaired Composite Panels-Static and Fatigue", 47Th AIAA/ASME/ASCE/AHS/ASC Structures, Structural Dynamics, and Materials Conference, 2006.

20 P. Davies, D. Choqueuse, B. Bigourdan, C. Gauthier, R. Joannic, P. Parneix, and J. L'Hostis, "Design, Manufacture and Testing of Stiffened Panels for Marine Structures Using Adhesively Bonded Poltruded Sections", Proc. Instn Mech. Engrs Vol. 218 Part M: J. Engineering for The Maritime Environment, 2004.

21 P. Daives and Jp. Sargent, "Fracture Mechanics Tests To Characterize Bonded Glass/Epoxy Composites: Application To Strength Prediction in Structural Assemblies", Proceedings of 3rd ESIS Conference on Fracture of Polymers, Composites and Adhesives, Elsevier, 2003.

22 K. B. Armstrong, "Effect of Absorbed Water in CFRP Composites on Adhesive Bonding", International Journal of Adhesion and Adhesives, 1996.

23 C. Soutis and F. Z. Hu, "Design and Performance of Bonded Patch Repairs of Composite Structures", Proceedings of Institution of Mechanical Engineers, Vol. 211, Part G, pp. 263-271, 1997.

24 S. H. Myhre, J. D. Labor, and S. C. Aker, "Moisture Problems in Advanced Composite Structural Repair", Composites, July, 1982.

25 A. J. Kinloch and S. J. Shaw, "The Fracture Resistance of A Toughened Epoxy Adhesive", Journal of Adhesion, Vol. 12, pp. 59-77, 1981.

26 G. Marom and L. J. Broutman, "Moisture in Epoxy Resin Composites", Journal of Adhesion, Vol. 12, pp. 153-154, 1981.

27 F. Ellyin and C. Rohrbacher, "The Influence of Aqueous Environment, Temperature and Cyclic Loading on Glass-Fiber/Epoxy Composite Laminates", Journal of Reinforced Plastics and Composites, Vol. 22, No. 7, 2003.

28 L. J. Hart-Smith, "An Engineer's Viewpoint on Design and Analysis of Aircraft Structural Joints", Proceedings of The Institution of Mechanical Engineers. Part G, Journal of Aerospace Engineering, 1995, 209(G2), pp.105-129, 1995.

29 L. J. Hart-Smith, "Adhesively Bonded Joints for Fibrous Composite Structures", 2003.

30 W. W. Wright, "The Effect of Diffusion of Water into Epoxy Resins and Their Carbon-Fiber Reinforced Composites", Composites, July, 1982.

31 M. V. Hosur, U. K. Vaidya, D. Mayers, and S. Jeelani, "Studies on The Repair of Ballistic Impact Damaged S2-Glass/Vinyl Ester Laminates", Composite Structures, pp. 281-290, 2003.

32 W. S. Chan and S. Vedhagiri, "Analysis of Composite Bonded/Bolted Joints Used in Repairing", Journal of Composite Materials, Vol. 35, No. 12, 2001.

33 D. M. Elliot and R. S. Trask, "Damage Tolerance and Repair of GFRP Warships", Journal of Thermoplastic Composite Materials, Vol. 14-May, 2001.

34 D. Zenkert, A. Shipsha, P. Bull, and B. Hayman, "Damage Tolerance Assessment of Composite Sandwich Panels With Localized Damage", Composites Science and Technology, 65, pp. 2597–2611, 2005.

35 K. B. Zimmerman and D. Liu, "An Experimental Investigation of Composite Repair", Journal of Experimental Mechanics, Vol. 36, 2, June, 1996.

36 U. K. Vaidya, G. Basappa and B. Mathew, "Flexural Fatigue Response of Repaired S2-Glass/Vinyl Ester Composites", 32Nd International SAMPE Technical Conference, Nov. 5-9, 2000.

37 T. J. Turtona, J. Dalzel-Jobb, and F. Livingstone, "Oil Platforms, Destroyers and Frigates—Case Studies of Qinetiq's Marine Composite Patch Repairs", Composites: Part A, 36, pp.1066–1072, 2005.

38 http://www.NetComposites.Com/Education.Asp, (NetComposites is a global research, consultancy and online media company, creating and using innovative technologies to advance the composites industry as well as running the industry's leading online portal for composites), visited March 2007.

39 P. Lazarus, "Resin Infusion of Marine Composites", Proceedings of The 1996 41St International SAMPE Symposium and Exhibition. Part 2 (of 2), 1996.

40 I. Grabovac, "Bonded Composite Solution to Ship Reinforcement", Composites: Part A 34, pp. 847–854, 2003.

41 J. R. Weitzenbock, A. T. Echtermeyer, F. Artiga-Dubois, and M. Parmar, "Nondestructive Inspection and Evaluation Methods for Composites Used in The Marine Industry", Iccm-12 Europe; International Conference on Composite Materials, Palais Des Congres, Paris, 5Th-9Th July, 1999.

42 Anon, "Bondship Partners Could Stick Ships Together", Warship Technology, N July/Aug., Jul, pp. 14-15, 2000.

43 R. C. Allan, J. Bird, and J. D. Clarke, "The Use of Adhesives in The Repair of Cracks in Ships' Structures", Mech E Conference Publications (Institution of Mechanical Engineers), pp. 169-178, 1986.

44 C. Soutis, D-M. Duan, and P. Goutas, "Compressive Behaviour of CFRP Laminates Repaired With Adhesively Bonded External Patches", Composite Structures 45, pp. 289-

301, 1999.

45 A. J. Gunnion and I. Herszberg, "Parametric Study of Scarf Joints in Composite Structures", Composite Structures, 75, pp. 364–376, 2006.

46 X. Liu and G. Wang, "Progressive Failure Analysis of Bonded Composite Repairs", Composite Structures, 2006.

47 A. M. Kumar and S.A. Hakeem, "Optimum Design of Symmetric Composite Patch Repair to Center Cracked Metallic Sheet", Composite Structures, 49, pp. 285-292, 2000.

48 A. C. Okafor and H. Bhogapurapu, "Design and Analysis of Adhesively Bonded Thick Composite Patch Repair of Corrosion Grind-Out and Cracks on 2024 T3 Clad Aluminum Aging Aircraft Structures", Composite Structures, 76, pp. 138–150, 2006.

49 M. A. Jarrah, M. S. M. Tahat, and S. V. Hoa, "Mode-II Fracture at The Interface Between A Base and A Repair Graphite/Epoxy Laminates", Journal of Reinforced Plastics and Composites, Vol. 21, No. 11, 2002.

50 L. P. Kollar and G. S. Springer, "Mechanics of Composite Structures", 2003.

51 W. F. Cole, "Technical Justification of Repairs to Composite Laminates", International Journal of Adhesion & Adhesives 19, pp. 107-120, 1999.

52 T. E. Tay, F. S. Chau, and C. J. Er, "Bonded Boron-Epoxy Composite Repair and Reinforcement of Cracked Aluminium Structures", Composite Structures 34, pp. 339-347, 1996.

53 V. Sabelkin, S. Mall, M.A. Hansen, R.M. Vandawaker, and M. Derriso, "Investigation into Cracked Aluminum Plate Repaired With Bonded Composite Patch", Composite Structures, V 79, N 1, June, pp. 55-66, 2007.

54 H. Hosseini-Toudeshky, S. Bakhshandeh, B. Mohammadi, and H. R. Daghyani, "Experimental Investigations on Fatigue Crack Growth of Repaired Thick Aluminum Panels in Mixed-Mode Conditions", Composite Structures, 75, pp. 437–443, 2006.

55 R. Jones and W. K. Chiu, Composite Repairs To Cracks In Thick Metallic Components", Composite Structures, 44, pp. 17-29, 1999.

56 A. A. Taib, R. Boukhili, S. Achiou, S. Gordon, and H. Boukehili, "Bonded Joints With Composite Adherends. Part I. Effect of Specimen Configuration, Adhesive Thickness, Spew Fillet and Adherend Stiffness on Fracture", International Journal of Adhesion & Adhesives, 26, pp. 226-236, 2006.

57 R. D. Adams and J. A. Harris, "The Infuence of Local Geometry on The Strength of Adhesive Joints", International Journal of Adhesion & Adhesives Vol. 7, No. 2, April., 1987.

58 http://www.FAA.Gov/Regulations_Policies, (Website of Federal Aviation Administration), visited December 2006.

59 F. Artiga-Dubois, M. Parmar, J. R. Weitzenbock, and A. T. Echtermeyer, "Non Destructive Testing of Composites for Naval Applications", Advanced Materials and Processes Affordabilities for The New Age (Paris La Défense, April 13-15 1999) Society for The Advancement of Material and Process Engineering. International SAMPE Europe Conference No20, Puteaux , France (13/04), pp. 491-502, 1999.

60 I. Grabovac,P. J. Pearce,A. Camilleri,K. Challis, and J. Lingard, "Are Composites Suitable for Reinforcement of Ship Structures?", Proceedings of The 12Th International Conference on Composite Materials, Paris, July 5–9, 1999.

61 Yoseph Bar-Cohen, "Emerging NDE Technologies and Challenges at the Beginning of the 3rd Millennium ",URL http://www.ndt.net/article/v05n02/barcohen/barcohen.htm#22, visited March 2007.

62 R.L. Keeney, H. Raiffa, Decisions With Multiple Objectives: Preferences and Value Tradeoffs, 1976.

Appendix A

Table 23: Comparison of most commonly used NDE methods.

	Specialized equipment	Well trained personnel	Time consuming for large areas	In depth detection	Most appropriate for	Least appropriate for	Detection of heat damage	Indication of defect depth	Accurate size/shape ind.	Calibration needed	Safety protection	Reference
Visual inspection	NO	NO	YES	NO			YES	NO	NO			4, 12, 13
Tap testing (electronic)	NO	NO	YES	Only for **thin** skins	[4]: Honeycomb panels		YES	NO		YES		4, 12, 13,41
Ultrasonic (pulse- echo)	YES	YES	YES	YES	[12], [41]: Thick single-skin composites	[4]: Honeycomb panels [41]: Thick sandwich composites	YES	YES	YES	YES		4, 7, 12, 13,41
X-ray inspection	YES	YES	YES		[4], [13]: Boron and **glass** fiber composites [12], [13]: Honeycomb panel in bonded sandwich assy	[4], [13]: **Carbon** fiber composites					YES	4, 12, 13
Eddy currents	YES	YES		NO	[4]: Conductive materials(**carbon** fiber composites)	[4]: Non conductive materials	YES	YES		YES		4, 13
Interferometry	YES	YES	NO	NO			YES					4, 7, 13
Bond testers	YES	YES	NO		[4]: Fast inspection of large areas, honeycomb structures [13]: Complex bonded structures	[4]: Small localized defects						4, 7, 13
Thermography	YES	YES	NO*	[13]: Poor and only with through transmission [41]: YES	[4]: Fast inspection of large areas	[41]: Complex geometries						4, 7, 13,41

Key:

1. Blank cells indicate that the component was not clarified by any of the researched references.
2. Cells without citations of references indicate concurrence of the researched references.

* Preparation of the surface, mounting of the TIC camera and heating of the surface is time consuming [41].

Appendix B

Example of Utility Determination Using the Standard Gamble Method

Let us assume that the utility of decision criterion Y_1 (see Table 17) needs to be determined. This criterion, "Single-skin delamination detection", reflects the ability of NDE methods to detect the described defect. Referring to GFRP warships' repairs D. M. Elliott and R.S. Trask state that:

> Realistically, it is not practical, due to the size of the structure and the time available, to search for delaminations that are below 100mm (4″) in diameter, unless they are surface breaking—i.e., visible. Hence, anything below this size is left unrepaired unless it could provide a moisture ingress path into the structural laminates. Having said this, it is a fact that 50% of all delamination defects found in service lie within the 100 mm (4″) to 300 mm (1') diameter size envelope.

Hence the range of 100 mm to 300 mm could be used as the magnitude range of decision criterion Y1. Let us also assume that experimental studies determined that a delamination size below 170 mm affects the tensile and compressive strength of the structure insignificantly, while sizes above 170 mm degrade these properties severely. Hence, it would be essential for the operator to know how close to 170 mm the defect size lies, to be able to assess the impact on the safe operation of the structure.

In this specific context the operator could determine that the threshold value for Y1 is 170 mm. This threshold value would represent that the operator requires a minimum delamination size detection of at least 170 mm. Thus, the utility of 0 could be designated to the capability of minimum delamination detection size of 170 mm. Additionally, the value of 1, in the utility scale, can be set for the capability of minimum defect size detection of 100 mm, since this is the best (minimum) practically detectable delamination size. Moreover, it can be assumed that the capability of minimum defect size detection of 300 mm represents the value of -1 in the utility scale, since the size of the defect is so extensive that would probably be detected without the need of NDE methods. Thus:

Equation 7

$$u(Y_1) = \begin{cases} 1 \text{ if } Y_1 = 100\text{mm} \\ 0 \text{ if } Y_1 = 170\text{mm} \\ -1 \text{ if } Y_1 = 300\text{mm} \end{cases}$$

The operator is requested to determine his certainty equivalent[1], CE1, for lottery L1 that has the following specifics:

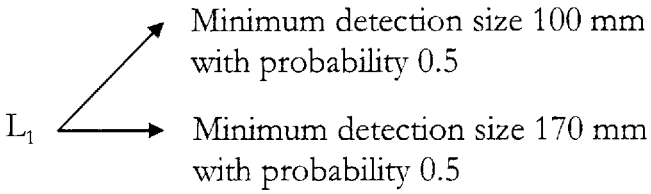

Theoretically the expected value of lottery L1 would be 0.5*(100+170) mm = 135 mm. This would mean that if the operator chooses the lottery he would have an expected minimum detection size of 135 mm. However, choosing the lottery L1 would provide the possibility of detecting defects of either greater than 100 mm or greater than 170 mm. Detecting defects as small as 100 mm would be meaningless for the operator since the structural integrity is not immediately threatened by sizes of that magnitude. On the other hand, detecting defects greater than 170 mm would be essential to determine whether the structure needs repair. Hence the operator could determine that his certainty equivalent for lottery L1 is 160 mm. This would reflect that he is risk averse since he is indifferent between having a detection scheme with minimum detection size of 160 mm and the detection scheme of lottery L1, with the expected value of 135 mm. Such a behavior would be justified by the operator's urge to be able to determine whether the defect size is greater than 170 mm. Hence the utility of CE1 would be the same as the utility of L1. Specifically:

[1] The certainty equivalent is the value of delamination size for which the operator would be indifferent between having defects greater or equal to this value detected with certainly, that is probability one, and having lottery L1.

$$u(CE_1) = u(L_1)$$
$$u(L_1) = 0.5 \cdot u(100mm) + 0.5 \cdot u(170mm)$$
$$u(L_1) = 0.5 \cdot 1 + 0.5 \cdot 0 = 0.5$$

Hence,

$$u(CE_1) = u(160\ mm) = 0.5$$

Thus, a third point of the utility curve of Y1 is obtained for the magnitude range that is below the threshold value Y_{1_T} (the other two are determined by Equation 7).

Accordingly the operator could be requested to determine his certainty equivalent, CE2, for the lottery L2 with the following specifics:

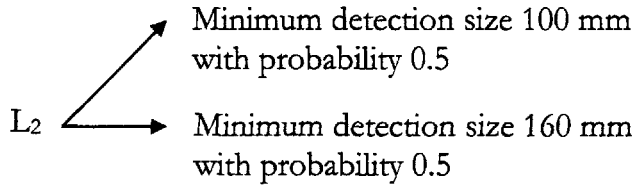

Theoretically the expected value of lottery L2 would be 0.5*(100+160) mm = 130 mm. This would mean that if the operator chooses the lottery he would have an expected minimum detection size of 130 mm. The operator could assess that his certainty equivalent, CE2, is 150 mm. This would reflect that he is risk averse since he is indifferent between having a detection scheme with minimum detection size of 150 mm and the detection scheme of lottery L2, with the expected value of 130 mm. Hence the utility of CE2 would be the same as the utility of L2. Specifically:

$$u(CE_2) = u(L_2)$$
$$u(L_2) = 0.5 \cdot u(100mm) + 0.5 \cdot u(160mm)$$
$$u(L_1) = 0.5 \cdot 1 + 0.5 \cdot 0.5 = 0.75$$

Hence,

$$u(CE_2) = u(150\ mm) = 0.75$$

Thus, a fourth point of the utility curve of Y1 is obtained for the magnitude range below the threshold value of 170 mm.

In addition the operator could be requested to determine his certainty equivalent, CE3, for the lottery L3 with the following specifics:

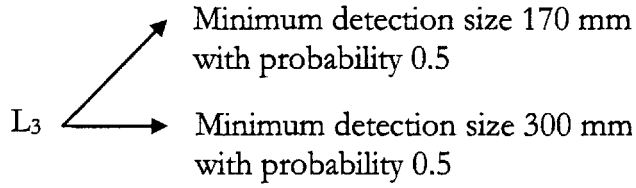

Theoretically the expected value of lottery L3 would be 0.5*(170+300) mm = 235 mm. This would mean that if the operator chooses the lottery he would have an expected minimum detection size of 235 mm. Let us assume that the operator's certainty equivalent, CE3, is 190 mm. This would reflect that he is risk prone since he is indifferent between having a detection scheme with minimum detection size of 190 mm and the detection scheme of lottery L3, with the expected value of 235 mm. Hence the utility of CE3 would be the same as the utility of L3. Specifically:

$$u(CE_3) = u(L_3)$$
$$u(L_3) = 0.5 \cdot u(170\text{mm}) + 0.5 \cdot u(300\text{mm})$$
$$u(L_3) = 0.5 \cdot 0 + 0.5 \cdot (-1) = -0.5$$

Hence,

$$u(CE_3) = u(190\text{ mm}) = -0.5$$

Hence, a third data point is generated for the utility function of Y1 for magnitude ranges above the threshold value of 170 mm.

Accordingly the operator could be requested to determine his certainty equivalent, CE4, for the lottery L4 with the following specifics:

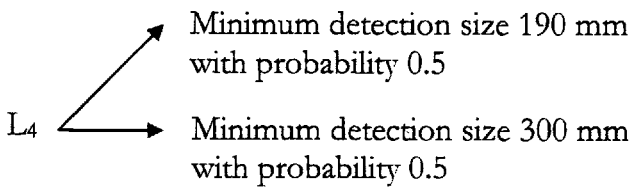

Theoretically the expected value of lottery L4 would be 0.5*(190+300) mm = 245 mm. This would mean that if the operator chooses the lottery he would have an expected minimum detection size of 245 mm. Let us assume that the operator's certainty equivalent, CE4, is 220 mm. This would reflect that he is risk prone since he is indifferent between having a detection scheme with minimum detection size of 220 mm and the detection scheme of lottery L4, with the expected value of 245 mm. Hence the utility of CE4 would be the same as the utility of L4. Specifically:

$$u(CE_4) = u(L_4)$$
$$u(L_4) = 0.5 \cdot u(190\text{mm}) + 0.5 \cdot u(300\text{mm})$$
$$u(L_4) = 0.5 \cdot 0.5 + 0.5 \cdot (-1) = -0.75$$

Hence,

$$u(CE_4) = u(220\text{ mm}) = -0.75$$

Hence, a fourth data point is generated for the utility function of Y1 for magnitude ranges above the threshold value of 170 mm.

Thusly, utilizing a set of standard gambles the operator managed to determine four data points of his utility function for Y1, in addition to the three initial ones determined by Equation 7. The procedure of standard gambles could continue until the number of data points is considered satisfactory for the precise representation of the utility curve. The operator's utility function, as determined by the data points obtained with the above analysis, is illustrated in Figure 30. The straight lines represent a two-part piecewise linear utility function for Y1, where the first and second part correspond to the linear utilities below and above the threshold value, respectively.

From the series of data points a utility function can be determined using curve fitting. In the example above, the utility of Y1 could be described by two functions:

Equation 8

$$u(Y_1) = \begin{cases} u_a(Y_1) & \text{if } Y_1 \geq Y_{1\_T} \\ u_b(Y_1) & \text{if } Y_1 < Y_{1\_T} \end{cases}$$

In Equation 8, subscripts "a" and "b" indicate that the utility function of Y1 assumes values above and below the threshold of 170 mm, respectively.

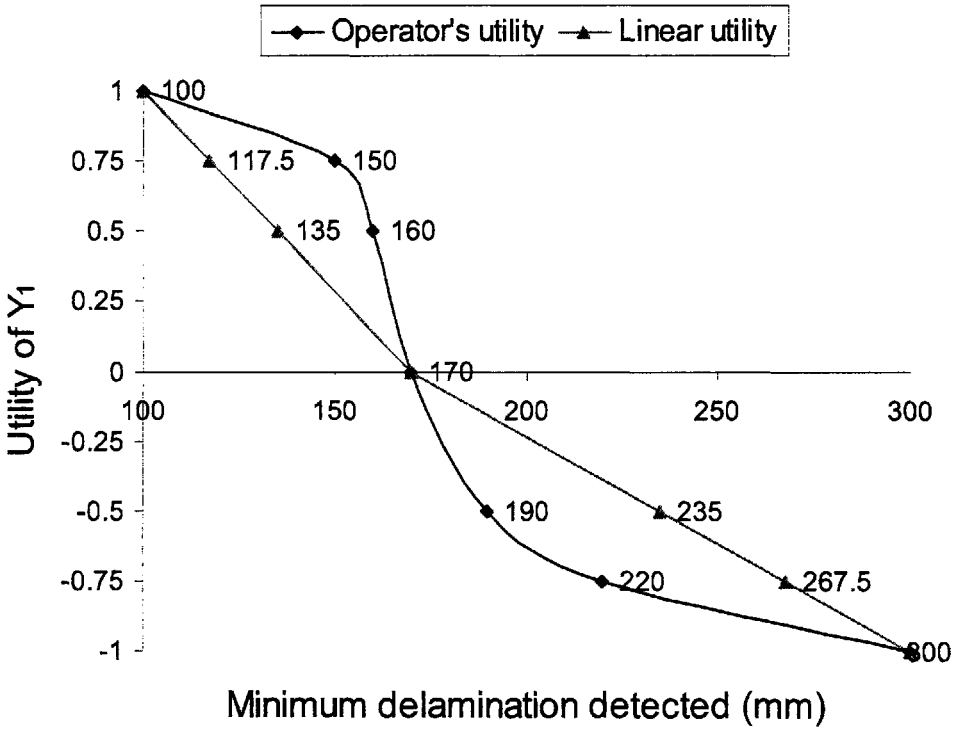

Figure 30: Operator's utility function of Y_1.

Appendix C

Determination of tensile stiffness for parent and repair composite lay-ups.

The parent lay up is: [(0/90/±45/90/0)2]s.
The patch lay up is: [±45].

Properties of the prepreg ply used for both parent and patch material:

Longitudinal Young modulus	$E_1 := 135\text{GPa}$
Transverse Young's modulus	$E_2 := 8.8\text{GPa}$
Longitudinal shear modulus	$G_{12} := 4.47\text{GPa}$
Longitudinal Poisson's ratio	$\nu_{12} := 0.33$
Transverse Poisson's ratio	$\nu_{23} := 0.48$

The parent thickness is 2.88 mm and consists of 24 plies. Hence, each ply has a thickness of:

$$h := \frac{2.88}{24}\text{mm} \qquad h = 1.2 \times 10^{-4}\ \text{m}$$

Of course this is an approximation since the adhesive thickness between the layers is disregarded.

For a transversely isotropic material, such as the prepreg used, under plane-stress condition, the stiffness matrix is:

$$\begin{pmatrix} Q_{11} & Q_{12} & Q_{16} \\ Q_{12} & Q_{22} & Q_{26} \\ Q_{16} & Q_{26} & Q_{66} \end{pmatrix} = \begin{pmatrix} S_{11} & S_{12} & S_{16} \\ S_{12} & S_{22} & S_{26} \\ S_{16} & S_{26} & S_{66} \end{pmatrix}^{-1}$$

where S_{ij} are the elements of the compliance matrix S_{TI} (the subscripts TI denote transversely isotropic material).

$$S_{TI} := \begin{pmatrix} \frac{1}{E_1} & \frac{-\nu_{12}}{E_1} & 0 \\ \frac{-\nu_{12}}{E_1} & \frac{1}{E_2} & 0 \\ 0 & 0 & \frac{1}{G_{12}} \end{pmatrix}$$

Stiffness matrix at 0° orientation of the fibers with respect to the load direction

$$Q_0 := S_{TI}^{-1} \qquad Q_0 = \begin{pmatrix} 1.36 \times 10^{11} & 2.925 \times 10^{9} & 0 \\ 2.925 \times 10^{9} & 8.863 \times 10^{9} & 0 \\ 0 & 0 & 4.47 \times 10^{9} \end{pmatrix} \text{ Pa}$$

Stiffness matrix at +45° orientation of the fibers with respect to the load direction

$$c = \cos\left(\frac{\pi}{4}\right) \qquad s = \sin\left(\frac{\pi}{4}\right)$$

$$T_{\sigma\_plus45} := \begin{pmatrix} c^2 & s^2 & 2 \cdot s \cdot c \\ s^2 & c^2 & -2 \cdot c \cdot s \\ -c \cdot s & c \cdot s & c^2 - s^2 \end{pmatrix} \qquad T_{\sigma\_plus45} = \begin{pmatrix} 0.5 & 0.5 & 1 \\ 0.5 & 0.5 & -1 \\ -0.5 & 0.5 & 0 \end{pmatrix}$$

$$T_{\varepsilon\_plus45} := \begin{pmatrix} c^2 & s^2 & s \cdot c \\ s^2 & c^2 & -s \cdot c \\ -2s \cdot c & 2s \cdot c & c^2 - s^2 \end{pmatrix} \qquad T_{\varepsilon\_plus45} = \begin{pmatrix} 0.5 & 0.5 & 0.5 \\ 0.5 & 0.5 & -0.5 \\ -1 & 1 & 0 \end{pmatrix}$$

$$Q_{plus45} := T_{\sigma\_plus45}^{-1} \cdot Q_0 \cdot T_{\varepsilon\_plus45}$$

$$Q_{plus45} = \begin{pmatrix} 4.214 \times 10^{10} & 3.32 \times 10^{10} & 3.178 \times 10^{10} \\ 3.32 \times 10^{10} & 4.214 \times 10^{10} & 3.178 \times 10^{10} \\ 3.178 \times 10^{10} & 3.178 \times 10^{10} & 3.474 \times 10^{10} \end{pmatrix} \text{ Pa}$$

Stiffness matrix at -45° orientation of the fibers with respect to the load direction

$$c = \cos\left(-\frac{\pi}{4}\right) \qquad s = \sin\left(-\frac{\pi}{4}\right)$$

$$T_{\sigma\_minus45} := \begin{pmatrix} c^2 & s^2 & 2\cdot s\cdot c \\ s^2 & c^2 & -2\cdot c\cdot s \\ -c\cdot s & c\cdot s & c^2 - s^2 \end{pmatrix} \qquad T_{\sigma\_minus45} = \begin{pmatrix} 0.5 & 0.5 & -1 \\ 0.5 & 0.5 & 1 \\ 0.5 & -0.5 & 0 \end{pmatrix}$$

$$T_{\varepsilon\_minus45} := \begin{pmatrix} c^2 & s^2 & s\cdot c \\ s^2 & c^2 & -s\cdot c \\ -2s\cdot c & 2s\cdot c & c^2 - s^2 \end{pmatrix} \qquad T_{\varepsilon\_minus45} = \begin{pmatrix} 0.5 & 0.5 & -0.5 \\ 0.5 & 0.5 & 0.5 \\ 1 & -1 & 0 \end{pmatrix}$$

$$Q_{minus45} := T_{\sigma\_minus45}^{-1} \cdot Q_0 \cdot T_{\varepsilon\_minus45}$$

$$Q_{minus45} = \begin{pmatrix} 4.214\times 10^{10} & 3.32\times 10^{10} & -3.178\times 10^{10} \\ 3.32\times 10^{10} & 4.214\times 10^{10} & -3.178\times 10^{10} \\ -3.178\times 10^{10} & -3.178\times 10^{10} & 3.474\times 10^{10} \end{pmatrix} \text{ Pa}$$

Stiffness matrix at 90° orientation of the fibers with respect to the load direction

$$c = \cos\left(\frac{\pi}{2}\right) \qquad s = \sin\left(\frac{\pi}{2}\right)$$

$$T_{\sigma\_90} := \begin{pmatrix} c^2 & s^2 & 2\cdot s\cdot c \\ s^2 & c^2 & -2\cdot c\cdot s \\ -c\cdot s & c\cdot s & c^2 - s^2 \end{pmatrix} \qquad T_{\sigma\_90} = \begin{pmatrix} 0 & 1 & 0 \\ 1 & 0 & 0 \\ 0 & 0 & -1 \end{pmatrix}$$

$$T_{\varepsilon\_90} := \begin{pmatrix} c^2 & s^2 & s\cdot c \\ s^2 & c^2 & -s\cdot c \\ -2s\cdot c & 2s\cdot c & c^2 - s^2 \end{pmatrix} \qquad T_{\varepsilon\_90} = \begin{pmatrix} 0 & 1 & 0 \\ 1 & 0 & 0 \\ 0 & 0 & -1 \end{pmatrix}$$

$$Q_{90} := T_{\sigma\_90}^{-1} \cdot Q_0 \cdot T_{\varepsilon\_90}$$

$$Q_{90} = \begin{pmatrix} 8.863 \times 10^{9} & 2.925 \times 10^{9} & 1.838 \times 10^{-7} \\ 2.925 \times 10^{9} & 1.36 \times 10^{11} & 7.599 \times 10^{-6} \\ 1.838 \times 10^{-7} & 7.599 \times 10^{-6} & 4.47 \times 10^{9} \end{pmatrix} \text{Pa}$$

The tensile stiffness matrices of the parent and patch laminates are:

$$A_{parent} := \begin{pmatrix} Q_0 + Q_{90} + Q_{minus45} + Q_{plus45} + Q_{90} \cdots \\ + Q_0 + Q_0 + Q_{90} + Q_{minus45} + Q_{plus45} + Q_{90} + Q_0 \end{pmatrix} \cdot 2 \cdot h$$

$$A_{patch} := \left(Q_{minus45} + Q_{plus45}\right) \cdot 2 \cdot h$$

Hence, the tensile stiffness in the direction of the loading can be calculated by the element of the first row and first column of each tensile stiffness matrix, divided by the total thickness of the corresponding laminate.

$$\frac{A_{parent_{1,1}}}{24 \cdot h} = 6.232 \times 10^{10} \text{ Pa} \qquad \frac{A_{patch_{1,1}}}{h} = 1.686 \times 10^{11} \text{ Pa}$$

For values of the patch to parent thickness ratio, r_t, between 0.6 and 0.7 the patch to parent membrane stiffness ratio assumes the following values:

$$r_{ms} := r_t \cdot \frac{\frac{A_{patch_{1,1}}}{2 \cdot h}}{\frac{A_{parent_{1,1}}}{24 \cdot h}}$$

$$r_{ms} = \begin{cases} 0.811 & \text{if } r_t = 0.6 \\ 0.947 & \text{if } r_t = 0.7 \end{cases}$$